Interfacial Properties of Dairy Ingredients:
Role of Various Proteins and Emulsifier Crystals

Xilong Zhou

Interfacial Properties of Dairy Ingredients: Role of Various Proteins and Emulsifier Crystals Xilong Zhou

Propositions

1. Casein micelles adsorb at neither oil-water nor air-water interfaces.
   (this thesis)
2. The Pickering stabilization mechanism is often incorrectly invoked in food emulsion or foam research.
   (this thesis)
3. People can be more easily influenced than they think.
   (Milkman, et al. "Megastudies improve the impact of applied behavioural science." Nature 600.7889 (2021): 478-483.)
4. Reducing racism and economic inequality strengthen resistance to global disasters.
   (Witze. "Racism is magnifying the deadly impact of rising city heat." Nature 595.7867 (2021): 349-351.)
5. The first thing a PhD candidate should learn is to ask proper questions.
6. Watching children's cartoons is beneficial for adults' mental health, since simple plots and positive themes can relieve stress.
7. Being gossipy is a useful social skill to make friends.

Propositions belonging to the thesis, entitled

'Interfacial properties of dairy ingredients: Role of various protein fractions and emulsifier crystals'

Xilong Zhou

Wageningen, 22 April 2022

Interfacial Properties of Dairy Ingredients:

Role of Various Protein Fractions and Emulsifier Crystals

Xilong Zhou

Thesis committee

Promoter

Dr Leonard M.C. Sagis
Associate professor, Physics and Physical Chemistry of Foods
Wageningen University & Research

Co-Promoter

Dr Guido Sala
Senior scientist, Physics and Physical Chemistry of Foods
Wageningen University & Research

Other members

Prof. Dr CGPH Schroën, Wageningen University & Research
Prof. Dr T. Huppertz, Wageningen University & Research
Prof. Dr P. Fischer, ETH Zürich, Switzerland
Dr W. Kloek, Friesland Campina Innovation Centre, Wageningen

This research was conducted under the auspices of graduate school VLAG (Advanced Studies in Food Technology, Agrobiotechnology, Nutrition and Health Sciences).

Interfacial Properties of Dairy Ingredients:

Role of Various Protein Fractions and Emulsifier Crystals

Xilong Zhou

Thesis

submitted in fulfilment of the requirements for the degree of doctor
at Wageningen University
by the authority of the Rector Magnificus,
Prof. Dr A.P.J. Mol,
in the presence of the
Thesis Committee appointed by the Academic Board
to be defended in public
on Friday 22 April 2022
at 1:30 p.m. in the Aula.

Xilong Zhou

Interfacial Properties of Dairy Ingredients: Role of Various Protein Fractions and Emulsifier Crystals, 190 pages

PhD thesis, Wageningen University, Wageningen, the Netherlands (2022)

With references, with summary in English

ISBN: 978-94-6447-142-7

DOI: https://doi.org/10.18174/566453

Table of contents

Chapter 1

General Introduction

1.1. Dairy based emulsions

In emulsions, when oil is dispersed in the water phase, the increase of surface area between oil and water results in an increase of the overall free energy of the system. According to thermodynamics, two immiscible phases tend to phase separate to spontaneously minimize surface area and free energy. Creaming and coalescence of oil droplets will then occur. Emulsifiers and proteins are normally used to stabilize emulsions, but by different mechanisms. Low molecular weight emulsifiers significantly decrease the interfacial tension, thereby decreasing the size of lipid droplets after homogenization. They also prevent the merging of lipid droplets by Marangoni effects, thus improving the stability against coalescence. Some recent research also claimed that emulsifiers with a high melting point can prevent (partial) coalescence by forming solid layers around the surface of the droplet (Fredrick, et al., 2013; Munk, et al., 2014), but this mechanism is not yet well investigated. Proteins, although they are not as surface active as low molecular weight surfactants (Liang, et al., 2017; Rosen, et al., 2012), are also amphiphilic and can adsorb at interfaces. Proteins form viscoelastic layers at interfaces, which can stabilize droplets by electrostatic and steric repulsion. The stability of droplets against coalescence and creaming is thereby improved during long-term storage.

In areas where dairy sources are scarce, dairy products are traditionally considered as luxury products. The spread of the consumption of dairy products is thus restricted to certain regions (Wu, et al., 2016). The development of recombined dairy products, for instance, milk reconstituted from milk powder, largely makes up for the shortage of dairy products in those areas. Such a development has significantly boosted the export and import of dairy ingredients among regions or countries. Recombined dairy cream (RDC) is one of these recombined dairy products and is a substitute for natural cream. RDC is composed of anhydrous milk fat, water, and some stabilizers. Compared with natural cream, recombined dairy cream has a number of competitive advantages. For example, the composition and desired properties of RDC can be standardized and adapted independently of the milking season, all the ingredients can be easily stored and transported, and its recipe can be adjusted if needed (van Lent, et al., 2008; Zhou, et al., 2016). However, compared with natural cream, recombined dairy cream has a main disadvantage that it is more kinetically unstable. In

natural cream, lipid droplets are covered with natural fat globule membranes, which can efficiently prevent coalescence and can protect lipid droplets from the activity of enzymes. Recombined dairy cream is made from anhydrous milk fat. During the manufacture of anhydrous milk fat, fat globule membranes are removed (Tamime, 2009). Without the protection of globule membranes around fat globules, the stability of RDC is much worse than that of natural dairy cream. Some instability phenomena may happen in RDC, for instance, coalescence, creaming, partial coalescence, aggregation and flocculation (Fredrick, et al., 2010). These instability phenomena can normally be prevented by utilizing stabilizers, including low molecular weight emulsifiers, proteins, and thickeners.

Taking production costs into consideration, normally, proteins and emulsifiers are mixed together in emulsion products, including RDC. This is also the reason why many researchers are interested in the interactions between emulsifiers and proteins in emulsion systems. Results have shown that low molecular weight emulsifiers can displace proteins from interfaces (J.-L. Courthaudon, et al., 1991; Wilde, et al., 2004). Moreover, some research demonstrated that the combined use of proteins and emulsifiers will results in a decrease of surface activity of proteins due to the formation of protein-emulsifier complexes (R. Miller, et al., 2000). This might impair the capacity of these proteins to form viscoelastic layers at interfaces of the oil droplets. Consequently, whether it is a good choice for emulsion stabilization to combine proteins and emulsifiers in the system is questionable. In practice, even for emulsions stabilized only by proteins, mixtures are often used, such a milk protein concentrates, which are mixtures of caseins and whey proteins (Scott, et al., 2003; Tomas, et al., 1994; Wu, et al., 2016; Zhou, et al., 2016). Many studies have shown that casein and whey have distinct functions, which are widely investigated with respect to adsorption dynamics, thermodynamics and rheological behaviors (Liang, et al., 2013a; Maldonado-Valderrama, et al., 2005; R Miller, et al., 2004; Raikos, 2010; Wüstneck, et al., 1996), but they are also reported to have interactions with each other (Dalgleish, Goff, Brun, et al., 2002; Dalgleish, Goff, & Luan, 2002; Dickinson & Matsumura, 1994), especially after heat treatment (Euston, et al., 2009; Liang, et al., 2013b). Whether these interactions improve or reduce emulsion stability needs to be evaluated.

Besides emulsions, foams are other important food lyophobic colloidal dispersions, and are also thermodynamically unstable systems. In foams,

coalescence, drainage and disproportionation can happen (Sánchez, et al., 2005; Shankaran, et al., 2019). Both low molecular weight emulsifiers and proteins are often used for stabilizing foams, and their functions at air-water (A-W) interfaces (foams) are similar to those at oil-water (O-W) interfaces (emulsions). Emulsifiers mainly decrease the surface tension, slowing down the rate of disproportionation and preventing coalescence by Marangoni effects. Proteins form viscoelastic networks at the interface, opposing its stretching. Large protein particles (i.e. insoluble aggregates) might remain in the lamellar films and can also retard drainage by pinning (Brent S. Murray, et al., 2004). Air bubbles are essential in determining texture, mouth feel and visual appeal of some dairy products (Campbell, et al., 1999), for example whipping cream, ice cream, or cappuccino-style beverages. In these products, foams should not just have a high volume fraction of air, but also a good stability. The optimization of both foam properties is thus of great interest for the food industry.

Synergistic or antagonistic effects among ingredients used in dairy or dairy-based emulsions and foams are often not well demonstrated or understood. The combined use of emulsifiers and proteins is normally based on an empirical approach. In order to acquire a more fundamental understanding of the role of the individual components and their potential synergy or antagonism in dairy systems, we need to focus on phenomena occurring at a length scale smaller than the macroscale of emulsions, i.e. on the structures formed at O-W or A-W interfaces by different components, and on their effect on the rheological properties of the interface. The interfacial composition and structure can significantly affect the stability, rheological properties and texture of food products (Chevallier, et al., 2016; Dickinson, 1999; Surel, et al., 2014). A fundamental understanding of compositions and structure of the interfaces is essential for designing the formulation and physical properties of dairy based emulsions or foams. In the following sections, we will briefly introduce some of the surface-active dairy ingredients often used in emulsions or foams, and the method used to study mechanical properties of their interfaces, namely interfacial rheology.

1.2. Surface active dairy ingredient

1.2.1. Casein

Casein is the main protein in milk, representing about 80% of its total proteins. It is mainly composed of four types of monomers, κ-casein, α_{S2}-casein, α_{S1}-casein, and β-casein, with a ratio 1.3 : 1 : 4 : 4 (Walstra, 1990). Alpha$_s$-casein and β-casein aggregate with each other by hydrophobic interactions, hydrogen bonds and interactions with colloidal calcium phosphates. In raw milk, over 95 % of caseins exists in the form of micelles (Dumpler, 2017). The conventional process to produce casein is isoelectric or enzymatic precipitation. Both processes will yield insoluble powders after drying. As a result, an additional processing step, alkalization is required to make casein soluble (Carr, et al., 2016). The product obtained after alkalization is sodium caseinate, which has a good solubility in water and is a well-known emulsifier for food emulsions. During the manufacturing of sodium caseinate, the micellar structure of casein is lost. In industry, micellar casein is isolated by microfiltration (Walstra, et al., 2005). The required filter membranes are expensive, which leads to a high price of the obtained products. Micellar casein is thus not widely used in food industry. This is the reason why in the last decades research studying emulsifying properties of caseins mainly focused on sodium caseinate, and not micellar casein. In practice, although sodium caseinate has good emulsifying properties and can reduce the surface tension to a great extent, it will induce another instability problem, i.e. flocculation (Dickinson, et al., 1997). It has been shown that casein fractions exhibit different hydrophobicity and surfactant properties at different state of structural aggregation (J. L. Courthaudon, et al., 1999; Roman, et al., 2006). Therefore, the emulsifying and stabilizing effect of micellar caseins can be remarkably different from sodium caseinate. Nowadays, the behavior of micellar casein at interfaces is still unclear. Some researchers believe that casein micelles can adsorb at O-W interfaces (San Martin-González, et al., 2009) and stabilize emulsions by a Pickering mechanism (Dickinson, 2015). However, this claim has not been fully proven, as a complete interfacial layer formed by micelles has never been observed. Full dairy protein products, for instance, skimmed milk power and milk protein concentrate, are usually used as stabilizers. In these products casein is mainly present in micellar form. Therefore, the interfacial properties of

micellar casein need to be further investigated to understand the function of each individual component and their interactions.

1.2.2. Whey protein

Whey protein makes up 20% of the total bovine milk protein and is also the main side product of the cheese industry. As whey protein contains all essential amino acids and is well digestible (Hoffman, et al., 2004), it is mainly used as nutritional ingredient in many products, like energy bars and protein powders for athletes. Whey protein is mainly composed of β-lactoglobulin and α-lactalbumin. β-lactoglobulin represents more than 50% of the whey proteins (Fox, et al., 2013), and is also the most well studied whey protein species at interfaces. β-lactoglobulin has a high level of secondary and tertiary structure, and is regarded as a globular protein held together by intramolecular disulfide bonds (McKenzie, et al., 1972; Papiz, et al., 1986), but it can have several forms, depending on the pH. It exists as a monomer when pH is lower than 3.5 or higher than 7.5, with a molecular weight around 18 kDa; at the natural pH of milk (6.6-6.7), β-lactoglobulin will associate into a dimer; in the pH range 3.5-5.2, it exists as an octamer (Swaisgood, 1982; Timasheff, et al., 1962). Due to its globular structure, β-lactoglobulin reorganizes its structure slowly when it adsorbs at interfaces, (Dickinson, 1997). After rearrangement at the interface, β-lactoglobulin molecules can have strong intermolecular interactions by a combination of ionic, hydrophobic and hydrogen bonds (Dickinson, 1998), thus forming strong viscoelastic layers at the surface of oil droplets or air bubbles. The only drawback of whey protein in stabilizing emulsions or foams is its heat sensitivity. Whey protein starts to denature around a temperature of 70 °C (Parris, et al., 1991), coupled with partial unfolding of its secondary and tertiary structure. Upon heating, the different protein species present in whey protein are capable of interacting with themselves and κ-casein to form heat-induced aggregates (Donato, et al., 2007; Jang, et al., 1990; Smits, et al., 1980), which can also result in flocculation or aggregation of emulsions stabilized with them (Kulmyrzaev, et al., 2000). Despite this, whey protein is still widely used as emulsifying and foaming agent in food products due to its unique interfacial properties (Nicorescu, et al., 2008). In the past decades, the consequence of physical or chemical modification of whey protein, for example using heat treatment to make aggregates, on emulsion stability was a frequently studied topic (Dybowska, 2011; Millqvist-Fureby, et al., 2001; Nicolai, et al., 2013). Whey protein aggregates have been reported to be

good stabilizers in emulsions, which can stabilize emulsion more efficiently than native whey protein due to the formation of thicker interfacial layers around oil droplets (Dybowska, 2011; Foley, et al., 1990). So far, the mechanical properties of the interfacial layers formed by whey protein or whey protein aggregates at O-W or A-W interfaces are not well studied, especially in the nonlinear viscoelastic regime, a regime highly relevant for the behavior of emulsions and foams during processing or consumption.

1.2.3. Polar lipids

Milk fat is the main ingredient of most dairy emulsions, like cream. It derives a high level of importance from the textural, sensory, and functionality it gives to products in which it is present, for example, yoghurt, liquid milk, butter and cream. Milk fat consists for about 98% of triacylglycerols (TAG) and other components being diacylglycerols (DAG), monoacylglycerols (MAG), free fatty acids, phospholipids, all comparatively more polar than TAG. A detailed composition of milk fat is reported in Tab. 1.1. DAG and MAG are natural surface-active ingredients in milk fat. Although the amount of MAG and DAG in fresh milk is small, their concentration will increase considerably due to the enzymatic hydrolysis of the ester bonds in triglycerides during storage. As a result, when milk fat is used as oil phase to make emulsions, DAG and MAG in the lipid phase will also adsorb at the interfaces. As mentioned above, many studies already revealed that small molecular weight emulsifiers interact with proteins adsorbed at the O-W interface. DAG and MAG were found having similar effects (Dickinson & Hong, 1994; McSweeney, et al., 2008; Munk, et al., 2014; B. M. C. Pelan, et al., 1997; Rahman, et al., 1982). Research evaluating the effects of these residual polar lipids on interfacial rheology or on emulsion properties is still scarce. However, in most research where proteins are used as stabilizers, these naturally present emulsifiers are assumed to have no effects in the system, and their effect on adsorbed proteins at the interfaces is ignored.

Besides being naturally present in the milk fat phase, MAG are also used as commercial emulsifiers in emulsions. Glycerol monooleate (MAG-O) and monostearate (MAG-S) are the two most often used monoglycerides in food emulsions, but have very different effects on emulsions. MAG-O is an unsaturated monoglyceride having a low melting point and is more effective in promoting partial coalescence during whipping of a cream (Goff, et al., 1989; B. Pelan, et al., 1997). MAG-S is a saturated monoglyceride with a high melting point. Emulsions made with MAG-S are more stable against (partial)

coalescence (Fredrick, et al., 2013; Goibier, et al., 2017). The stabilization by MAG-S in water-in-oil emulsion was also observed and is often assumed to be by a Pickering mechanism, in which MAG-S crystals cover the surface of dispersed water droplets to prevent coalescence (Ghosh, et al., 2011). However, the mechanism by which MAG-S stabilizes oil-in-water emulsions against (partial) coalescence is less clear. Both Fredrick, et al. (2013) and Goibier, et al. (2017) proposed two different mechanisms. The first one is that MAG-S forms a rigid barrier protecting fat droplets from (partial) coalescence. A similar mechanism was also proposed by Munk, et al. (2014), and was assumed to be Pickering stabilization. The second one is that MAG-S crystals in droplets serve as templates for further milk fat crystallization and lead to a higher crystallization rate. The formed milk fat crystals are thereby smaller and cannot piece through the droplet over a long distance and become incorporated into another droplet. However, so far, both two mechanisms have not been convincingly proven in oil-in-water emulsion.

Tab. 1.1. Compositions of lipids in cow's milk (Walstra, et al., 2005).

Lipid class	% of total
Triacylglycerols	98.3
Diacylglycerols	0.3
Monoacylglycerols	0.03
Free fatty acids	0.1
Phospholipids	0.8
Sterols	0.3
Carotenoids	Trace
Fat-soluble vitamins	Trace
Flavor compounds	Trace

1.3. Interfacial rheology

Interfacial rheology is a powerful tool to study the mechanical properties of interfaces, which can be done with two methods, shear and dilatational rheology (Chen, et al., 2017; Danov, et al., 2015; Li, et al., 2018; Wan, et al., 2016). Shear rheology measures the response of interfacial layers to shear deformation, in which the shape of surface elements is varied while keeping their area constant. Oppositely, dilatational rheology determines the response of the interfacial layer against expansion and compression of

surface elements, while maintaining their shape. Within both modes several types of tests can be used, such as frequency sweeps, amplitude sweeps and step strain relaxation tests, and the results obtained with these measurements can provide insights into the structure of the interfaces.

In interfacial shear rheology, there is no area change of the interface. Therefore, for a protein-stabilized interface, the stress output is only affected by the network formed by proteins at the interface (Brent S Murray, 2002). For dilatational rheology, in addition to the network formed by proteins, the stress response is also affected by the density change of proteins adsorbed at the interface. Upon compression, the density of proteins increases and a jammed protein layer can even be formed, which can result in strong molecular interactions (Freer, et al., 2004). As a result, for the same interface, the stress response from interfacial dilatational rheology is often larger than the one from interfacial shear rheology. A protein stabilized A-W interface can normally be studied by both shear and dilatational rheology. However, shear rheology is hardly applied on a protein stabilized O-W interface, because in general, intermolecular interactions among adsorbed proteins at O-W interfaces are much weaker than at A-W interfaces (Hinderink, et al., 2020). A low stress (torque) response from shear tests on O-W interfaces results in inaccurate or even invalid results, which is the main reason interfacial shear rheology is not used in this thesis research.

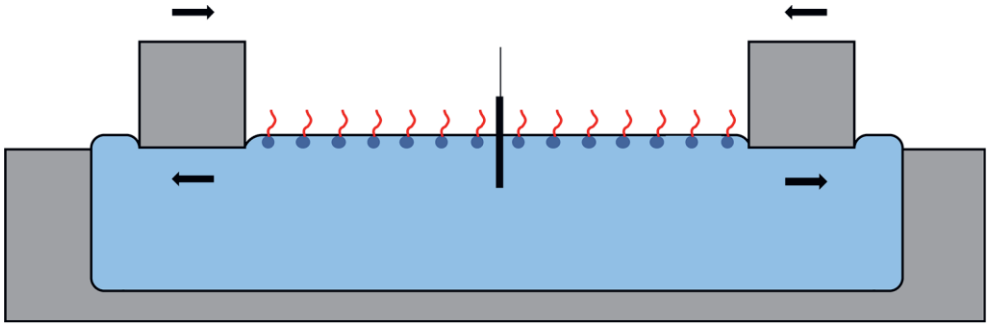

Fig. 1.1. Schematic of a dilatational rheology experiment performed with a Langmuir trough.

Dilatational rheology can be performed with both a Langmuir trough (Fig. 1.1) or droplet tensiometer (Fig. 1.2). In a Langmuir trough experiment, the area of the interfacial layer is controlled by moving two Teflon barriers,

which are hydrophobic. The surface tension is measured with a Wilhelmy plate. In a droplet tensiometer, a droplet or bubble can be formed at the tip of a needle immersed in air or a liquid. The area of the droplet can be adjusted by injecting/withdrawing fluid into/from the droplet or bubble. The area change in droplet tensiometry is (close to) an all-sided compression/expansion, and the modulus which is determined is indeed the dilatational modulus (the two-dimensional equivalent of the three-dimensional bulk modulus). The deformation of interfaces in a Langmuir trough is uni-axial, and the response contains a shear component. In essence, this device determines the two-dimensional Young's modulus. For this reason, the dilatational moduli determined using a droplet tensiometer can be considered more accurate than the ones from a Langmuir trough, particularly for interfaces in which the shear contribution is not negligible. The most common mode to apply area dilatation of the interface is by using sinusoidal deformations. In the linear response regime (i.e. in the limit of small amplitude deformations), the output tension or stress is also sinusoidal. The output data can be analyzed by two methods: Fourier transformation of the stress response and analysis of the intensity and phase of the first harmonic, or by graphical methods, using Lissajous plots.

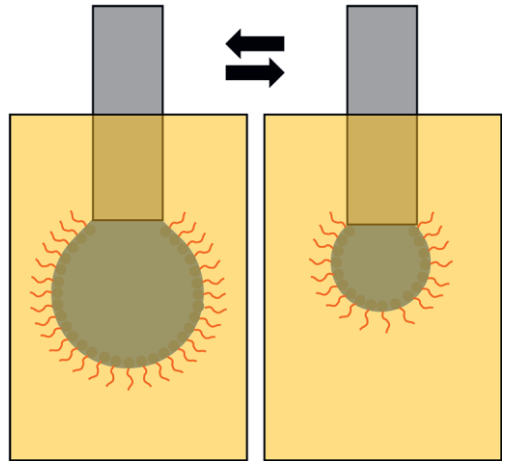

Fig. 1.2. Schematic of a dilatational rheology experiment performed with a droplet tensiometer.

1.3.1. Fourier transformation

Fourier transformation is a mathematical transformation that can decompose time dependent functions into frequency dependent functions. For a sinusoidal strain input $\gamma(t) = \gamma_0 \, sin(\omega t)$, the stress σ can be expressed by the Fourier series (Dealy, et al., 2012),

$$\sigma(t; \omega, \gamma_0) = \gamma_0 \sum_n \{E_n'(\omega, \gamma_0) \, sin(n\omega t) + E_n''(\omega, \gamma_0) \, cos(n\omega t)\} \qquad \text{Eq. 1.1}$$

where $\gamma(t)$ is the strain at time t; γ_0 and ω are the amplitude and frequency of the strain, respectively; σ is the surface stress; n represents the order of the harmonics; E_n' and E_n'' are the elastic and viscous moduli with order n.

In the linear viscoelastic regime, the stress response is still an ideal sinusoidal curve. The frequency spectrum of the stress will show only the first harmonic. When the strain is in the nonlinear viscoelastic regime, the stress curve will be a distorted sinusoidal function, and the Fourier series of the surface stress will have higher harmonics. To use E_1' and E_1'' to represent the moduli of interfaces in the nonlinear regime will be inaccurate, as all the information present in the higher harmonics is discarded. The rheological properties of interfaces in the nonlinear regime are sometimes very important, as in food processing and consumption, large and fast deformations of interfaces often occur. The rheological properties of interfaces in the nonlinear regime have therefore high practical relevance (Sagis, et al., 2014).

1.3.2. Lissajous plots

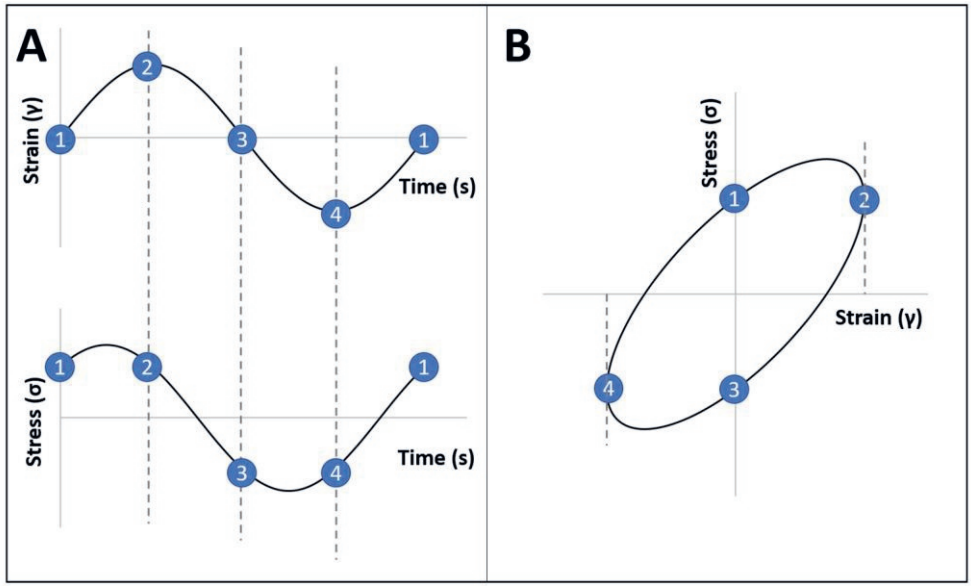

Fig. 1.3. Schematic of the construction of Lissajous plots. A: stress and strain over time. B: Lissajous plots (stress is plotted versus strain).

Lissajous plots are constructed by directly plotting the surface stress versus time-dependent strain, as illustrated in Fig. 1.3. In the linear viscoelastic regime, Lissajous plots will display an ellipse shape, whereas in the nonlinear regime, the shape of Lissajous plots will be distorted, and even asymmetrical in dilatational rheology, as shown in Fig. 1.4. Nonlinear behavior, such as strain softening or hardening, can be directly observed from Lissajous plots (Fig. 1.4). From the shape of Lissajous plots, the changes of the structure of the interface upon deformation can be deduced. For example, expansion softening is normally linked with the break-up of bonds in an interconnected structure; a steep increase of the stress upon compression indicates stronger molecular interactions among the structures. Therefore, compression hardening is normally related with the formation of jammed structures.

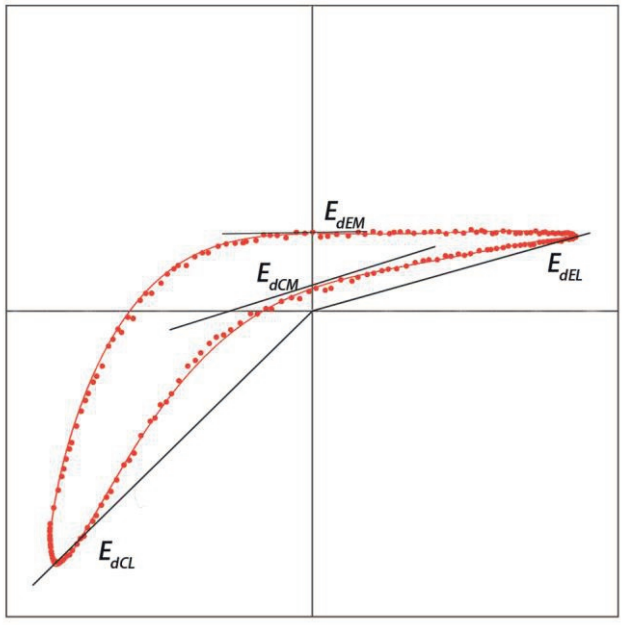

Fig. 1.4. Example of a Lissajous plot in the nonlinear viscoelastic regime (Expansion softening/yielding and compression hardening). E_{dEM} and E_{dEL} are the tangent modulus and secant modulus upon expansion, respectively. Likewise, E_{dCM} and E_{dCL} are the tangent modulus and secant modulus upon compression, respectively.

The shape of Lissajous plots can provide not only a qualitative description of structural changes at the interface, but can also provide quantitative parameters. The quantification of Lissajous plots has already been introduced by Ewoldt, et al. (2008), and applied in dilatational rheology by van Kempen, et al. (2013). Basically, the tangent of the Lissajous plot at strain zero (E_{dEM} upon expansion, E_{dCM} upon compression) and the slope of the secant line at maximum strain (E_{dEL} upon expansion, E_{dCL} upon compression) can be used to quantify softening or hardening behavior (Fig. 1.4). Moghimikheirabadi, et al. (2019) developed a method to determine the tangential and secant moduli from the Fourier coefficients E_n' and E_n'', using the following equations (Eq. 1.2 - Eq. 1.5):

$$E_{dEM} = \left.\frac{d\sigma}{d\gamma}\right|_{\gamma_{exp}=0} = \left.\frac{d\sigma}{d\gamma}\right|_{t=2k\pi/\omega} = \sum_{n=1}^{\infty} nE_n' \qquad \text{Eq. 1.2}$$

$$E_{dEL} = \frac{\sigma}{\gamma}\Big|_{\gamma_{exp}=\gamma_{max}} = \frac{\sigma}{\gamma}\Big|_{t=\frac{\pi}{2\omega}+2k\pi/\omega} = \sum_{n=1}^{\infty}(-1)^n(E_{2n}'' - E_{2n-1}'') \quad \text{Eq. 1.3}$$

$$E_{dCM} = \frac{d\sigma}{d\gamma}\Big|_{\gamma_{comp}=0} = \frac{d\sigma}{d\gamma}\Big|_{t=\frac{\pi}{w}+2k\pi/\omega} = \sum_{n=1}^{\infty} nE_n'\,(-1)^{n+1} \quad \text{Eq. 1.4}$$

$$E_{dEL} = \frac{\sigma}{\gamma}\Big|_{\gamma_{comp}=\gamma_{max}} = \frac{\sigma}{\gamma}\Big|_{t=\frac{3\pi}{2\omega}+2k\pi/\omega} = \sum_{n=1}^{\infty}(-1)^{n+1}(E_{2n}'' + E_{2n-1}'') \quad \text{Eq. 1.5}$$

1.4. Research aim and outline of this thesis

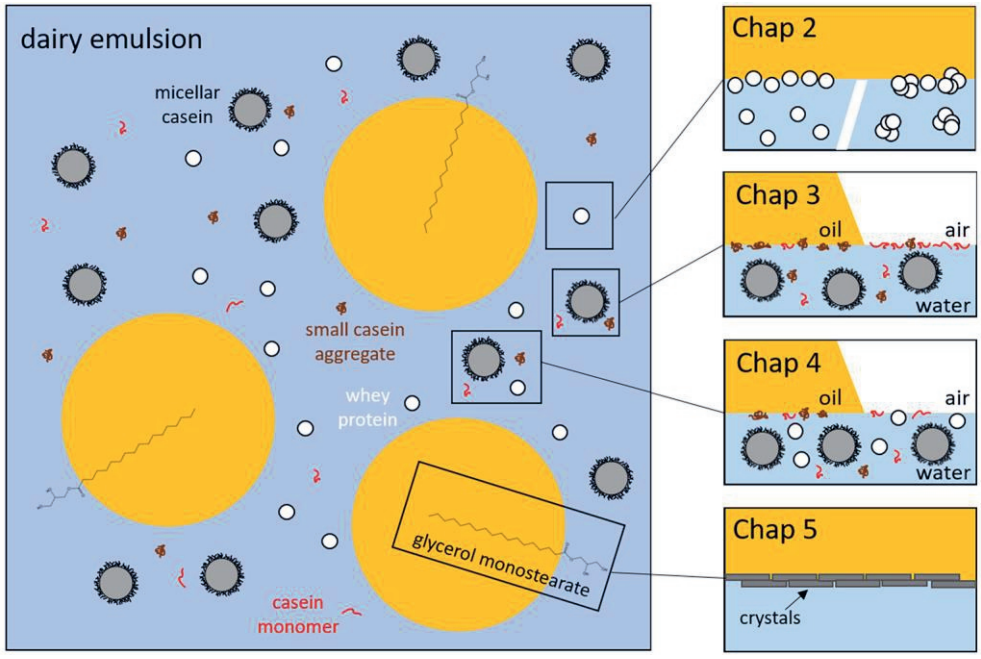

Fig. 1.5. Graphical outline of the experimental chapters of this thesis.

In this research, we mainly focused on O-W and A-W interfaces stabilized by dairy proteins and their mixtures, and on O-W interfaces stabilized by emulsifier crystals. We aimed at understanding the interfacial properties of the individual dairy proteins, casein, whey protein, and their mixtures; we also aimed at improving our understanding of how high melting point emulsifiers stabilize oil-in-water emulsion against (partial) coalescence. The mechanical properties of the interfaces were tested by dilatational rheology. Combining results obtained from rheological measurements and results from several interface visualization techniques, the composition/structure

of the interfaces was deduced. The outline of the experimental chapters is illustrated in Fig. 1.5.

Before investigating the interfacial composition and mechanical properties of the interface in mixed systems, we first studied the surface-active species individually. In Chapter 2, we investigated the mechanical properties of O-W interfaces stabilized with whey proteins or whey protein aggregates in the nonlinear viscoelastic regime. The dynamic stability of the cream made from whey protein was also compared to that of a cream made with whey protein aggregates. In chapter 3, we fractionated casein micelle dispersions into different fractions. The interfacial properties of micellar caseins, small casein aggregates or monomers were subsequently investigated at both the O-W and A-W interfaces, and the dominant protein species at these interfaces were identified. After gathering insights into the linear and nonlinear interfacial properties of casein and whey protein, these proteins were mixed at different ratios. The relative contribution of casein and whey protein to the rheological properties of O-W and A-W interfaces, and the composition/structure of these interfaces were studied. In chapter 5, the interests shifted to the crystallization process of MAG-S at O-W interfaces. MAG-S crystallization at a planar O-W interface and in an oil-in-water emulsion was investigated. In this specific study a new phenomenon, i.e. repeated deformation-relaxation of lipid droplets was found and is described in this thesis for the first time. Whey protein and casein have distinctive molecular properties, and in this research we have shown that these properties lead to specific interfacial mechanical behaviors. Based on the findings in chapter 2-5, the effects of protein size, structure and flexibility on their adsorption behavior, structures formed at the interfaces and their applications in emulsions or foams are discussed in chapter 6. The effects of surface active components naturally present in oils on rheology tests and on the properties of emulsions, as well as the role of Pickering stabilization in protein stabilized interfaces or MAG-S stabilized emulsions are also discussed.

References

Campbell, G. M., & Mougeot, E. (1999). Creation and characterisation of aerated food products. Trends in Food Science & Technology, 10(9), 283-296.

Carr, A., & Golding, M. (2016). Functional Milk Proteins Production and Utilization: Casein-Based Ingredients. In P. L. H. McSweeney & J. A. O'Mahony (Eds.), Advanced Dairy Chemistry: Volume 1B: Proteins: Applied Aspects (pp. 35-66). New York, NY: Springer New York.

Chen, M., Sala, G., Meinders, M. B., van Valenberg, H. J., van der Linden, E., & Sagis, L. M. (2017). Interfacial properties, thin film stability and foam stability of casein micelle dispersions. Colloids and Surfaces B: Biointerfaces, 149, 56-63.

Chevallier, M., Riaublanc, A., Lopez, C., Hamon, P., Rousseau, F., & Croguennec, T. (2016). Aggregated whey proteins and trace of caseins synergistically improve the heat stability of whey protein-rich emulsions. Food Hydrocolloids, 61, 487-495.

Courthaudon, J.-L., Dickinson, E., Matsumura, Y., & Williams, A. (1991). Influence of emulsifier on the competitive adsorption of whey proteins in emulsions. Food Structure, 10(2), 1.

Courthaudon, J. L., Girardet, J. M., Campagne, S., Rouhier, L. M., Campagna, S., Linden, G., & Lorient, D. (1999). Surface active and emulsifying properties of casein micelles compared to those of sodium caseinate. International Dairy Journal, 9(3-6), 411-412.

Dalgleish, D. G., Goff, H. D., Brun, J. M., & Luan, B. B. (2002). Exchange reactions between whey proteins and caseins in heated soya oil-in-water emulsion systems - overall aspects of the reaction. Food Hydrocolloids, 16(4), 303-311.

Dalgleish, D. G., Goff, H. D., & Luan, B. B. (2002). Exchange reactions between whey proteins and caseins in heated soya oil-in-water emulsion systems - behavior of individual proteins. Food Hydrocolloids, 16(4), 295-302.

Danov, K. D., Kralchevsky, P. A., Radulova, G. M., Basheva, E. S., Stoyanov, S. D., & Pelan, E. G. (2015). Shear rheology of mixed protein adsorption layers vs their structure studied by surface force measurements. Adv Colloid Interface Sci, 222, 148-161.

Dealy, J. M., & Wissbrun, K. F. (2012). Melt rheology and its role in plastics processing: theory and applications: Springer Science & Business Media.

Dickinson, E. (1997). Properties of Emulsions Stabilized with Milk Proteins: Overview of Some Recent Developments. Journal of Dairy Science, 80(10), 2607-2619.

Dickinson, E. (1998). Proteins at interfaces and in emulsions stability, rheology and interactions. Journal of the Chemical Society, Faraday Transactions, 94(12), 1657-1669.

Dickinson, E. (1999). Adsorbed protein layers at fluid interfaces: interactions, structure and surface rheology. Colloids and Surfaces B-Biointerfaces, 15(2), 161-176.

Dickinson, E. (2015). Microgels—an alternative colloidal ingredient for stabilization of food emulsions. Trends in Food Science & Technology, 43(2), 178-188.

Dickinson, E., & Golding, M. (1997). Depletion flocculation of emulsions containing unadsorbed sodium caseinate. Food Hydrocolloids, 11(1), 13-18.

Dickinson, E., & Hong, S.-T. (1994). Surface Coverage of. beta.-Lactoglobulin at the Oil-Water Interface: Influence of Protein Heat Treatment and Various Emulsifiers. Journal of agricultural and food chemistry, 42(8), 1602-1606.

Dickinson, E., & Matsumura, Y. (1994). Proteins at liquid interfaces: Role of the molten globule state. Colloids and Surfaces B: Biointerfaces, 3(1), 1-17.

Donato, L., Guyomarc'h, F., Amiot, S., & Dalgleish, D. G. (2007). Formation of whey protein/κ-casein complexes in heated milk: Preferential reaction of whey protein with κ-casein in the casein micelles. International Dairy Journal, 17(10), 1161-1167.

Dumpler, J. (2017). Heat Stability of Concentrated Milk Systems.

Dybowska, B. E. (2011). Whey protein-stabilized emulsion properties in relation to thermal modification of the continuous phase. Journal of food Engineering, 104(1), 81-88.

Euston, S. R., Al-Bakkush, A.-A., & Campbell, L. (2009). Comparing the heat stability of soya protein and milk whey protein emulsions. Food Hydrocolloids, 23(8), 2485-2492.

Ewoldt, R. H., Hosoi, A., & McKinley, G. H. (2008). New measures for characterizing nonlinear viscoelasticity in large amplitude oscillatory shear. Journal of Rheology, 52(6), 1427-1458.

Foley, J., & O'Connell, C. (1990). Comparative emulsifying properties of sodium caseinate and whey protein isolate in 18% oil in aqueous systems. Journal of Dairy Research, 57(3), 377-391.

Fox, P. F., & McSweeney, P. L. (2013). Advanced Dairy Chemistry: Volume 1: Proteins, Parts A&B: Springer.

Fredrick, E., Heyman, B., Moens, K., Fischer, S., Verwijlen, T., Moldenaers, P., Van der Meeren, P., & Dewettinck, K. (2013). Monoacylglycerols in dairy recombined cream: II. The effect on partial coalescence and whipping properties. Food Research International, 51(2), 936-945.

Fredrick, E., Walstra, P., & Dewettinck, K. (2010). Factors governing partial coalescence in oil-in-water emulsions. Adv Colloid Interface Sci, 153(1-2), 30-42.

Freer, E. M., Yim, K. S., Fuller, G. G., & Radke, C. J. (2004). Interfacial rheology of globular and flexible proteins at the hexadecane/water interface: comparison of shear and dilatation deformation. The Journal of Physical Chemistry B, 108(12), 3835-3844.

Ghosh, S., Tran, T., & Rousseau, D. (2011). Comparison of Pickering and Network Stabilization in Water-in-Oil Emulsions. Langmuir, 27(11), 6589-6597.

Goff, H., & Jordan, W. (1989). Action of emulsifers in promoting fat destabilization during the manufacture of ice cream. Journal of Dairy Science, 72(1), 18-29.

Goibier, L., Lecomte, S., Leal-Calderon, F., & Faure, C. (2017). The effect of surfactant crystallization on partial coalescence in O/W emulsions. Journal of colloid and interface science, 500, 304-314.

Hinderink, E., Sagis, L., Schroën, K., & Berton-Carabin, C. C. (2020). Behavior of plant-dairy protein blends at air-water and oil-water interfaces. Colloids and Surfaces B: Biointerfaces, 111015.

Hoffman, J. R., & Falvo, M. J. (2004). Protein–which is best? Journal of sports science & medicine, 3(3), 118.

Jang, H. D., & Swaisgood, H. E. (1990). Disulfide Bond Formation Between Thermally Denatured β-Lactoglobulin and κ-Casein in Casein Micelles. Journal of Dairy Science, 73(4), 900-904.

Kulmyrzaev, A., Bryant, C., & McClements, D. J. (2000). Influence of sucrose on the thermal denaturation, gelation, and emulsion stabilization of

whey proteins. Journal of agricultural and food chemistry, 48(5), 1593-1597.

Li, W., Wang, Y., Zhao, H., He, Z., Zeng, M., Qin, F., & Chen, J. (2018). Effects of soluble soy polysaccharides and gum arabic on the interfacial shear rheology of soy β-conglycinin at the air/water and oil/water interfaces. Food Hydrocolloids, 76, 123-130.

Liang, Y., Matia-Merino, L., Gillies, G., Patel, H., Ye, A., & Golding, M. (2017). The Heat Stability of Milk Protein-stabilized Oil-in-water Emulsions: A Review. Current Opinion in Colloid & Interface Science.

Liang, Y., Patel, H., Matia-Merino, L., Ye, A., & Golding, M. (2013a). Effect of pre-and post-heat treatments on the physicochemical, microstructural and rheological properties of milk protein concentrate-stabilised oil-in-water emulsions. International Dairy Journal, 32(2), 184-191.

Liang, Y., Patel, H., Matia-Merino, L., Ye, A., & Golding, M. (2013b). Structure and stability of heat-treated concentrated dairy-protein-stabilised oil-in-water emulsions: A stability map characterisation approach. Food Hydrocolloids, 33(2), 297-308.

Maldonado-Valderrama, J., Fainerman, V., & ... (2005). Dilatational Rheology of β-Casein Adsorbed Layers at Liquid− Fluid Interfaces. The Journal of ….

McKenzie, H., Ralston, G., & Shaw, D. (1972). Location of sulfhydryl and disulfide groups in bovine. beta.-lactoglobulins and effects of urea. Biochemistry, 11(24), 4539-4547.

McSweeney, S. L., Healy, R., & Mulvihill, D. M. (2008). Effect of lecithin and monoglycerides on the heat stability of a model infant formula emulsion. Food Hydrocolloids, 22(5), 888-898.

Miller, R., Fainerman, V., Aksenenko, E., Leser, M., & Michel, M. (2004). Dynamic surface tension and adsorption kinetics of β-casein at the solution/air interface. Langmuir, 20(3), 771-777.

Miller, R., Fainerman, V. B., Makievski, A. V., Krägel, J., Grigoriev, D. O., Kazakov, V. N., & Sinyachenko, O. V. (2000). Dynamics of protein and mixed protein/surfactant adsorption layers at the water/fluid interface. Adv Colloid Interface Sci, 86(1), 39-82.

Millqvist-Fureby, A., Elofsson, U., & Bergenståhl, B. (2001). Surface composition of spray-dried milk protein-stabilised emulsions in relation to pre-heat treatment of proteins. Colloids and Surfaces B: Biointerfaces, 21(1-3), 47-58.

Moghimikheirabadi, A., Fischer, P., Kröger, M., & Sagis, L. M. C. (2019). Relaxation Behavior and Nonlinear Surface Rheology of PEO–PPO–PEO Triblock Copolymers at the Air–Water Interface. Langmuir, 35(44), 14388-14396.

Munk, M. B., Larsen, F. H., Van Den Berg, F., Knudsen, J. C., & Andersen, M. L. (2014). Competitive displacement of sodium caseinate by low-molecular-weight emulsifiers and the effects on emulsion texture and rheology. Langmuir, 30(29), 8687-8696.

Murray, B. S. (2002). Interfacial rheology of food emulsifiers and proteins. Current Opinion in Colloid & Interface Science, 7(5-6), 426-431.

Murray, B. S., & Ettelaie, R. (2004). Foam stability: proteins and nanoparticles. Current Opinion in Colloid & Interface Science, 9(5), 314-320.

Nicolai, T., & Durand, D. (2013). Controlled food protein aggregation for new functionality. Current Opinion in Colloid & Interface Science, 18(4), 249-256.

Nicorescu, I., Loisel, C., Vial, C., Riaublanc, A., Djelveh, G., Cuvelier, G., & Legrand, J. (2008). Combined effect of dynamic heat treatment and ionic strength on denaturation and aggregation of whey proteins – Part I. Food Research International, 41(7), 707-713.

Papiz, M., Sawyer, L., Eliopoulos, E., North, A., Findlay, J., Sivaprasadarao, R., Jones, T., Newcomer, M., & Kraulis, P. (1986). The structure of β-lactoglobulin and its similarity to plasma retinol-binding protein. Nature, 324(6095), 383-385.

Parris, N., Purcell, J. M., & Ptashkin, S. M. (1991). Thermal denaturation of whey proteins in skim milk. Journal of agricultural and food chemistry, 39(12), 2167-2170.

Pelan, B., Watts, K., Campbell, I., & Lips, A. (1997). The stability of aerated milk protein emulsions in the presence of small molecule surfactants. Journal of Dairy Science, 80(10), 2631-2638.

Pelan, B. M. C., Watts, K. M., Campbell, I. J., & Lips, A. (1997). The Stability of Aerated Milk Protein Emulsions in the Presence of Small Molecule Surfactants. Journal of Dairy Science, 80(10), 2631-2638.

Rahman, A., & Sherman, P. (1982). Interaction of milk proteins with monoglycerides and diglycerides. Colloid and Polymer Science, 260(11), 1035-1041.

Raikos, V. (2010). Effect of heat treatment on milk protein functionality at emulsion interfaces. A review. Food Hydrocolloids, 24(4), 259-265.

Roman, J. A., & Sgarbieri, V. C. (2006). The hydrophilic, foaming and emulsifying properties of casein concentrates produced by various methods. International Journal of Food Science and Technology, 41(6), 609-617.

Rosen, M. J., & Kunjappu, J. T. (2012). Surfactants and interfacial phenomena: John Wiley & Sons.

Sagis, L. M., & Fischer, P. (2014). Nonlinear rheology of complex fluid–fluid interfaces. Current Opinion in Colloid & Interface Science, 19(6), 520-529.

San Martin-González, M. F., Roach, A., & Harte, F. (2009). Rheological properties of corn oil emulsions stabilized by commercial micellar casein and high pressure homogenization. LWT - Food Science and Technology, 42(1), 307-311.

Sánchez, C. C., & Patino, J. M. R. (2005). Interfacial, foaming and emulsifying characteristics of sodium caseinate as influenced by protein concentration in solution. Food Hydrocolloids, 19(3), 407-416.

Scott, L. L., Duncan, S. E., Sumner, S. S., & Waterman, K. M. (2003). Physical properties of cream reformulated with fractionated milk fat and milk-derived components. J Dairy Sci, 86(11), 3395-3404.

Shankaran, P. I., & Chinnaswamy, A. (2019). Instant coffee foam: An investigation on factors controlling foamability, foam drainage, coalescence, and disproportionation. Journal of Food Process Engineering, 42(6), e13173.

Smits, P., & Van Brouwershaven, J. H. (1980). Heat-induced association of β-lactoglobulin and casein micelles. Journal of Dairy Research, 47(3), 313-325.

Surel, C., Foucquier, J., Perrot, N., Mackie, A., Garnier, C., Riaublanc, A., & Anton, M. (2014). Composition and structure of interface impacts texture of O/W emulsions. Food Hydrocolloids, 34, 3-9.

Swaisgood, H. E. (1982). Chemistry of milk protein. Developments in dairy chemistry, 1, 1-59.

Tamime, A. Y. (2009). Dairy fats and related products: John Wiley & Sons.

Timasheff, S. N., & Townend, R. (1962). Structural and Genetic Implications of the Physical and Chemical Differences Between β-Lactoglobulins A and B. Journal of Dairy Science, 45(2), 259-266.

Tomas, A., Paquet, D., Courthaudon, J. L., & Lorient, D. (1994). Effect of Fat and Protein Contents on Droplet Size and Surface Protein Coverage in Dairy Emulsions. Journal of Dairy Science, 77(2), 413-417.

van Kempen, S. E., Schols, H. A., van der Linden, E., & Sagis, L. M. (2013). Non-linear surface dilatational rheology as a tool for understanding microstructures of air/water interfaces stabilized by oligofructose fatty acid esters. Soft Matter, 9(40), 9579-9592.

van Lent, K., Le, C. T., Vanlerberghe, B., & Van der Meeren, P. (2008). Effect of formulation on the emulsion and whipping properties of recombined dairy cream. International Dairy Journal, 18(10-11), 1003-1010.

Walstra, P. (1990). On the stability of casein micelles. Journal of Dairy Science, 73(8), 1965-1979.

Walstra, P., Wouters, J. T., & Geurts, T. J. (2005). Dairy science and technology: CRC press.

Wan, Z., Yang, X., & Sagis, L. M. (2016). Contribution of Long Fibrils and Peptides to Surface and Foaming Behavior of Soy Protein Fibril System. Langmuir, 32(32), 8092-8101.

Wilde, P., Mackie, A., Husband, F., Gunning, P., & Morris, V. (2004). Proteins and emulsifiers at liquid interfaces. Adv Colloid Interface Sci, 108, 63-71.

Wu, S., Wang, G., Lu, Z., Li, Y., Zhou, X., Chen, L., Cao, J., & Zhang, L. (2016). Effects of glycerol monostearate and Tween 80 on the physical properties and stability of recombined low-fat dairy cream. Dairy Science & Technology, 96(3), 377-390.

Wüstneck, R., Krägel, J., Miller, R., Wilde, P., & Clark, D. (1996). The adsorption of surface-active complexes between β-casein, β-lactoglobulin and ionic surfactants and their shear rheological behaviour. Colloids and Surfaces A: Physicochemical and Engineering Aspects, 114, 255-265.

Zhou, X., Chen, L., Han, J., Shi, M., Wang, Y., Zhang, L., Li, Y., & Wu, W. (2016). Stability and physical properties of recombined dairy cream: Effects of soybean lecithin. International Journal of Food Properties, 20(10), 2223-2233.

Chapter 2

Bulk and interfacial properties of milk fat emulsions stabilized by whey protein isolate and whey protein aggregates

Abstract

Whey protein is widely used in the food industry as an emulsion stabilizer because of its outstanding emulsifying ability. Recent studies have shown that heat-induced whey protein aggregates may also have potential to stabilize emulsions. The interfacial behavior of whey protein and whey protein aggregates adsorbed at the milk fat-water interface has not been well investigated, especially not in the nonlinear regime, which is highly relevant for the preparation of products such as recombined dairy cream.

In this study, the interfacial properties of milk fat-water interfaces stabilized by whey protein isolate (WPI) and whey protein aggregates (WPA) at different bulk concentrations (0.1 wt% - 4.0 wt%) were studied by Large Amplitude Oscillatory Dilatation (LAOD). Lissajous plots were used to analyze the nonlinear response of the interfaces as a function of strain amplitude and frequency. The elastic modulus was quantified based on the tangent modulus at zero instantaneous strain in expansion and in compression. Bulk stability of creams stabilized with the mentioned proteins was studied by determining creaming rate, droplet size distribution, ζ-potential and viscosity of the continuous phase.

At low concentrations (<2.0 wt%) WPI-stabilized cream had smaller oil droplets than WPA-stabilized cream, indicating that at these concentrations WPI had better emulsifying ability. For concentrations higher than 2.0 wt%, WPA was a better emulsifier in terms of creaming stability because of the higher viscosity of the continuous phase of the emulsions. Both WPI and WPA could prevent coalescence equally well if the concentration was higher than 0.5 wt%. LAOD measurements showed that at a protein concentration of 0.1 wt% there was little difference between WPI- and WPA-stabilized interfaces. At 4.0 wt%, WPI showed abrupt intra-cycle yielding followed by a predominantly viscous behavior at large expansion. The WPA interfacial layer had a larger maximum linear strain, and showed a more gradual softening in expansion and mild strain hardening in compression. We hypothesize that WPI formed denser and more brittle (quasi-) 2d structures at the interface, while the interfaces formed by WPA might have a thicker and more stretchable 3d structure. The WPA-stabilized emulsion was less resistant to coalescence upon drastic stirring, which can be explained with

its different large deformation behavior, and is relevant for applications where the cream is subjected to large deformations (whipping or stirring).

2.1. Introduction

Kinetic stability of oil-in-water (o/w) emulsions has been a topic of considerable interest for a long time. A frequent aim of studies on this subject is to link aspects like creaming rate, droplet size distribution and viscosity of the continuous phase to the composition of the continuous phase and/or properties of the interface between the two immiscible phases. Low molecular weight surfactants or proteins are the most frequently used stabilizers for food emulsions. For small surfactants, the Gibbs-Marangoni effect is the main mechanism of stabilization of an interface (Tadros, Izquierdo, Esquena, & Solans, 2004). Proteins adsorb at the interface more slowly than low molecular weight surfactants because of their larger molecular size and complex structure. After emulsion formation, proteins form viscoelastic interfacial layers that, apart from mechanical stabilization, can provide steric and electrostatic repulsion among emulsions droplets. This way, several instability phenomena could be retarded (Damodaran, 2005; E. Dickinson, 1999; Dickinson, 2001; Wilde, 2000). Different proteins contribute differently to emulsion properties, mainly because of differences in the interfacial structures they form and in the interfacial composition (Dalgleish, 2006).

Milk fat based emulsions, such as recombined dairy cream and recombined milk, are a group of emulsions of increasing economic interest. In the production of these emulsions, anhydrous milk fat is mixed with a solution of non-fat milk solids, and subsequently homogenized. Compared with other emulsions, milk fat based emulsions have some potential differences, which mainly result from the complicated chemical composition of milk fat. Milk fat has a wide variety of triglycerides containing fatty acids with varying levels of saturation (Yener & van Valenberg, 2019), and bimodally distributed in terms of carbon numbers (Yener, et al., 2019). Because of the presence of short-chain fatty acids in the triglycerides, but also of aldehydes, ketones and lactones, milk fat has a unique flavor and cannot easily be replaced by other animal fats or plant oils (Mortensen, 2016).

However, in contrast to milk fat globules in natural milk, which have substantial long-time stability imparted by the milk fat globule membranes,

the milk fat droplets in recombined dairy cream tend to be much less stable, and additional stabilizers need to be added to improve emulsion stability. Several stabilizers have been proposed for this purpose, such as proteose-peptone, glycerol monostearate, tween 80, lecithin and phospholipid-enriched dairy products. Most of the studies on the effect of the mentioned components in recombined milk fat emulsions focused on whipping properties (Fredrick, et al., 2013; Han, et al., 2018; Phan, Moens, Le, Van der Meeren, & Dewettinck, 2014; van Lent, Le, Vanlerberghe, & Van der Meeren, 2008; Vanderghem, Danthine, Blecker, & Deroanne, 2007) and little on the macroscopic stability of the system as a function of composition (Fredrick, et al., 2013; Vanderghem, et al., 2007; S. Wu, et al., 2016; Zhou, et al., 2016). Studies on milk fat-water interfaces are still scarce, in spite of the important role of interfacial properties in milk fat emulsion stability, both under quiescent conditions and during whipping.

Whey protein is widely used in the food industry, not only because it contains all essential amino acids and is well digestible (Hoffman & Falvo, 2004), but also because of its good emulsifying ability. The physicochemical properties of whey protein and its applications in emulsion are clearly discussed in several reviews (Damodaran, 2005; Nicolai, Britten, & Schmitt, 2011). Many studies have been devoted to the interfacial properties of whey protein-stabilized interfaces (Davis & Foegeding, 2004; Petkov, Gurkov, Campbell, & Borwankar, 2000; Rodríguez Patino, Rodríguez Niño, & Sánchez, 1999; Wooster & Augustin, 2007), Most of these either focused on air-water interfaces or on plant oil-water interfaces, and very few studies are available on the interfacial properties in the large deformation (i.e. nonlinear response) regime. However, during manufacturing (e.g. homogenization, pumping, whipping) the droplets in emulsions are routinely subjected to large deformations. Consequently, studying the interfacial properties of oil-water interfaces at large and fast dynamic strains is extremely relevant, and for the dynamic stability of emulsions it is surely more relevant than small amplitude oscillatory deformations at low frequencies. Lissajous plots are a powerful tool to study the interfacial properties of protein-stabilized interfaces in the nonlinear regime and have already been utilized in several studies. Schröder, Berton-Carabin, Venema, and Cornacchia (2017); Wan, Yang, and Sagis (2016) Chen, et al. (2017) have studied the interfacial properties of interfaces stabilized by whey protein hydrolysates, soy protein fibrils and casein micelles, respectively, using large amplitude oscillatory

dilatations. The anhydrous milk fat-water interface has so far not been studied with this approach.

In recent decades, several studies have appeared in which the effects of modifications of native whey proteins, such as (partial) hydrolyzation, enzymatic modification, or heat induced aggregation, on the emulsifying properties, were investigated. Some studies claim that after heating between 60 and 90 °C, whey protein will lose its emulsifying ability to a great extent (Dybowska, 2011; Millqvist-Fureby, Elofsson, & Bergenståhl, 2001). However, according to Dybowska (2011); Nicolai and Durand (2013), whey protein aggregates prepared by controlled heat treatment can improve emulsion stability. Dybowska (2011) hypothesized that the improved stability is the result of the formation of thicker interfacial layers around the oil droplets. This opinion is supported by transmission electron micrographs made by Foley and O'Connell (1990). In summary, although the emulsifying ability of whey protein aggregates is worse than that of native whey protein, aggregates can apparently still stabilize emulsions, mainly because of the interfacial structures they form. The mechanical properties of these interfacial structures have not been well studied. Recently, the application of whey protein microgel particles in emulsion stabilization has also attracted much attention. Microgels are claimed to adsorb at the interface to form Pickering emulsions, and efficiently prevent coalescence. Whey protein microgels are made without cross-linking agents (Schmitt, et al., 2010), and are promising materials to encapsulate emulsions to delay lipid digestion (Sarkar, et al., 2016) or for drug delivery (Jiang, Chen, Deng, Suuronen, & Zhong, 2014). A few studies have investigated the effects of pH, ionic strength, protein concentration on the stability of emulsions stabilized by whey protein microgels and on the microstructure of the interfaces (Destribats, Rouvet, Gehin-Delval, Schmitt, & Binks, 2014; J. Wu, et al., 2015). Again, the mechanical properties of these structures at the interface have not been investigated in detail. In particular, data in the nonlinear response regime are lacking, and the relation between (nonlinear) interfacial properties and emulsion stability under quiescent conditions and far from equilibrium conditions still needs to be explored. Considering the application of plant protein is quickly gaining interest nowadays, an accurate characterization of the properties of dairy ingredients provides benchmarks for future studies on non-dairy materials.

The aim of the present study was to investigate the interfacial properties of anhydrous milk fat-water interfaces stabilized by native whey protein (WPI) and heat-induced aggregates (WPA), and link these properties and bulk properties of the continuous phase to the stability of model milk fat emulsions at quiescent and dynamic conditions. The interfacial properties of anhydrous oil-water interfaces were studied by large amplitude oscillatory dilatation (LAOD). Lissajous plots were utilized to characterize the nonlinear response of WPI- and WPA-stabilized interfaces at different bulk concentrations (0.1 wt% and 4.0 wt%). The bulk stability of the milk fat emulsion was studied in terms of droplet size distribution, viscosity of the continuous phase, creaming rate, and ζ-potential. The stability of the milk fat emulsions in dynamic conditions was also investigated by subjecting the emulsions to vigorous stirring, and monitoring the effects of this processing step on emulsion stability.

2.2. Materials and methods

2.2.1. Materials

Anhydrous milk fat was kindly donated by FrieslandCampina (Wageningen, Netherlands). Whey protein isolate (WPI, BiPRO, 88.8% protein content) was purchased from Agropur (Canada). According to the specification sheet provided by Agropur, the lactose and calcium content of WPI were 0.2 wt%, and 0.1 wt%, respectively. Florisil (60-100 mesh), 8-anilino-1-naphtalenesulfonic acid ammonium salt (ANS), sodium dodecyl sulfate (SDS) and sodium azide were purchased from Sigma (Netherlands). The phosphate buffer (PB, 0.01M, pH 7.0) used to measure protein hydrophobicity was made from sodium dihydrogen phosphate monohydrate ($NaH_2PO_4 \cdot H_2O$) and di-sodium hydrogen phosphate dihydrate ($Na_2HPO_4 \cdot 2H_2O$) (Merck, Germany).

2.2.2. Methods

2.2.2.1. Sample preparation

2.2.2.1.1. Purification of anhydrous milk fat

Florisil was desiccated overnight at 120 ^{o}C in an oven, then cooled down to room temperature. Anhydrous milk fat was melted at 60 ^{o}C and mixed with 10 wt% Florisil. The mixture was stirred while being heated in water bath set

at 60 ^{o}C. Samples of anhydrous milk fat were taken every hour to measure the interfacial tension of a milk fat - Milli-Q water interface, until a constant value was obtained. Finally, Florisil was removed from the milk fat using filter papers (Whatman, Grade 4, diam.90mm, England). The purified anhydrous milk fat was stored at -20 ^{o}C.

2.2.2.1.2. Whey protein solutions and whey protein aggregate (WPA) solutions

WPI powder was dissolved in Milli-Q water overnight to obtain a 6.25 wt% WPI solution; 0.02 wt% sodium azide was added to prevent spoilage. The WPI solution was centrifuged for 30 min at 10^4 g to remove non-dissolved material (most likely insoluble aggregates). The supernatant was subsequently filtered by a syringe filter with pore size 0.45 µm and then stored as a WPI stock solution. The protein content of the stock solution was 5.49 wt%, as determined by Dumas (conversion coefficient: 6.25) and the pH was 6.8-7.0. Subsequently, the stock solution was diluted with Milli-Q water to make samples with concentrations of 0.1, 0.2, 0.5, 1.0, 2.0 and 4.0 wt%.

The WPA aggregate dispersion was made from WPI stock solution. The stock solution was poured into a glass 250 mL beaker, and subjected to heat treatment in a water bath (80 ^{o}C, 30 min). During the heat treatment, the solution was stirred (300 rpm) with a magnetic stirrer (Framo, M20/1, Germany). The stirring bar had a length of 4 cm. Afterwards, the sample was cooled down by ice water, and diluted by Milli-Q water to obtain samples with concentrations of 0.1, 0.2, 0.5, 1.0, 2.0, and 4.0 wt%.

2.2.2.1.3. Cream preparation

Cream samples with different stabilizer concentrations, both WPI and WPA, were prepared. The anhydrous milk fat was melted at 60 ^{o}C, then poured into the protein solutions to produce a mixture with 20 wt% fat. The mixture was kept at 60 ^{o}C in a water bath for 15 min. Subsequently, it was pre-homogenized using an Ultra-Turrax (IKA T25, Germany) at 6000 rpm, and finally homogenized by two-steps homogenization (Delta Instruments, Netherlands). Pressure was set at 100 bar for the first step and 40 bar for the second step. Samples were sealed in blue cap bottles and stored overnight at room temperature before analysis.

2.2.2.2. Characterization of the protein samples

2.2.2.2.1. Particle size distribution

The particle size distribution of WPI or WPA was determined using a Malvern Zetasizer Nano-ZS (Malvern Instruments Ltd, United Kingdom) at 20 °C, with cell type DTS0012. Protein solutions were filtered by syringe filter with pore size 0.45 μm and subsequently diluted to 0.4 wt% with Milli-Q water. The refractive and absorption indices were 1.450 and 0.001 respectively. The refractive index of dispersant (water) was 1.330. Before each test, samples were equilibrated for 2 min.

2.2.2.2.2. Hydrophobicity

Protein surface hydrophobicity was measured with methods described by Lam and Nickerson (2015). WPI solutions were diluted with PB buffer (0.01 M, pH 7.0) to obtain a concentration range from 0.02 wt% to 0.1 wt%. WPA solutions were diluted to a range from 0.005 wt% to 0.04 wt%. For each protein sample, 1 mL was added in a cuvette (10×10×45mm, SARSTEDT, Germany) and mixed with 10 μL of 8 mmol/L 8-anilino-1-naphtalenesulfonic acid ammonium salt (ANS) solution (in 10 mM PB, pH 7.0). The mixture was incubated in the dark, while being shaken for 1 h. PB-ANS without protein was used as a blank, and PB-protein was the control. Fluorescence was measured using a Fluorimeter (PerkinElmer, UK) at excitation wavelength of 390 nm, and emission wavelength of 470 nm. The slit width was set at 5 nm. The intensities of blank and control were subtracted for each protein sample to obtain the net fluorescence. The slope of the net fluorescence as the function of protein concentration was used to quantify the extent of hydrophobicity. All measurements were made in triplicate.

2.2.2.3. Characterization of the milk fat emulsions

2.2.2.3.1. Creaming rate

A LUMiFuge (LUM LUMGmbH, Germany) was used to test the creaming behavior of samples at a constant gravitational acceleration value at room temperature (20 °C). The samples were centrifuged at 1000 g for 2600 s, which is equivalent to approximately one month of storage at 1 g. The light factor was set to 1.0. The measurement time interval was equal to 10 s. The creaming rate was calculated using the LUMiFuge Front Tracking module,

and the tracked transmission value was 25%. The creaming rate v is defined as:

$$v = \frac{|\Delta L|}{\Delta t} \quad \text{Eq. 2.1}$$

where, ΔL is the change of position of the layer with 25% transmission, in the time period Δt. Only the linear part of the curve of layer position versus time was considered.

In order to analyze the degree of coalescence or aggregation during centrifugation, samples were carefully taken from the tubes with a syringe and their droplet size distribution was measured as described here below.

2.2.2.3.2. Oil droplet size distribution

The oil droplet size distribution of the emulsions was tested using a MasterSizer 2000 (Malvern Instruments Ltd., UK) with static light scattering. The cream was dispersed in distilled water until the obscuration was 15%. The refractive indices used for the dispersed phase (anhydrous milk fat) and dispersant were 1.461 and 1.330, respectively. The absorption index was 0.01. The weight-volume mean oil droplet diameter $d_{4,3}$ (μm) was calculated with Eq. 2.2.

$$d_{4,3} = \frac{\sum n_i {d_i}^4}{\sum n_i {d_i}^3} \quad \text{Eq. 2.2}$$

where n_i is the number of particles with the same diameter, and d_i is the particle size.

For checking the degree of aggregation of droplets, the oil droplet size distribution of emulsion samples with added SDS was also tested. Samples were mixed in a 1:1 volume ratio with 1.0 wt% SDS solution, and then 100 times diluted by distilled water, before measuring the droplet size distribution.

2.2.2.3.3. Viscosity of continuous phase

The viscosity of continuous phase was tested with an Ubbelodhe capillary viscometer with constant 0.01078 $mm^2 \cdot s^{-2}$ (SI Analytics GmbH, Germany) at 20 °C. The dynamic viscosity η (mPa·s) can be calculated with Eq. 2.3.

$$\eta = Ct\rho \cdot 10^{-3} \quad \text{Eq. 2.3}$$

where C is the constant of the Ubbelodhe capillary viscometer ($mm^2 \cdot s^{-2}$), t is the time taken by the liquid front to pass from the upper to lower marks (s). ρ is the density of protein solution ($kg \cdot m^3$).

2.2.2.3.4. ζ-potential

The ζ-potential of emulsion droplets was measured using a ZetaSizer Nano ZS (Malvern Instruments Ltd., UK). The samples were diluted 1000 times with Milli-Q water. Each measurement was performed 3 times at room temperature (20 °C). The refractive and absorption indices used for the oil droplets were set to 1.461 and 0.001 respectively. Milli-Q water was used as dispersant with refractive index 1.330 and dielectric constant 80.4. The cell type was DTS1070.

2.2.2.3.5. Stability of cream at dynamic conditions

Recombined dairy creams made with 4.0 wt% WPI or WPA were put in a water bath to warm up to 40 ^{o}C. Then the samples were subjected to stirring with a Turrax (IKA T25, Germany) at 3000 rpm for 15 min. During the described experiment, the droplet size distribution of the samples was measured every 5 min. Tests were also conducted at different stirring speeds, i.e. 3000, 9000 and 10000 rpm.

2.2.2.4. Interfacial properties

2.2.2.4.1. Interfacial tension measurements

The interfacial tension of the purified milk fat-water interface was determined using a Tracker Automated Droplet Tensiometer (ADT) (Teclis, France). The purified anhydrous milk fat was poured into the cuvette of this system. A temperature control module was used to keep the temperature of the fat at 40 ^{o}C. A pendent drop of water or the protein samples was formed at the tip of a motored syringe (Trajan, Australia), submerged in the oil phase. The surface area of the droplet was 20 mm^2. The density of the droplet fluid and anhydrous milk fat at 40 ^{o}C were determined using a density meter (DMA 5000, Anton Paar, Germany), and the values were 0.9922 g/mL and 0.9041 g/mL, respectively. The time evolution of the interfacial tension was monitored for 1 h.

2.2.2.4.2. Large amplitude oscillatory dilatation (LAOD)

After monitoring the interfacial tension for 1 h, sinusoidal oscillatory area deformations were applied to the droplet interface. The oscillation frequency was set as 0.005 Hz, and an amplitude sweep was performed in which the amplitude was set to 5, 10, 15, 20, 25 and 30%. For each amplitude, 5 cycles of oscillation were applied, followed by 300 s of recovery. The middle 3 cycles were used for constructing Lissajous Plots. Lissjaous Plots were made using the method described by Sagis and Fischer (2014). According to this method, the surface pressure, (π), is plotted against the relative area deformation (γ), in a cyclic plot. The deformation and surface pressure were calculated using Eq. 2.4 and Eq. 2.5:

$$\gamma = \frac{A_t - A_0}{A_0} \qquad \text{Eq. 2.4}$$

$$\pi = \sigma_t - \sigma_0 \qquad \text{Eq. 2.5}$$

where A_t and σ_t are the interfacial area and interfacial tension at time *t*, and A_0 and σ_0 are the initial interfacial area and interfacial tension. The Lissajous Plots were analysed in terms of the dilatational moduli at minimum and large extension (E_{dEM} and E_{dEL}, respectively), and the dilatational moduli at minimum and large compression (E_{dCM} and E_{dCL}, respectively), introduced earlier by van Kempen, Schols, van der Linden, and Sagis (2013) and based on a scheme introduced by Ewoldt, Hosoi, and McKinley (2008).

Once the amplitude sweep was completed, a new droplet was formed and the test was repeated at a higher frequency. The frequencies applied in this study were 0.005 Hz, 0.01 Hz, 0.02 Hz, 0.05 Hz and 0.1 Hz.

2.2.2.5. Statistical analysis

In this study, all samples were prepared at least in duplicates, and all tests were conducted at least twice. For the samples with the same protein, statistical differences among concentrations were checked by ANOVA analysis, followed by Tukey's post hoc test, and significant differences were marked with different letters. For the samples with the same concentration, statistical differences between WPI and WPA were checked by T-test, and significant differences were marked with an asterisk (*). All analyses were conducted by IBM SPSS 25 (IBM SPSS Inc., Chicago, IL, USA). Significance was set as $P < 0.05$.

2.3. Results and discussion

2.3.1. Hydrophobicity and particle size distribution of the protein samples

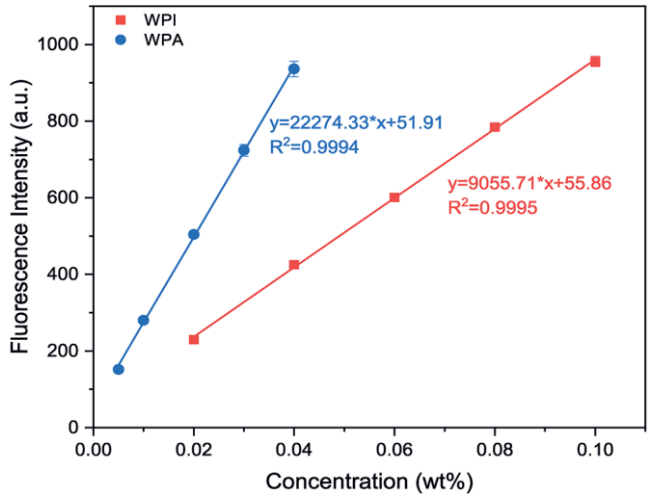

Fig. 2.1. Fluorescence intensity of WPI-ANS or WPA-ANS in PB buffer (0.01 M, pH 7.0, 20°C) as function of protein concentrations and their linear fits. The slope of the curve represents the relative hydrophobicity of the proteins.

As shown in Fig. 2.1, the slope of WPA was much higher than WPI, which meant that WPA was more hydrophobic than WPI. This is the result of the formation mechanism of WPA (Aguilera, 1995; Spiegel, 1999; Wijayanti, Bansal, & Deeth, 2014). First of all, during heat treatment globular proteins unfolded and reactive groups were exposed. The unfolded molecules aggregated, but the shear forces induced by stirring prevented the formation of a connected gel network, and individual protein aggregates were produced. As a result of the unfolding, more hydrophobic groups were exposed in WPA compared to native whey protein.

The scattering intensity scales with the size of particles to the power six, and the scattering of smaller particles can be somewhat obscured by the scattering of a few larger particles (Fig. S 2.1). Therefore, the results are shown in terms of the volume-weight distribution rather than the intensity-weight distribution. As shown in Fig. 2.2, the size of WPI was smaller than 10 nm and distributed around 2 nm, while the peak of the size distribution of WPA was around 20 nm. These size distributions of WPI and WPA are in line

with the results from Yang, Thielen, Berton-Carabin, van der Linden, and Sagis (2020).

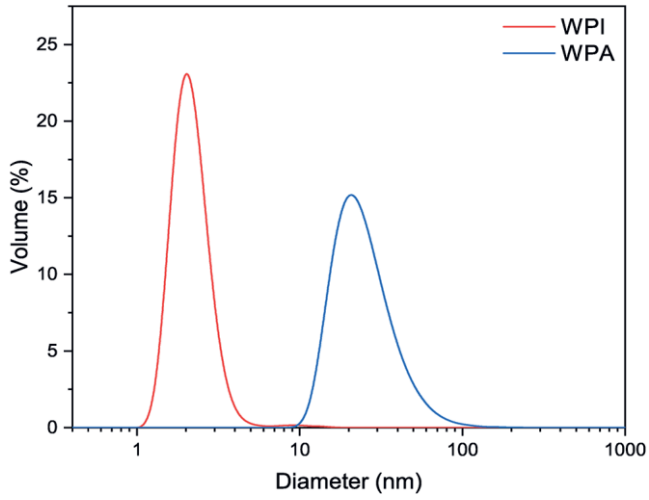

Fig. 2.2. Volume-weighted size distribution of WPI and WPA at room temperature (20 °C). Protein samples were diluted to 0.4 wt% with Milli-Q water before testing.

2.3.2. Bulk stability

To explore whether aggregation of the protein can affect emulsion stability, the creaming rate of the droplets, their size distribution over time, their ζ-potential, and the effects of continuous phase viscosity on creaming were studied for milk fat emulsions stabilized by either WPI or WPA (at various concentrations). The emulsion tests were done with both purified and non-purified milk fat (results for the latter are included in the supplementary information; Fig. S 2.2 - Fig. S 2.5). There were only minor differences in stability between the two systems, which were mainly observed at low protein concentrations. At high protein concentrations, purified or non-purified milk fat emulsion systems had no difference in stability. Apparently, at low protein concentrations, the surface active components in anhydrous milk fat like mono- or di-glycerides could compete with proteins for adsorption at the interface (Eric Dickinson, 1999; Dickinson & Tanai, 1992; Granger, Barey, Combe, Veschambre, & Cansell, 2003), and as a result, the stability was influenced by these surface active components. At a high protein concentration, the effects of proteins became more dominant in the

system and as a result, the differences between emulsions with purified milk fat or non-purified milk fat diminished. Therefore, the data of the interfacial characterization of the samples with purified milk fat and a high protein concentration can also be used for interpreting stability data of the non-purified milk fat emulsions.

2.3.2.1. Creaming rate

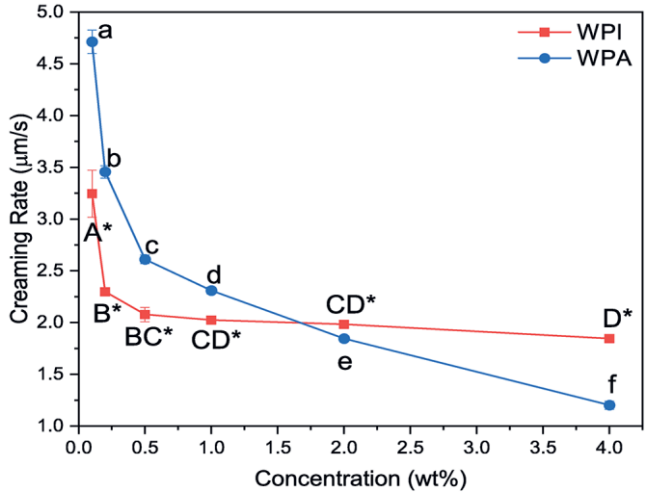

Fig. 2.3. Creaming rate of milk fat emulsions stabilized with WPI or WPA as function of protein concentrations, measured at room temperature (20 °C), and 10^3 g. An asterisk (*) is used to denote statistical differences between proteins at the same concentrations. Different letters mark the statistical differences between concentrations of the samples with the same protein.

The creaming rate of the emulsions decreased dramatically as the WPI or WPA concentration increased from 0.1 to 0.5 wt% (Fig. 2.3). Above 0.5 wt%, WPI-stabilized emulsions showed a nearly constant creaming rate. For WPA-stabilized emulsions, the creaming rate kept decreasing with increasing protein concentration. When the protein concentration was below 1.5 wt%, WPI-stabilized emulsions had a slower creaming rate than WPA-stabilized emulsions. Above 2.0 wt%, WPA-stabilized emulsions creamed more slowly than WPI-stabilized ones. To explain these observations we investigated the droplet size distribution of the emulsions (section 2.3.2.2) and the continuous phase viscosity of the samples (section 2.3.2.3).

2.3.2.2. Droplet size distribution

The oil droplet size distribution of fresh milk fat emulsions (0d) and of samples centrifuged under conditions simulating a storage of 30 days (30d) was measured with (+SDS) and without SDS. This surfactant was added to unveil the presence of oil droplet aggregates, which would be disrupted by it. Our results suggest that at concentrations of 0.1 wt% and 0.2 wt% neither WPI nor WPA could stabilize the emulsions. Fresh emulsions prepared with 0.1 wt% or 0.2 wt% WPI showed a single peak (Fig. 2.4). The 30d samples stabilized with these WPI concentrations had a bimodal distribution, while 30d+SDS showed a single peak, close to the original size distribution. Hence, for these emulsions the main destabilization mechanism was flocculation, and not coalescence. Similar behavior was observed for the samples with the same concentrations of WPA. However, during storage, coalescence or irreversible aggregation occurred in these emulsions, since the particle size distribution of the 30d WPA sample did not shift back to the original distribution after adding SDS. A significant shoulder remained at the right of the main peak.

At 0.5 wt% both WPI and WPA could stabilize the emulsions against coalescence or aggregation, as the droplet size distribution of the 30d samples and 0d samples overlapped. Compared with WPI, the use of WPA always led to the formation of larger oil droplets, especially when the concentration was lower than 2.0 wt%. This is an indication that WPA had a weaker emulsifying ability. Above 2.0 wt%, the difference in mean oil droplet size $d_{4,3}$ (Tab. 2.1) between WPI- and WPA-stabilized emulsions was negligible (<0.10 μm).

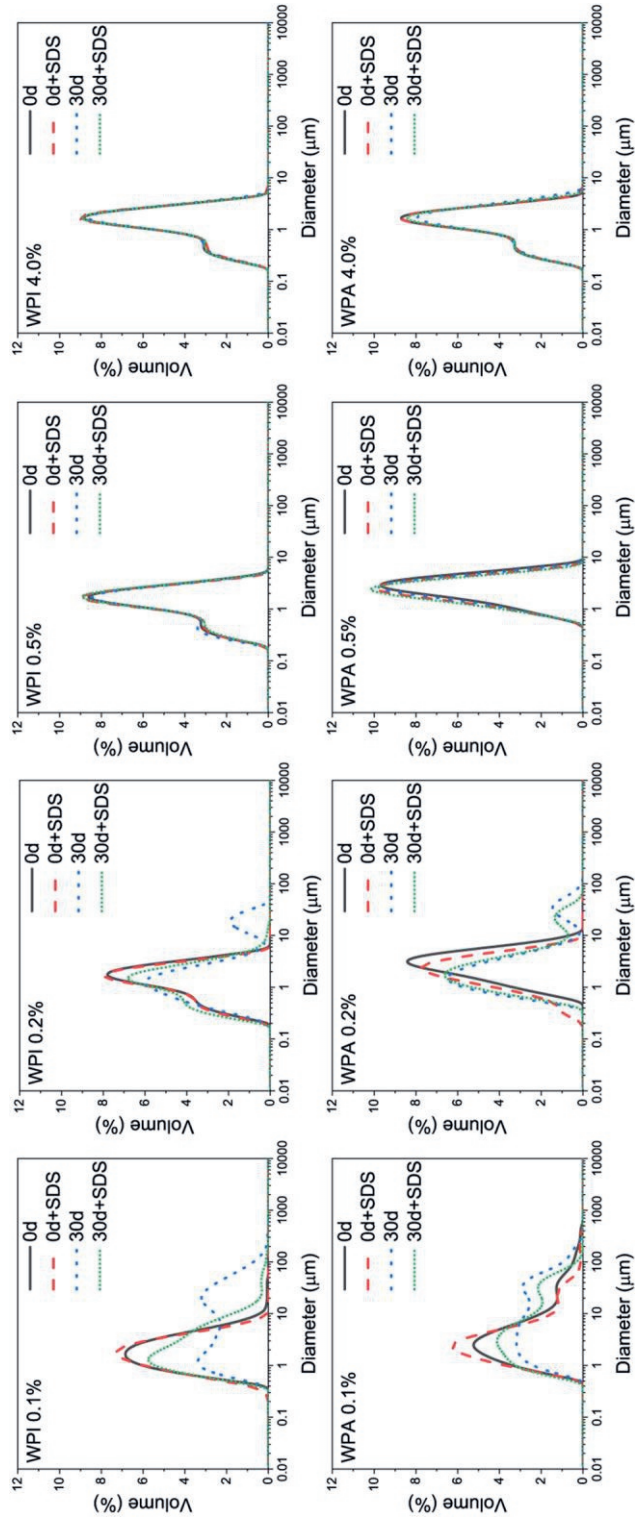

Fig. 2.4. Droplet size distribution of milk fat emulsions stabilized with WPI and WPA at various protein concentrations, including fresh samples (0d) with (+SDS) and without SDS, and samples after a simulated storage of 30 days (30d), with (+SDS) and without SDS.

Tab. 2.1. $d_{4,3}$ (µm) of fresh milk fat emulsions (0d) made from WPI or WPA. An asterisk (*) is used to indicate statistical differences between the two protein samples at the same concentrations. Different letters indicate statistical differences among different concentrations of the samples with the same protein.

Proteins	Concentrations (wt%)					
	0.1	0.2	0.5	1.0	2.0	4.0
WPI	2.31±0.29 ^{A*}	1.50±0.05 ^{B*}	1.42±0.07 ^{B*}	1.42±0.05 ^{B*}	1.39±0.04 ^{B*}	1.40±0.02 ^{B*}
WPA	13.00±3.76 ^{a}	2.92±0.10 ^{b}	2.63±0.01 ^{b}	1.92±0.05 ^{b}	1.49±0.01 ^{b}	1.37±0.01 ^{b}

2.3.2.3. Viscosity of the continuous phase

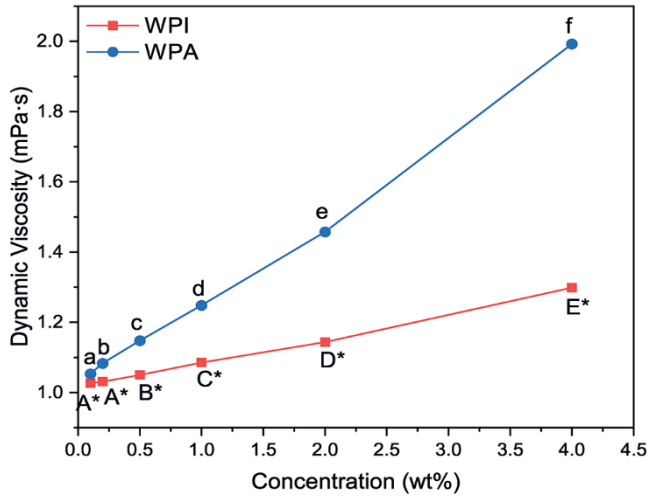

Fig. 2.5. Viscosity of WPI solutions and WPA dispersions at protein concentrations of 0.1 wt%, 0.2 wt%, 0.5 wt%, 1.0 wt%, 2.0 wt%, 4.0 wt%, at 20 °C. An asterisk (*) is used to indicate statistical differences between the two protein samples at the same concentrations. Different letters indicate statistical differences among different concentrations of the samples with the same protein.

With an increase in protein concentration, the viscosity of both WPI and WPA solutions increased. Fig. 2.5 shows that the viscosity of the WPA solution was significantly higher than that of the WPI solution, particularly at the highest concentrations. This implied that WPA was a more efficient thickener. Combined with the data of the mean oil droplet size, $d_{4,3}$, shown in Tab. 2.1, the viscosity differences between WPI solutions and WPA dispersions could explain the differences in creaming rate we observed in section 2.3.2.1. At low concentrations (0.1% wt-1.0 wt%), where the viscosities of the emulsions stabilized with the two proteins were still similar, the droplet size difference between the WPI- and WPA-stabilized emulsions was responsible for the higher creaming rate of the WPA emulsions. At higher concentrations (>1.0 wt%), the mean droplet sizes of the two emulsions were close, but the difference in viscosity of the continuous phase was much larger. As a result, the WPA emulsions had a lower creaming rate.

2.3.2.4. ζ-potential

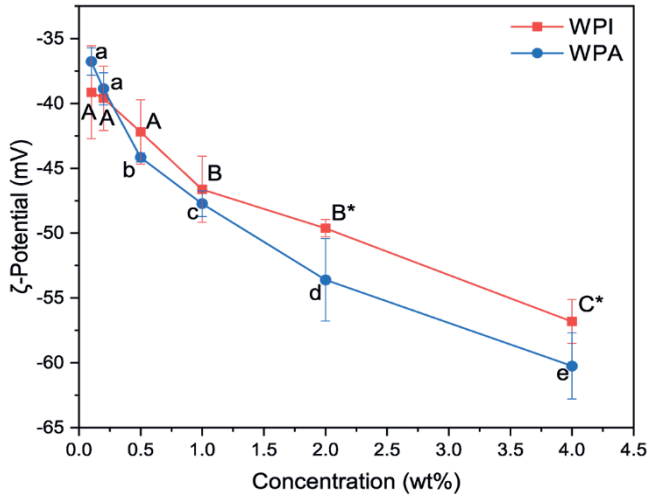

Fig. 2.6. ζ-potential of milk fat emulsions made with WPI or WPA at various protein concentrations, measured at 20 °C. The emulsions were 1000 times diluted by Milli-Q water before testing. An asterisk (*) is used to indicate statistical differences between the two protein samples at the same concentrations. Different letters indicate statistical differences among different concentrations of the samples with the same protein.

The pH of the milk fat emulsions was approximately neutral (around 7), and at this pH whey protein is negatively charged. Upon increasing protein concentration from 0.1 to 4.0 wt%, the ζ-potential of WPI-stabilized emulsions gradually and significantly ($P<0.05$) decreased from -39.13±3.59 mV to -56.82±1.68 mV (Fig. 2.6). In the same concentration range, the ζ-potential of WPA-stabilized emulsions decreased from -36.77±1.06 mV to -60.23±2.56 mV. Although at a concentration of 4.0 wt%, the values of the ζ-potential of the emulsions stabilized by the two proteins were significantly different, the difference was marginal (<5 mV), and we can conclude that differences in stability between the two emulsions were unlikely to be related to differences in electrostatic repulsion among droplets.

2.3.3. Interfacial properties

All measurements of interfacial properties were done with purified milk fat, as the surface tension of the interface between non-purified milk fat and the protein solutions was too low, resulting in detachment of the droplet from

the tip of the needle of the tensiometer. As a result of the much lower surface to volume ratio, tensiometry measurements are more sensitive to these impurities. As we pointed out above (section 2.3.2), the differences in macroscopic properties between purified and non-purified milk fat emulsions were negligible at higher protein concentrations, so interfacial data for purified milk fat can also be used for interpreting stability data of the non-purified milk fat emulsions.

2.3.3.1. Interfacial tension

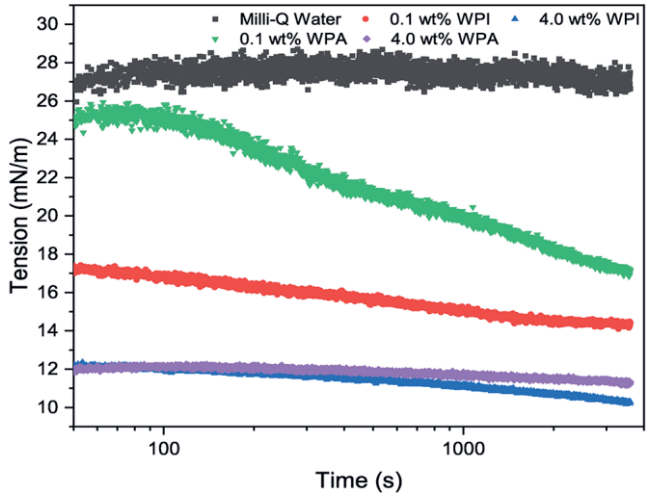

Fig. 2.7. Interfacial tension between anhydrous milk fat and a WPI solution or a WPA dispersion at 40 °C. Data before 50 s is not shown, since the droplet was not yet in thermal equilibrium with the continuous oil phase.

The interfacial tension as a function of time, from 50 s to 3600 s, is shown in Fig. 2.7. The data obtained before 50 s is not shown, because the droplets had not yet reached their target temperature of 40 °C, and were therefore not in thermal equilibrium with the continuous oil phase. At a concentration 0.1 wt%, WPI decreased the interfacial tension of the milk fat-water interface to a nearly constant value of about 15 mN/m in approximately 1000 s, while for WPA the interfacial tensions decreased much less and much more slowly, in spite of the fact that WPA has a higher surface hydrophobicity (see Fig. 2.1) and was therefore expected to more readily adsorb at the interface. It has been shown that molecular size can have a significant influence on the rate of adsorption (Beverung, Radke, & Blanch,

1999; Dybowska, 2011; Jung, Gunes, & Mezzenga, 2010; Sobhaninia, Nasirpour, Shahedi, & Golkar, 2017). Larger molecules and particles may diffuse towards and adsorb at the interface more slowly than smaller ones. Increased rigidity could also be a factor (Dybowska, 2011; Segall & Goff, 2002; Wijayanti, et al., 2014), since it would cause aggregates to unfold more slowly and to a lesser extent at the interface. Beverung, et al. (1999) showed that compared to smaller size proteins, larger molecules need a higher surface coverage to achieve the same decrease in interfacial tension. All these would explain why at a low concentration, WPA reduced interfacial tension much slower than WPI. When the concentration increased to 4.0 wt%, the initial diffusion-controlled phase could not be observed, which meant at a high protein concentration, the interface quickly became saturated with WPI or WPA, within the 50 s start-up phase in which thermal equilibrium was not yet attained. Once the interfaces have become saturated, WPI and WPA decrease the interfacial tension to a similar extent. This explains the nearly equal droplet size of the emulsions prepared at this protein concentration (Tab. 2.1 in section 2.3.2.2). During emulsion formation, convection contributed to the transfer of proteins to the interface, together with diffusion, quickly saturating the interfaces with proteins. Since WPI and WPA decreased interfacial tension to a similar extent at saturation, similar oil droplet size would be achieved in emulsion formation when the energy input was the same.

2.3.3.2. Large amplitude oscillatory dilatation

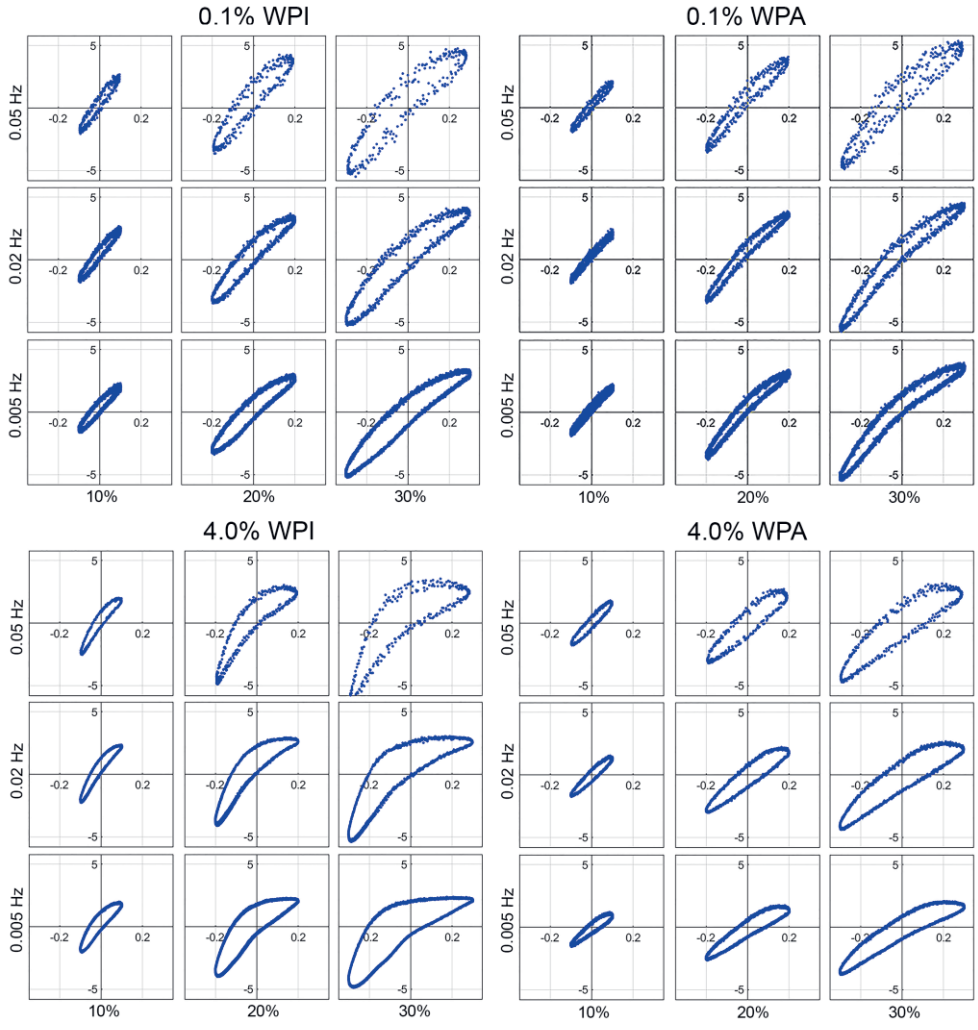

Fig. 2.8. Pipkin Plots showing the evolution of the surface pressure of WPI- and WPA-stabilized milk fat-water interfaces at protein concentrations of 0.1 and 4.0 wt%. Strain amplitude was varied from 10% to 30%. Frequency was varied from 0.005 Hz to 0.05 Hz.

In order to study the interfacial properties of WPI- and WPA-stabilized milk fat-water interfaces in the nonlinear regime, large amplitude oscillatory dilatational (LAOD) measurements were performed, including amplitude and frequency sweeps. The obtained Pipkin plots are shown in Fig. 2.8. In

general, the Lissajous plots became increasingly asymmetric with increasing amplitude, which meant that the response became progressively nonlinear. In expansion, strain softening was observed both for WPI- and WPA-stabilized interfaces, as evident from the decrease of the slope in the upper right quadrant of the plot. At a low concentration (0.1%) the response of both WPI- and WPA-stabilized interfaces was dominated by the elastic contribution (Fig. 2.8), since the Lissajous plots were very narrow. The plots for the WPA-stabilized interfaces were narrower, indicating that the structure at the interface had a lower loss tangent and was relatively more solid-like. The stiffness of the two interfaces was however comparable at this concentration. At a high concentration (4.0 wt%), the strain softening behavior was more pronounced for WPI-stabilized interfaces. Particularly at 30% deformation, the plots for these interfaces had a high initial slope at the start of the expansion part of the cycle (the lower left corner of the plot), followed by an abrupt change in the slope, after which the slope was near zero. This pointed to intra-cycle yielding, which meant that the structure had been disrupted to such an extent that it started to flow, and the response became predominantly viscous. Compared with WPI, WPA-stabilized interfaces had a milder and more gradual strain softening in expansion, and a larger maximum linear strain. So, although the two types of interfaces appeared to be similar in stiffness, the WPA-stabilized interfaces were more stretchable and less brittle than the WPI-stabilized interfaces.

The Lissajous plots were analyzed using a method introduced by Ewoldt, et al. (2008), and modified by van Kempen et al. (2013). The elastic modulus E_{dCM} (the tangent modulus in compression at minimum strain) and E_{dEM} (the tangent modulus in expansion at minimum strain) were calculated and plotted in Fig. 2.9. Additional plots for the modulus E_{dCM} (the tangent modulus in compression at minimum strain), E_{dCL} (the secant modulus in compression at largest strain) and E_{dEL} (the secant modulus in expansion at largest strain) are provided in the supplementary information (Fig. S *2.6* – Fig. S 2.8). For E_{dEM}, there was no difference between WPI- and WPA-stabilized interfaces at a low concentration (Fig. 2.9). However, at a high concentration, the value of E_{dEM} of the WPI-stabilized interface decreased substantially as a function of amplitude, from a maximum value of 18.0 mN/m to a value of 2.6 mN/m (when the frequency was 0.005 Hz). This clearly showed the yielding of the structure, in which the interfacial behavior changed from viscoelastic solid to viscoelastic liquid behavior. The stronger

frequency dependence observed for WPI at high strains could be attributed to an

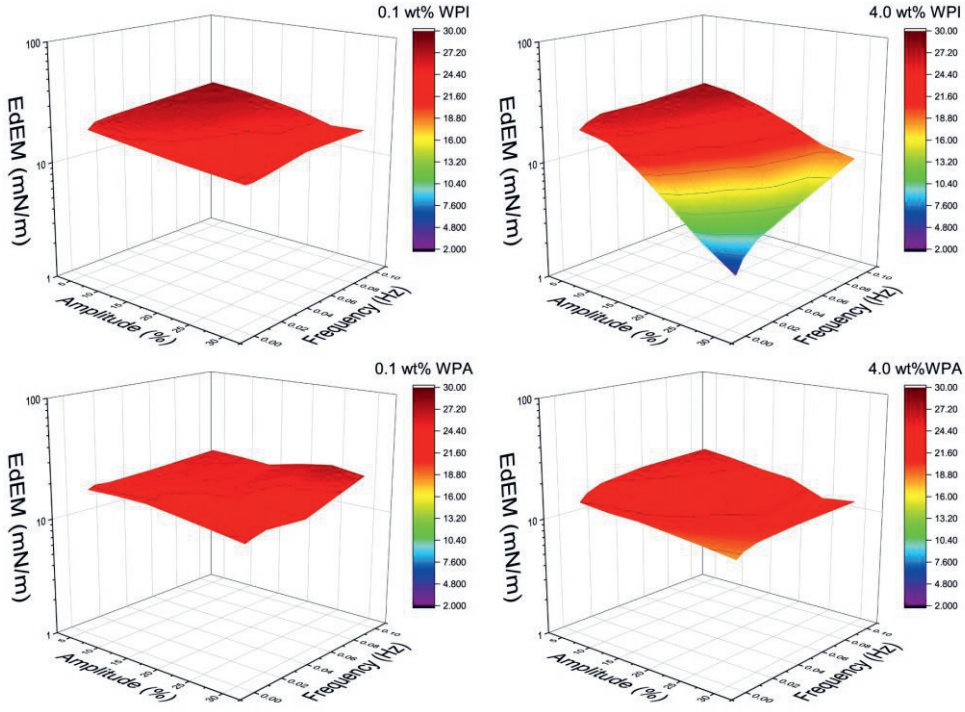

Fig. 2.9. E_{dEM} of WPI- and WPA-stabilized milk-fat-water interfaces at protein concentrations of 0.1 and 4.0 wt% as the function of strain amplitude and strain frequency.

increased mobility within the interface, which led to shorter relaxation times, and, as a result, the frequency range where the response was still frequency-dependent was shifted to higher frequencies. In contrast, the value of E_{dEM} of the WPA-stabilized interfaces showed a much smaller and more gradual decrease with increasing amplitude. This decrease was virtually independent of frequency, which implied that the interface retained a more viscoelastic solid like behavior, even at the highest amplitudes tested. At a high protein concentration, adsorption to and desorption from the interface could play a role in the response to oscillatory deformations. However, when plotting the elastic moduli as a function of frequency, in the linear regime, we observed a power law behavior ($E' \sim \omega^n$), with a value of the power n for WPI or WPA between 0.1 and 0.2 (Fig. S 2.9). This was significantly lower than the value

of n=0.5, predicted by the Lucassen van den Tempel model, for interfaces in which the response is dominated by diffusion between bulk and interface (Lucassen & Van Den Tempel, 1972; Sagis, et al., 2019). Combined with the low loss tangent (Tab. S1), the power law behavior we observed was indicative of an interface with a soft viscoelastic disordered solid structure, which implied that the response of WPI or WPA stabilized interfaces to dilatation was dominated by in-plane interactions.

Based on the facts that, 1) WPA has a larger size than WPI, 2) at 4.0 wt%, WPI showed abrupt intra-cycle yielding followed by a predominantly viscous behavior at large expansion, and 3) the WPA interfacial layer had a larger maximum linear strain, and showed a more gradual softening in expansion and mild strain hardening in compression, we formulate the hypothesis that WPI might form a denser and more brittle (quasi-) 2d interfacial structure, and WPA might form a coarser and thicker 3d interfacial structure (Fig. 2.10). For WPI, molecules were further compressed and concentrated during the compression, which resulted in a higher connectivity among molecules. Subsequently, during the expansion, the interface initially showed a solid elastic response, followed by yielding, which was evidenced by a steep initial slope in the expansion part of Lissajous plots, followed by a zero slope. For WPA, the coarser and thicker 3d structure led to a lower connectivity among aggregates. Consequently, the plots had a smaller initial slope and the interfaces retained more of their elastic behavior in the expansion part of the Lissajous plots, and only a gradual softening was found at the end of the expansion. These differences in structure between WPI and WPA-stabilized interfaces also implied that the WPI and WPA-stabilized emulsions may have differences at dynamic conditions. In the following, the stability of WPI and WPA-stabilized emulsions under dynamic conditions will be discussed in section 2.3.4.

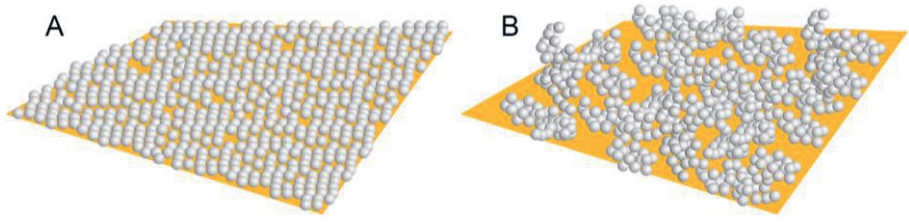

Fig. 2.10. Schematic representation of the (quasi-) 2d structure on oil-water interfaces formed by WPI (A), and the 3d structure formed by WPA (B).

2.3.4. Stability of the emulsions at dynamic conditions

The stability of the emulsions under dynamic conditions was tested by determining the droplet size distribution after stirring at various speeds and stirring times (Fig. 2.11). Microscopic images of the samples after stirring are shown in the supplementary information (Fig. S 2.10 and Fig. S 2.11). At a stirring speed of 3000 rpm, both WPI- and WPA-stabilized emulsions were stable against coalescence (data is not shown). The emulsions started to destabilize once the stirring speed was increased to 9000 rpm, where another peak at around 20 µm could be observed in the size distribution. At 9000 rpm, the difference between WPI- and WPA-stabilized emulsions was still negligible. However, at 10000 rpm WPA, compared with WPI, always had a slightly higher peak at 11 µm and a lower peak at 1.5 µm. This meant that the WPA-stabilized emulsion was somewhat less resistant to the strong stirring than WPI, although the difference was quite small.

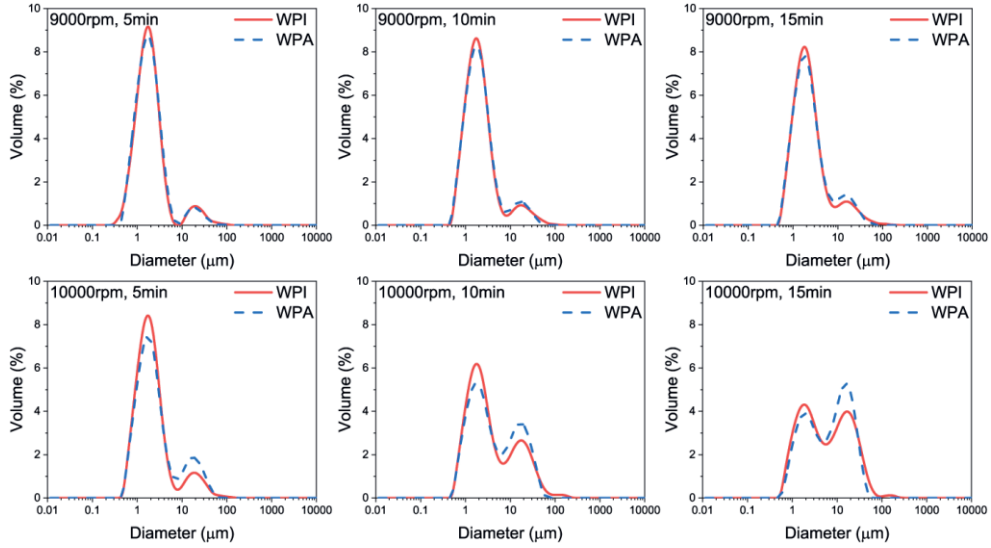

Fig. 2.11. Evolution of the droplet size distribution of emulsions made with 4.0 wt% WPI or WPA upon stirring at different speeds.

The results of section 2.3.3.2 proved that under dynamic conditions the interface stabilized by WPI displayed intra cycle yielding behavior and behaved more like a (quasi-) 2d viscoelastic liquid at large deformations, while the WPA layer did not show this yielding behavior, but a more gradual softening, retaining more of a solid-like behavior. As a result, the WPA

interfacial layer could break at large and fast deformations, leading to exposure of parts of the interface, and to an increase in the rate of coalescence. Although at high protein concentration the interface formed by WPI was more brittle than the WPA interfacial layer, WPI could flow and remain at the interface during fast and large deformation. Consequently, it could protect oil droplets by a mechanism similar to the Marangoni effect demonstrated for small molecular surfactants.

2.4. Conclusion

In this study the stability of milk fat emulsions prepared with WPI or WPA is explained in terms of bulk and interfacial properties. For emulsions with a low protein content, WPI displays better emulsifying ability than WPA, even though in the linear regime the viscoelastic properties of interfaces formed by the two proteins are similar. At high concentrations, WPA can stabilize emulsions better than WPI, as WPA can thicken the continuous phase of the emulsion more effectively. However, emulsions made with WPA are less stable when they are subjected to vigorous stirring. This may be caused by the fact that the WPI-stabilized interface has a denser and more brittle (quasi-) 2d structure. At large deformations, the WPI-stabilized interface shows yielding, thus preventing coalescence by a mechanism similar to the Marangoni effect. On the other hand, WPA forms a coarser and thicker 3d interfacial structure that is more solid-like, but may break at a large deformation. The results presented here are not only useful for developing more stable recombined dairy products, but also shed light on the effect of heat-induced whey protein modification on emulsifying ability and emulsion stability.

Reference

Aguilera, J. M. (1995). Gelation of whey proteins: Chemical and rheological changes during phase transition in food. Food technology (Chicago), 49(10), 83-89.

Beverung, C., Radke, C. J., & Blanch, H. W. (1999). Protein adsorption at the oil/water interface: characterization of adsorption kinetics by dynamic interfacial tension measurements. Biophysical chemistry, 81(1), 59-80.

Chen, M., Sala, G., Meinders, M. B., van Valenberg, H. J., van der Linden, E., & Sagis, L. M. (2017). Interfacial properties, thin film stability and foam stability of casein micelle dispersions. Colloids and Surfaces B: Biointerfaces, 149, 56-63.

Dalgleish, D. G. (2006). Food emulsions—their structures and structure-forming properties. Food Hydrocolloids, 20(4), 415-422.

Damodaran, S. (2005). Protein stabilization of emulsions and foams. Journal of Food Science, 70(3), R54-R66.

Davis, J., & Foegeding, E. (2004). Foaming and interfacial properties of polymerized whey protein isolate. Journal of Food Science, 69(5), C404-C410.

Destribats, M., Rouvet, M., Gehin-Delval, C., Schmitt, C., & Binks, B. P. (2014). Emulsions stabilised by whey protein microgel particles: towards food-grade Pickering emulsions. Soft Matter, 10(36), 6941-6954.

Dickinson, E. (1999). Adsorbed protein layers at fluid interfaces: interactions, structure and surface rheology. Colloids and Surfaces B-Biointerfaces, 15(2), 161-176.

Dickinson, E. (1999). Adsorbed protein layers at fluid interfaces: interactions, structure and surface rheology. Colloids and Surfaces B: Biointerfaces, 15(2), 161-176.

Dickinson, E. (2001). Milk protein interfacial layers and the relationship to emulsion stability and rheology. Colloids and Surfaces B: Biointerfaces, 20(3), 197-210.

Dickinson, E., & Tanai, S. (1992). Protein displacement from the emulsion droplet surface by oil-soluble and water-soluble surfactants. Journal of agricultural and food chemistry, 40(2), 179-183.

Dybowska, B. E. (2011). Whey protein-stabilized emulsion properties in relation to thermal modification of the continuous phase. Journal of food Engineering, 104(1), 81-88.

Ewoldt, R. H., Hosoi, A., & McKinley, G. H. (2008). New measures for characterizing nonlinear viscoelasticity in large amplitude oscillatory shear. Journal of Rheology, 52(6), 1427-1458.

Foley, J., & O'Connell, C. (1990). Comparative emulsifying properties of sodium caseinate and whey protein isolate in 18% oil in aqueous systems. Journal of Dairy Research, 57(3), 377-391.

Fredrick, E., Heyman, B., Moens, K., Fischer, S., Verwijlen, T., Moldenaers, P., Van der Meeren, P., & Dewettinck, K. (2013). Monoacylglycerols in dairy recombined cream: II. The effect on partial coalescence and whipping properties. Food Research International, 51(2), 936-945.

Granger, C., Barey, P., Combe, N., Veschambre, P., & Cansell, M. (2003). Influence of the fat characteristics on the physicochemical behavior of oil-in-water emulsions based on milk proteins-glycerol esters mixtures. Colloids and Surfaces B: Biointerfaces, 32(4), 353-363.

Han, J., Zhou, X., Cao, J., Wang, Y., Sun, B., Li, Y., & Zhang, L. (2018). Microstructural evolution of whipped cream in whipping process observed by confocal laser scanning microscopy. International Journal of Food Properties, 21(1), 593-605.

Hoffman, J. R., & Falvo, M. J. (2004). Protein–which is best? Journal of sports science & medicine, 3(3), 118.

Jiang, Y., Chen, J., Deng, C., Suuronen, E. J., & Zhong, Z. (2014). Click hydrogels, microgels and nanogels: emerging platforms for drug delivery and tissue engineering. Biomaterials, 35(18), 4969-4985.

Jung, J.-M., Gunes, D. Z., & Mezzenga, R. (2010). Interfacial activity and interfacial shear rheology of native β-lactoglobulin monomers and their heat-induced fibers. Langmuir, 26(19), 15366-15375.

Lam, R. S., & Nickerson, M. T. (2015). The effect of pH and temperature pre-treatments on the physicochemical and emulsifying properties of whey protein isolate. LWT-Food Science and Technology, 60(1), 427-434.

Lucassen, J., & Van Den Tempel, M. (1972). Dynamic measurements of dilational properties of a liquid interface. Chemical Engineering Science, 27(6), 1283-1291.

Millqvist-Fureby, A., Elofsson, U., & Bergenståhl, B. (2001). Surface composition of spray-dried milk protein-stabilised emulsions in relation to pre-heat treatment of proteins. Colloids and Surfaces B: Biointerfaces, 21(1-3), 47-58.

Mortensen, B. (2016). Anhydrous Milk Fat/Butter Oil and Ghee.

Nicolai, T., Britten, M., & Schmitt, C. (2011). β-Lactoglobulin and WPI aggregates: formation, structure and applications. Food Hydrocolloids, 25(8), 1945-1962.

Nicolai, T., & Durand, D. (2013). Controlled food protein aggregation for new functionality. Current Opinion in Colloid & Interface Science, 18(4), 249-256.

Petkov, J. T., Gurkov, T. D., Campbell, B. E., & Borwankar, R. P. (2000). Dilatational and shear elasticity of gel-like protein layers on air/water interface. Langmuir, 16(8), 3703-3711.

Phan, T. T. Q., Moens, K., Le, T. T., Van der Meeren, P., & Dewettinck, K. (2014). Potential of milk fat globule membrane enriched materials to improve the whipping properties of recombined cream. International Dairy Journal, 39(1), 16-23.

Rodríguez Patino, J. M., Rodríguez Niño, M. R., & Sánchez, C. C. (1999). Adsorption of whey protein isolate at the oil− water interface as a function of processing conditions: A rheokinetic study. Journal of agricultural and food chemistry, 47(6), 2241-2248.

Sagis, L. M., & Fischer, P. (2014). Nonlinear rheology of complex fluid–fluid interfaces. Current Opinion in Colloid & Interface Science, 19(6), 520-529.

Sagis, L. M., Liu, B., Li, Y., Essers, J., Yang, J., Moghimikheirabadi, A., Hinderink, E., Berton-Carabin, C., & Schroen, K. (2019). Dynamic heterogeneity in complex interfaces of soft interface-dominated materials. Scientific reports, 9(1), 2938.

Sarkar, A., Murray, B., Holmes, M., Ettelaie, R., Abdalla, A., & Yang, X. (2016). In vitro digestion of Pickering emulsions stabilized by soft whey protein microgel particles: influence of thermal treatment. Soft Matter, 12(15), 3558-3569.

Schmitt, C., Moitzi, C., Bovay, C., Rouvet, M., Bovetto, L., Donato, L., Leser, M. E., Schurtenberger, P., & Stradner, A. (2010). Internal structure and colloidal behaviour of covalent whey protein microgels obtained by heat treatment. Soft Matter, 6(19), 4876.

Schröder, A., Berton-Carabin, C., Venema, P., & Cornacchia, L. (2017). Interfacial properties of whey protein and whey protein hydrolysates and their influence on O/W emulsion stability. Food Hydrocolloids, 73, 129-140.

Segall, K., & Goff, H. (2002). Secondary adsorption of milk proteins from the continuous phase to the oil–water interface in dairy emulsions. International Dairy Journal, 12(11), 889-897.

Sobhaninia, M., Nasirpour, A., Shahedi, M., & Golkar, A. (2017). Oil-in-water emulsions stabilized by whey protein aggregates: Effect of aggregate size, pH of aggregation and emulsion pH. Journal of Dispersion Science and Technology, 38(9), 1366-1373.

Spiegel, T. (1999). Whey protein aggregation under shear conditions–effects of lactose and heating temperature on aggregate size and structure. International journal of food science & technology, 34(5-6), 523-531.

Tadros, T., Izquierdo, P., Esquena, J., & Solans, C. (2004). Formation and stability of nano-emulsions. Adv Colloid Interface Sci, 108, 303-318.

van Kempen, S. E., Schols, H. A., van der Linden, E., & Sagis, L. M. (2013). Non-linear surface dilatational rheology as a tool for understanding microstructures of air/water interfaces stabilized by oligofructose fatty acid esters. Soft Matter, 9(40), 9579-9592.

van Lent, K., Le, C. T., Vanlerberghe, B., & Van der Meeren, P. (2008). Effect of formulation on the emulsion and whipping properties of recombined dairy cream. International Dairy Journal, 18(10-11), 1003-1010.

Vanderghem, C., Danthine, S., Blecker, C., & Deroanne, C. (2007). Effect of proteose-peptone addition on some physico-chemical characteristics of recombined dairy creams. International Dairy Journal, 17(8), 889-895.

Wan, Z., Yang, X., & Sagis, L. M. (2016). Nonlinear surface dilatational rheology and foaming behavior of protein and protein fibrillar aggregates in the presence of natural surfactant. Langmuir, 32(15), 3679-3690.

Wijayanti, H. B., Bansal, N., & Deeth, H. C. (2014). Stability of whey proteins during thermal processing: A review. Comprehensive Reviews in Food Science and Food Safety, 13(6), 1235-1251.

Wilde, P. (2000). Interfaces: their role in foam and emulsion behaviour. Current Opinion in Colloid & Interface Science, 5(3-4), 176-181.

Wooster, T. J., & Augustin, M. A. (2007). Rheology of whey protein–dextran conjugate films at the air/water interface. Food Hydrocolloids, 21(7), 1072-1080.

Wu, J., Shi, M., Li, W., Zhao, L., Wang, Z., Yan, X., Norde, W., & Li, Y. (2015). Pickering emulsions stabilized by whey protein nanoparticles

prepared by thermal cross-linking. Colloids and Surfaces B: Biointerfaces, 127, 96-104.

Wu, S., Wang, G., Lu, Z., Li, Y., Zhou, X., Chen, L., Cao, J., & Zhang, L. (2016). Effects of glycerol monostearate and Tween 80 on the physical properties and stability of recombined low-fat dairy cream. Dairy Science & Technology, 96(3), 377-390.

Yang, J., Thielen, I., Berton-Carabin, C. C., van der Linden, E., & Sagis, L. M. (2020). Nonlinear interfacial rheology and atomic force microscopy of air-water interfaces stabilized by whey protein beads and their constituents. Food Hydrocolloids, 101, 105466.

Yener, S., & van Valenberg, H. J. (2019). Characterisation of triacylglycerols from bovine milk fat fractions with MALDI-TOF-MS fragmentation. Talanta.

Zhou, X., Chen, L., Han, J., Shi, M., Wang, Y., Zhang, L., Li, Y., & Wu, W. (2016). Stability and physical properties of recombined dairy cream: Effects of soybean lecithin. International Journal of Food Properties, 20(10), 2223-2233.

Appendix

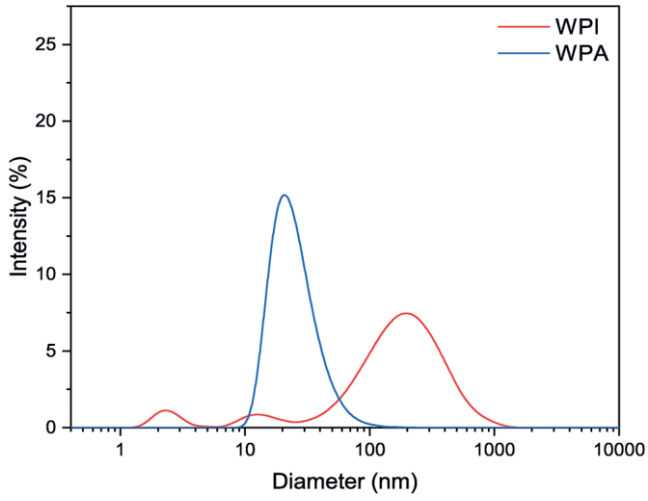

Fig. S 2.1. Intensity-weighted size distribution of WPI and WPA at room temperature (20 °C). Protein samples were diluted to 0.4 wt% with Milli-Q water before testing.

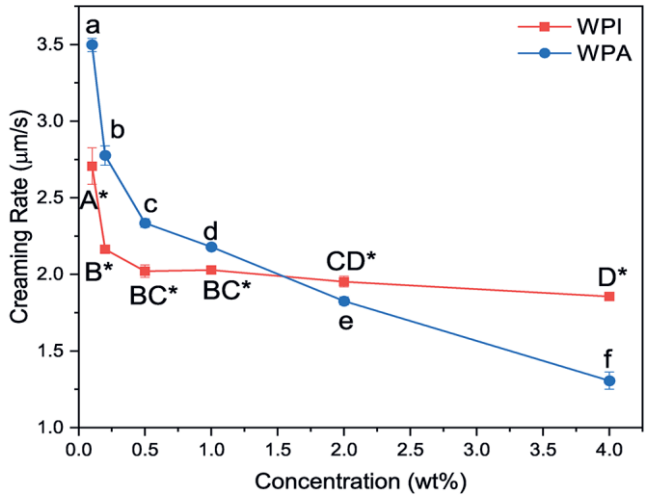

Fig. S 2.2. Creaming rate of milk fat emulsions stabilized with WPI or WPA as function of protein concentrations, measured at room temperature (20 °C), and 103 g. An asterisk (*) is used to denote statistical differences between proteins at the same concentrations. Different letters mark the statistical differences between concentrations of the samples with same protein.

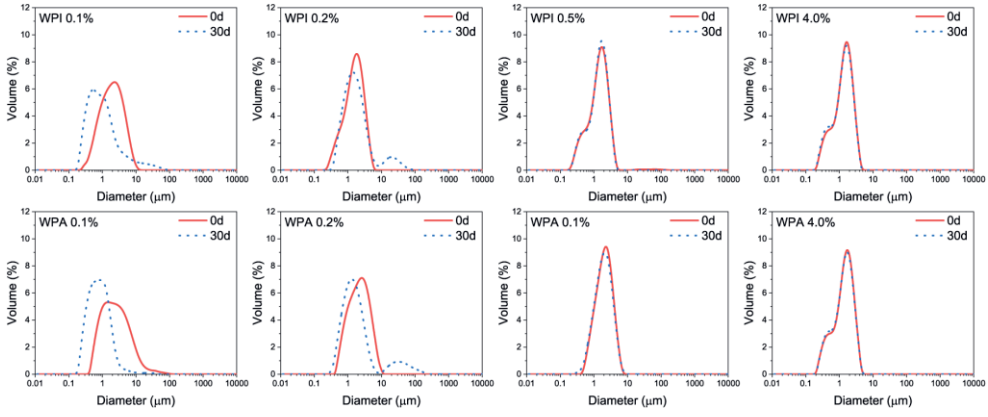

Fig. S 2.3. Droplet size distribution of milk fat emulsions stabilized with WPI and WPA at various protein concentrations, including fresh samples (od), samples after a simulated storage of 30 days (30d).

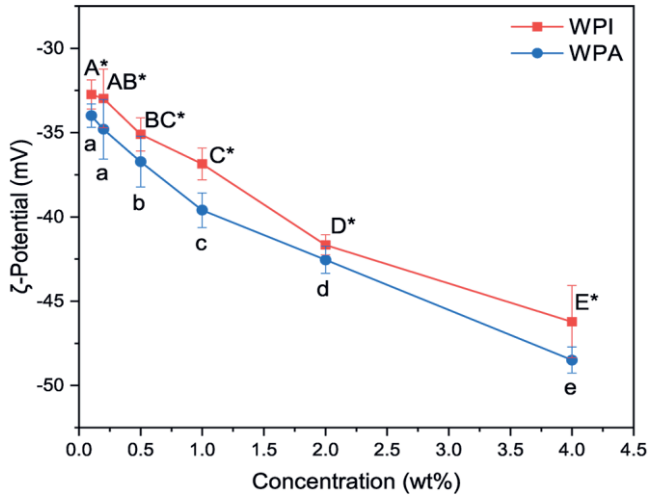

Fig. S 2.4. ζ-potential of milk fat emulsions made with WPI or WPA at various protein concentrations, measured at 20 °C. The emulsions were 1000 times diluted by Milli-Q water before testing. An asterisk (*) is used to denote statistical differences between proteins at the same concentrations. Different letters mark the statistical differences between concentrations of the samples with the same protein.

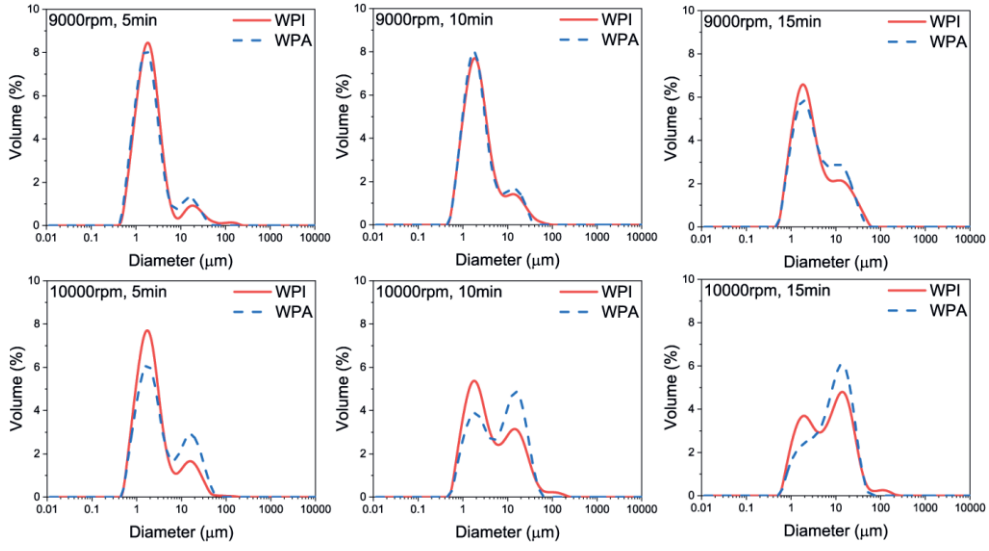

Fig. S 2.5. Evaluation of droplet size distribution of milk fat emulsions during stirring at different speeds. The milk fat emulsions were made by 4.0 wt% WPI or WPA.

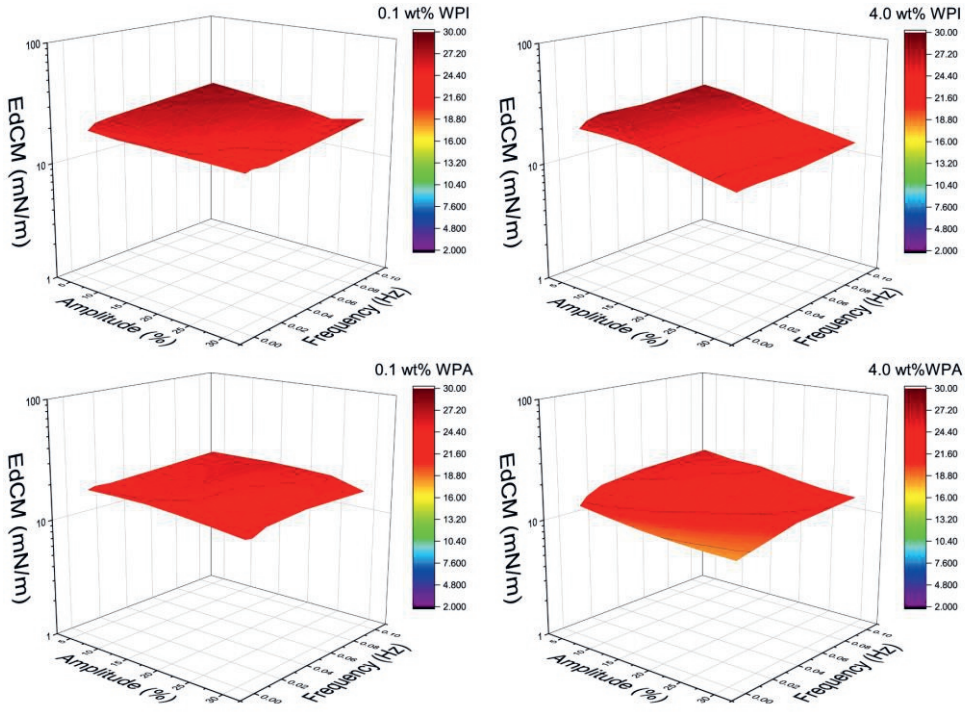

Fig. S 2.6. E_{dCM} of WPI- and WPA-stabilized milk fat-water interfaces at protein concentrations of 0.1 and 4.0 wt% as the function of strain amplitude and strain frequency.

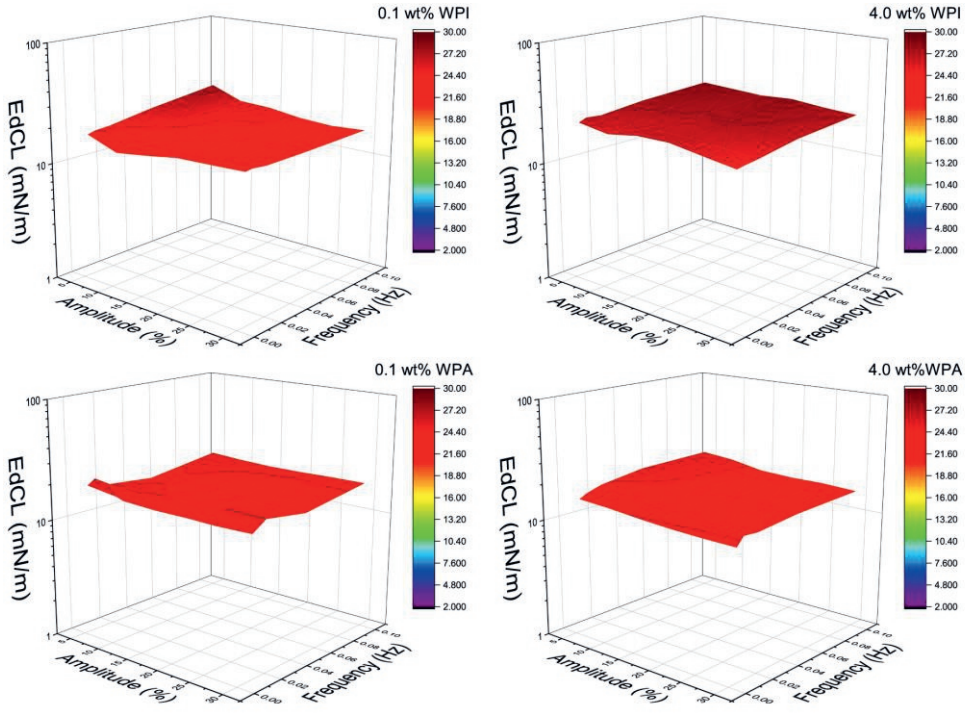

Fig. S 2.7. E_{dCL} of WPI- and WPA-stabilized milk fat-water interfaces at protein concentrations of 0.1 and 4.0 wt% as the function of strain amplitude and strain frequency.

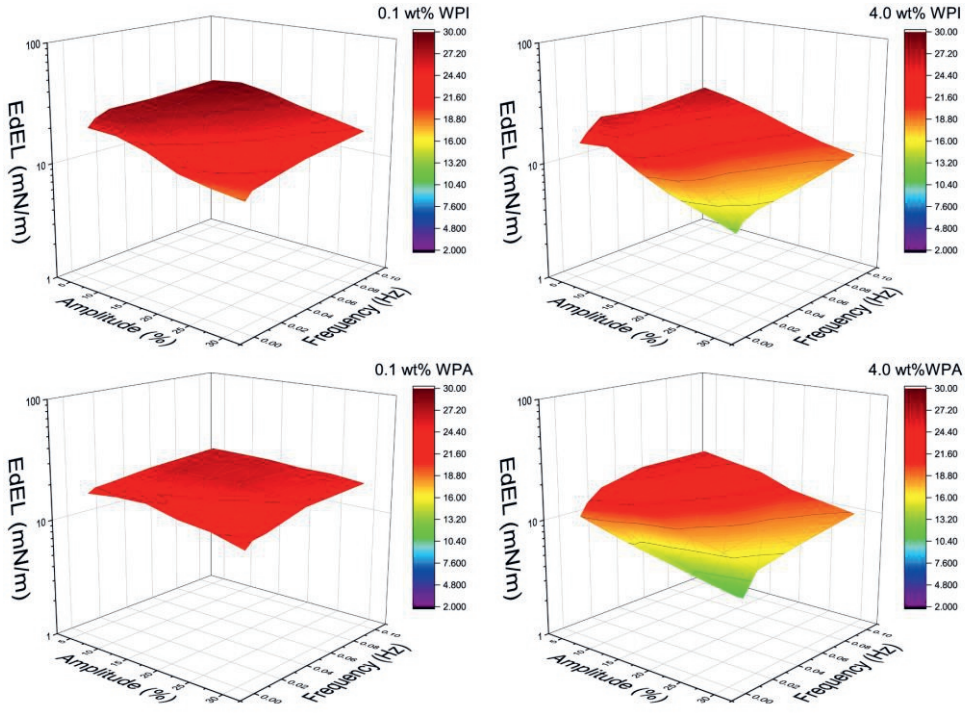

Fig. S 2.8. E_{dEL} of WPI- and WPA-stabilized milk fat-water interfaces at protein concentrations of 0.1 and 4.0 wt% as the function of strain amplitude and strain frequency.

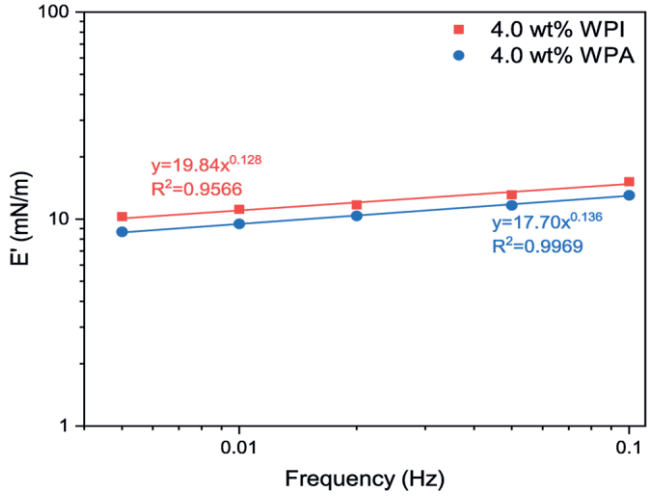

Fig. S 2.9. Elastic modulus (*E'*) of WPI or WPA-stabilized interface as a function of frequency and fitted by a power law. The amplitude was fixed as 30%.

Tab. S 2.1. Loss tangent (*E''/E'*) of 4.0 wt% WPI- or WPA-stabilized interface at different frequencies, with fixed amplitude 30%.

Protein	Frequency				
	0.005	0.01	0.02	0.05	0.1
WPI	0.51092	0.472415	0.446421	0.568403	0.426571
WPA	0.239702	0.266367	0.256305	0.264725	0.241682

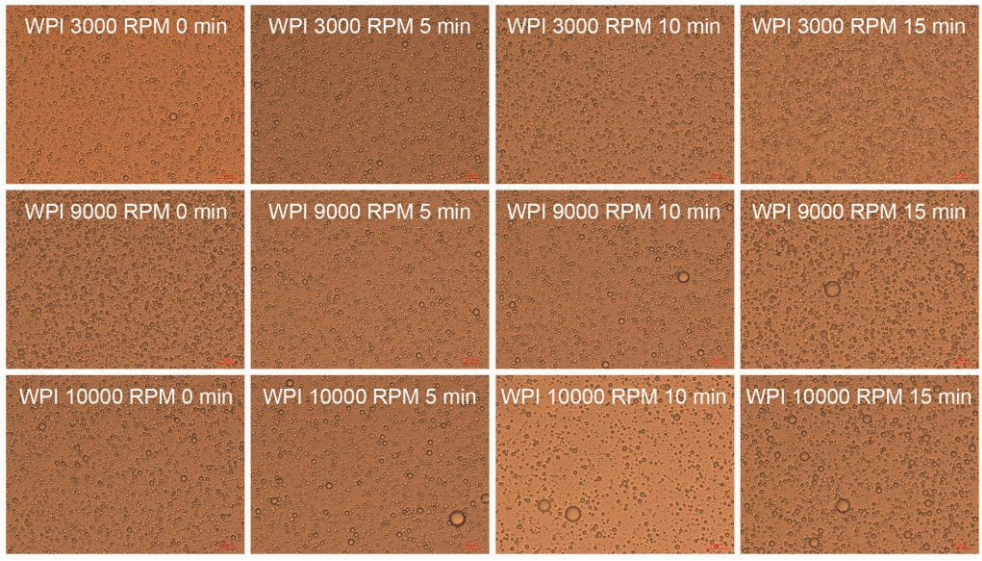

Fig. S 2.10. Microscopic pictures of emulsions made with 4.0 wt% WPI upon stirring at different speeds. The red scale bar is 20 µm. Samples were 10 times diluted by Milli-Q water.

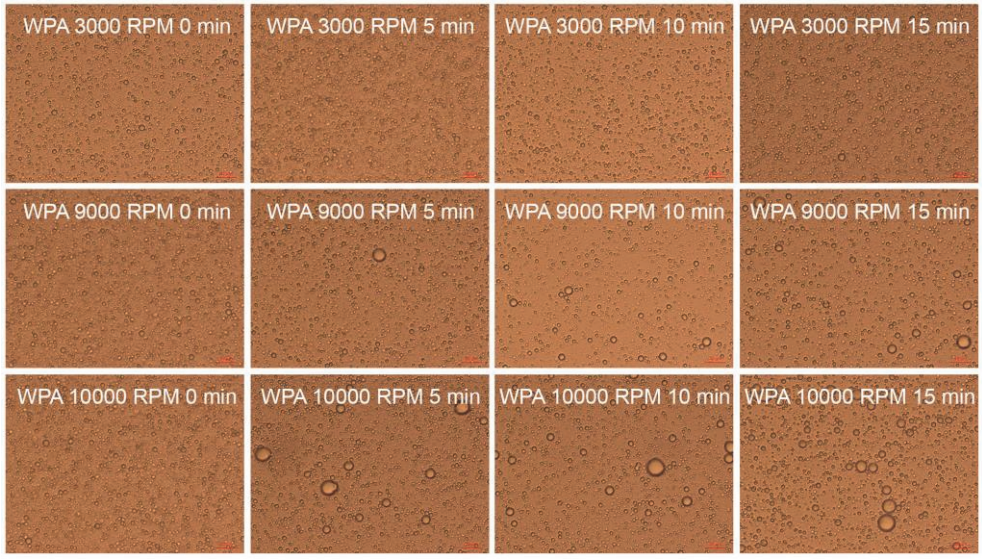

Fig. S 2.11. Microscopic pictures of emulsions made with 4.0 wt% WPA upon stirring at different speeds. The red scale bar is 20 µm. Samples were 10 times diluted by Milli-Q water.

Chapter 3

Are micelles actually at the interface in micellar casein stabilized foam and emulsions

Abstract

Different casein preparations are used for stabilizing emulsions and foams. For systems made with aqueous micellar casein dispersions, the molecular and colloidal mechanisms responsible for the stabilization of oil-water and air-water interfaces have not been conclusively ascertained. Whether the micelles themselves, small casein aggregates, or individual casein molecules are at the interface is still an open question. Understanding these mechanisms is important for food industries to improve product formulations. We investigated the nonlinear rheology and microstructure of oil-water and air-water interfaces stabilized with casein micelle dispersions and their fractions. Our results convincingly show that the micelles themselves are not adsorbed at the interfaces. For air-water interfaces, the behavior appears to be dominated by β-casein, whereas the properties of oil-water interfaces are dominated by small casein aggregates. These findings are important to understand the stabilization mechanisms of emulsions and foams prepared with caseins or milk.

3.1. Introduction

Dairy proteins are widely used as stabilizers in food emulsions and foams (Scott, Duncan, Sumner, & Waterman, 2003; Tomas, Paquet, Courthaudon, & Lorient, 1994; Wu, et al., 2016; Zhou, et al., 2016). Huppertz (2010) and Ho, Bhandari, and Bansal (2021) comprehensively reviewed the influence of milk protein composition and different processing parameters on milk protein stabilized foams. A detailed review of emulsifying and emulsion stabilizing properties of milk proteins can be found in Dickinson's review papers (Dickinson, 1997, 2001). There is a consensus that dairy proteins form viscoelastic interfacial layers at air-water or oil-water interfaces, providing steric and electrostatic repulsion, thus stabilizing emulsion droplets or foam bubbles against coalescence. The rheological properties of interfaces stabilized with α_{S1}-, β-casein or β-lactoglobulin are extensively studied in the small deformation regime (Dickinson, 1998). However, the interfacial rheology of oil-water or air-water interfaces in the nonlinear regime is hardly reported, in spite of its high relevance for processing and consumption (Sagis & Fischer, 2014). In previous studies on the microstructure and dilatational properties of whey proteins at the oil-water (Zhou, Sala, & Sagis, 2020) and

air-water interfaces (Yang, Thielen, Berton-Carabin, van der Linden, & Sagis, 2020), we showed that native whey proteins form viscoelastic solid-like interfaces, which have a yield stress. Beyond this yield stress the interface shows significant softening and behaves more like a viscoelastic fluid. For the other major constituent of dairy protein, casein, more research is needed to establish its behavior in the nonlinear regime.

Casein is regarded as a good emulsifier that can reduce the surface tension to a great extent (Jackson & Pallansch, 1961; Leman, Kinsella, & Kilara, 1989). It is mainly composed of four types of monomers, κ-casein, α_{S2}-casein, α_{S1}-casein, and β-casein, with a ratio 1.3 : 1 : 4 : 4 (Walstra, 1990). These monomers form micelles, where they are linked to each other by hydrophobic interactions and hydrogen bonds, and by colloidal calcium phosphates. Over 95% of the casein in milk is present in the casein micelles (Dumpler, 2017). In the past decades, most research investigating the role of casein in emulsions, foams, or interfaces in general, were mostly based on sodium caseinate, and to a lesser extent on micellar casein. It has been shown that casein exhibits different hydrophobicity and surfactant properties depending on its structural aggregation state (Courthaudon, et al., 1999; Roman & Sgarbieri, 2006). The results obtained for sodium caseinate cannot be extrapolated to micellar caseins, as the micelles are broken down during the manufacturing of sodium caseinates (Carr & Golding, 2016). Only a few studies cast light on the application of casein micelles in emulsions and foams. Lazzaro, et al. (2017) disaggregated casein micelles into different sizes by gradually demineralizing casein micelles, and found monomers or smaller casein micelles have better emulsifying properties, but are less stable to creaming and flocculation. Zhang and Goff (2004) utilized EDTA to disaggregate casein micelles in milk protein solution and achieved better foamability. Some other studies investigated the effects of pH, ionic strength (Zhang, Dalgleish, & Goff, 2004), and heat treatment (Liang, Patel, Matia-Merino, Ye, & Golding, 2013) on the stability of emulsions or foams stabilized by casein micelles or by full milk proteins. A common observation of these studies is that nonmicellar caseins always display a better emulsifying property or formability than micellar casein. Although the foamability of casein micelles is not comparable with nonmicellar caseins, micellar casein appears to provide better foam stability. Li, et al. (2020) applied casein micelles in recombined dairy cream and achieved better foam stability after whipping. Ewert, et al. (2016) also proved that comparing with sodium caseinate, micellar caseins produced a

more stable foam. Casein micelles (Dombrowski, Dechau, & Kulozik, 2016) or casein micelle aggregates (Chen, et al., 2016) have larger molecular size and likely to retard the drainage of liquid from the films separating the bubbles, thus improving the stability of foams. However, the molecular and colloidal mechanisms behind the stabilization of oil-water (O-W) and air-water (A-W) interfaces by micellar casein, are still under debate, and published studies even contradict each other.

For foams, casein micelles (Dombrowski, et al., 2016) and casein micelle aggregates (Chen, et al., 2016) appeared not to adsorb at the interface, and were assumed to either remain in the bulk phase, or attach to the interface as a sublayer, leading to pinning of the foam lamellae and slowing down drainage (Chen, et al., 2017). However, this behavior has not been fully proved, and contradictory findings were reported in other research (Silva, Saint-Jalmes, de Carvalho, & Gaucheron, 2014), where casein micelles are claimed to adsorb at the A-W interface and subsequently fall apart. Regarding emulsions, some researchers stated that casein micelles can adsorb at the O-W interface (San Martin-González, Roach, & Harte, 2009) and stabilize the emulsions by the so-called Pickering mechanism (Dickinson, 2015). Although electron microscopy pictures do illustrate that micelles can be at oil-water or air-water interfaces (Anderson, Brooker, & Needs, 1987; Brooker, 1985; Jensen, 2013), it is difficult to distinguish whether in these cases the micelles adsorbed at the interfaces or just attached to the interface as a sublayer. Moreover, in those pictures, only a few complete micelles could be found at the interfaces. Whether those sparse micelles at the interfaces can stabilize the droplets or foams is questionable. So, whether micellar casein can adsorb at O-W interfaces and thus prevent oil droplet coalescence is also not completely clear yet.

In this study, a casein micelle dispersion was fractionated by ultracentrifugation into a pellet (which was subsequently redispersed in water), and a supernatant. The pellet redispersion was mainly composed of micellar caseins, and the supernatant contained small aggregates and monomers of all casein fractions. We investigated the nonlinear rheology of O-W and A-W interfaces stabilized with the casein micelle dispersion and the other two fractions separately. We analyzed the interfaces using multiphoton excitation microscopy (MPM) and ellipsometry. The microstructure of A-W interfaces was also visualized by atomic force microscopy on Langmuir-Blodgett films. We aimed at explaining how casein

micelles stabilize O-W and A-W interfaces on the basis of molecular and colloidal mechanisms.

3.2. Methods

3.2.1. Materials

Micellar casein isolate (84.15% protein, lactose 3.0%, ash 7.3%, moisture 3.3 %, fat 1.1%) was kindly donated by FrieslandCampina (Netherlands). Beta-casein powder (79.33% protein) was purchased from Eurial (France). Florisil (60-100 mesh), dimethyl sulfoxide (DMSO), bis-tris buffer, DL-dithiothreitol (DTT), trifluoroacetic acid (TFA), urea (99,5% purity), tri-sodium citrate dehydrate, syringe filters (PVDF, 5.0 µm, d 25 mm; PVDF, 0.45 µm, d 33 mm; PVDF, 0.1 µm, d 33 mm) and filter membrane (PVDF, 0.45 µm, d 47 mm) were purchased from Merck (Netherlands). Medium chain triglyceride (MCT) was purchased from IMCD (France). Cyanine 5 (Cy5) was purchased from Lumiprobe (Europe). Acetonitrile (HPLC Ultra–Gradient) was purchased from Biosolve-Chemicals (Netherlands). UV glue, nylon rings (M10) and metal washers (diameter 7 mm) were purchased online (Amazon). Glass slides (#1.5) were purchased from Thermo (Netherlands). Dialysis membranes (3.5 kD, #3) were purchased from Spectrum Labs (Greece). Skim milk powder was kindly donated by NIZO (Netherlands).

3.2.2. Fractionation of casein micelle dispersion

A casein micelle dispersion with 2.0 wt% protein was made by dissolving micellar casein isolate in Milli-Q water and stirring overnight at room temperature; 0.02 wt% sodium azide was added to prevent spoilage. The casein micelle dispersion was filtered through syringe filters with a cut off 5.0 µm and 0.45 µm, successively.

Twenty gram of casein micelle dispersion was centrifuged at 15,000 g for 1 h using an ultracentrifuge (Beckman Coulter, US). The supernatant was carefully transferred to a serum bottle with a volume of 20 mL, and the mass was compensated to 20 g by adding Milli-Q water. The supernatant was subsequently filtered using a syringe filter with a cut off 0.1 µm.

After the first ultracentrifugation, the pellet still contained a significant amount of liquid. To get rid of the monomers and small aggregates in that fluid, the pellet was washed. First, Milli-Q water was added to the tube to

achieve a total mass of 20 g. Then the pellet was re-dispersed using a Turrax (IKA T25, Germany) at 8000 rpm. Subsequently, the dispersion was ultracentrifuged at 50,000 g for 30 min. The new supernatant was discarded, and the new pellet was washed again. After two full washing steps, the final pellet was re-dispersed, and sonicated for 10 min (160 W, 35 kHz) using an ultrasonic bath (RK510, Bandelin, Germany), then filtered through syringe filters with a cutoff of 5.0 µm and 0.45 µm, successively.

The protein concentration of the casein micelle dispersion, supernatant and pellet redispersion was determined by DUMAS with conversion coefficient 6.38, and the contents were 1.90 ± 0.06, 0.31 ± 0.02, and 1.26 ± 0.01 wt%, respectively.

3.2.3. Particle size distribution of the samples

The particle size distribution of casein micelle dispersion, supernatant and pellet were determined using a Malvern Zetasizer Nano-ZS (Malvern Instruments Ltd, United Kingdom). All samples were diluted to a protein concentration 0.1 wt% with Milli-Q water. Approximately 1 mL sample was pipetted into a cuvette (type DTS0012). The refractive and absorption indices of protein dispersions/solutions were 1.450 and 0.001, respectively. The refractive index of dispersant (water) was 1.330. Before each test, the sample was equilibrated for 2 min.

3.2.4. High pressure liquid chromatography (HPLC)

To identify the monomers present in the supernatant, we used the method of HPLC analysis described by de Vries, et al. (2015). Three hundred microliter supernatant prepared as described in section 2.2 was mixed with 900 µL 0.1% v/v TFA (pH 2.0). The mixtures were vortexed for 10 s and filtered through a filter with a cut off 0.1 µm. Reconstituted skim milk was taken as a qualitative reference. It was prepared by dissolving 1 g skim milk power in 9 g warm water (40 °C), while stirring for 30 min at room temperature. The skim milk was mixed with solution A (0.1 M Bis-Tris buffer, 8 M urea, 5.37 mM sodium citrate and 19.5 mM DTT, pH 7.0) at a ratio of 1:3 (v:v) and kept for 1 h at room temperature. Then the sample was centrifuged for 5 min at 16,000 g to remove any remaining fat. A volume of 300 µL of sample was pipetted into a new tube and mixed with 900 µL solution B (6M urea in 0.1% v/v TFA, pH 2.0). The mixtures were vortexed for 10 s and filtered through a syringe filter with a cut off 0.1 µm.

All the supernatant or skim milk samples were stored in HPLC vials. The analysis was carried out using an Ultimate 3000 LC module equipped with an Aeris Widepore 3.6 µm XB-C18 column (250 × 4.6 mm, Phenomenex, Netherlands). A security guard cartridge system was used as a precolumn (AJ0–8769, Phenomenex). The temperature of the auto-sampler and the column were set as 4 and 45 °C, respectively. The injection volume was 5 µL. The wavelength of the UV detector was 214 nm. The protein eluent consisted of solvent A (0.1% FTA in Milli-Q water, v/v) and solvent B (0.1% FTA in acetonitrile, v/v). The elution method described by de Vries, et al. (2015) was used. The peaks for b-casein were analyzed with Chromeleon 7.1.2 software to obtain an estimate for the concentration of this component to be used in the surface rheology experiments. All the measurements were conducted in triplicate. The amount of β-casein was calculated using the following equation:

$$C_{\beta-casein} = C_{sup} \times A_{\beta-casein}/A_{total} \quad \text{Eq. 3.1}$$

where $C_{\beta-casein}$ is the content of β-casein in the supernatant; C_{sup} is the total protein content of the supernatant; $A_{\beta-casein}/A_{total}$ represents the ratio between the peak area of β-casein and the total area of all peaks in the HPLC spectrum. In this research, only β-casein was quantified. The reason is explained in the results part (section 3.3.2).

3.2.5. Fat purification

The anhydrous milk fat (AMF) used for the study of the rheological properties of O-W interfaces prepared with the different protein samples and for the other analyses described here below, was previously purified. Florisil was desiccated overnight at 105 °C in an oven, then cooled down to room temperature. AMF was melted at 60 °C and mixed with 10 wt% Florisil. The mixture was stirred at 60 °C for at least 2 h. Subsequently, 10 mL of the mixture was sampled and filtered with a syringe filter to remove Florisil particles. The surface tension of the interface between the filtered AMF and Milli-Q water was tested for at least 1 h. If the tension decreased over time, AMF needed to be purified further by repeating the steps described above. Once the surface tension stayed constant, the AMF and Florisil mixture were filtered using vacuum filtration with a filter membrane (PVDF, 0.45 µm, d 47 mm). The filtered AMF was sealed in blue cap bottles and kept in the dark at room temperature.

The medium chain triglyceride oil (MCT) for the microscopy tests was also purified according to the same protocol, but at room temperature.

3.2.6. Oscillatory dilatational measurements

Oscillatory dilatational deformations were applied to the O-W or A-W interfaces using a Tracker Automated Droplet Tensiometer (Teclis, France) according to the method described by Zhou, Sala, and Sagis (2020). For O-W interfaces, purified AMF was transferred to the cuvette and kept melted at 40 °C in the cell. A pendent droplet of the protein samples was formed at the tip of the needle, which was immersed in the oil phase. The surface area of the droplet was 20 mm^2. The density of the droplet fluid and AMF at 40 ^oC were 0.9922 and 0.9041 g/mL, respectively. For the A-W interface, a pendent droplet of protein solution was formed at the tip of the needle at 20 °C. A small amount of water was added at the bottom of cuvette to saturate the air phase with water and limit evaporation during the test. For that same purpose, the cuvette was covered with parafilm. The area of the droplet was adjusted to 15 mm^2. The density of the droplet fluid and air at 20 ^oC were 0.9982 and 0.0012 g/mL, respectively.

The interface was firstly equilibrated for 3 h, followed by sinusoidal area deformations. An amplitude sweep was performed with amplitudes of 5, 10, 15, 20 and 30%, at a fixed frequency of 0.01 Hz. For every amplitude, 5 oscillation cycles were performed and followed by a 900 s of rest. For every amplitude, only the middle 3 cycles were used to construct Lissajous plots, where surface pressure (π) is plotted against strain amplitude (γ). The method of constructing Lissajous plots was introduced by Sagis, et al. (2014). The surface pressure and deformation were calculated using:

$$\gamma = \frac{A_t - A_0}{A_0} \qquad \text{Eq. 3.2}$$

$$\pi = \sigma_t - \sigma_0 \qquad \text{Eq. 3.3}$$

where A_t and σ_t are interfacial area and interfacial tension at time t; A_0 and σ_0 are initial interfacial area and interfacial tension.

3.2.7. Visualization of interfaces with multiphoton excitation microscopy (MPM)

3.2.7.1. Object slides for MPM

Pictures of the object slides used for MPM are shown in Fig. 3.1a. A metal washer and a nylon ring were attached on a glass slide using liquid UV glue, then the whole setup was incubated with UV light overnight to solidify the glue.

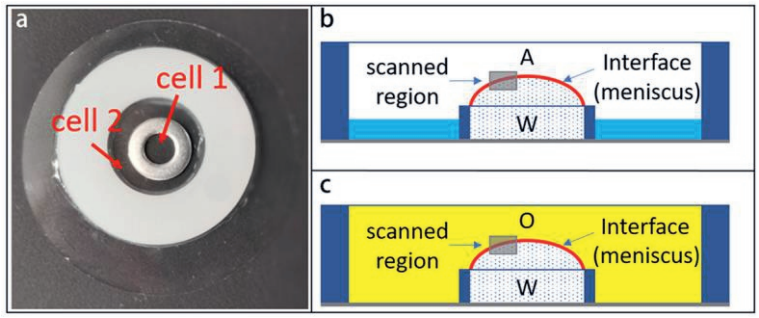

Fig. 3.1. Picture and schematics of slides for MPM. (a) top view of the slide; (b) side view of the slide for the A-W interface; (c) side view of the slide for the O-W interface. 'A' represents air; 'W' represents the water phase with proteins; 'O' represents oil.

3.2.7.2. Protein dialysis

Cyanine 5 was dissolved in dimethyl sulfoxide (DMSO) to a concentration of 1 mg/mL. Then, 10 and 50 µL Cyanine 5 solution were added to 1 mL supernatant solution and pellet redispersion, respectively. The corresponding blank samples were made by adding the same amount of dye to 1 mL Milli-Q water. The samples were incubated in the dark for 2 h at room temperature. Subsequently, the samples were dialyzed with a cutoff size of 3.5 kDa for 7 h by flowing Milli-Q water at room temperature.

3.2.7.3. Visualization of the interfaces

The dialyzed sample was slowly pipetted into cell 1 (Fig. 3.1a), until the sample formed a meniscus. For O-W interfaces, the outside of the meniscus was covered with MCT oil (Fig. 3.1c). For A-W interfaces, the slide was covered by parafilm to prevent evaporation. A small amount of water was added in cell 2 to limit sample evaporation (Fig. 3.1b). O-W and A-W

interfaces were visualized by a Leica SP8Dive multiphoton excitation microscope (Leica, Germany), using a HC FLUOTAR L 25×/0.95 W VISIR objective. The laser excitation wavelength was set at 840 nm, and the emission range for the detector was 650-700 nm. A 3-dimensional region (240*240*200 µm) was scanned by the MPM.

3.2.8. Topography of interfacial microstructure

3.2.8.1. Interfacial pressure isotherms

Interfacial pressure isotherms (area vs. surface pressure) were made using a Langmuir trough (KSV NIMA/Biolin Scientific Oy, Finland). Casein micelle dispersion, supernatant, and pellet redispersion were diluted to 0.2 wt%. The samples were injected (200 µL) at the bottom of a Langmuir trough filled with Milli-Q water using a gas-tight syringe. Afterwards, the system was equilibrated for 3 h, while monitoring the surface pressure using a platinum Wilhelmy plate (perimeter 20 mm, height 10 mm). At last, the interfacial area was reduced by compressing the film with Teflon barriers, moving with a speed of 5 mm/min.

3.2.8.2. Preparation of Langmuir-Blodgett (LB) films

LB films were made based on the same protocol described for the interfacial pressure isotherms. A freshly cleaved mica sheet (Highest Grade V1 Mica, Ted Pella, USA) was fixed vertically with respect to the interface. The mica sheet was completely immersed in the water phase. An amount of 200 µL of sample was injected at the bottom of the trough, while monitoring the surface pressure using a platinum Wilhelmy plate. After equilibrating for 3 h, the films formed at the interface were compressed to a target surface pressure of 13 or 23 mN/m. The interfacial films were deposited on the sheet mica by withdrawing the sheet vertically at a speed of 1 mm/min, while the Teflon barriers maintained the target surface pressure. All films were produced in duplicate and dried for two days in a desiccator at room temperature.

3.2.8.3. Atomic force microscopy (AFM)

The topography of the LB-films was studied using AFM (MultiMode 8-HR, Bruker, USA). The films were analyzed in tapping mode with a Scanayst-air model non-conductive pyramidal silicon nitride probe (Briker, USA). A normal spring constant of 0.40 N/m and a lateral scan frequency of 0.977 Hz

were applied for the analysis. The films were scanned for a 2.0 × 2.0 μm^2 area with a lateral resolution of 512 × 512 $pixels^2$. To ensure good representativeness, at least two locations of each replicate were scanned. The images were analyzed with Nanoscope Analysis v1.5 software (Bruker, USA).

3.2.8.4. Ellipsometry

The thickness of A-W and O-W interfacial films prepared with casein micelle dispersion, supernatant or redispersed pellet were analyzed with an imaging nulling ellipsometer EP4 (Accurion, Germany). A-W interfacial films were created by injecting 10 mL of protein solutions in Petri dishes. Afterward, the measurement spot was aligned on the interfacial layer. For evaluation of the O-W interfaces, the light source and objective lens coupled to the analyzer were extended with light guides. O-W interfacial films were created in a Teflon trough by first injecting 15 mL protein solutions, followed by the alignment of measurement spot. The MCT oil was then carefully pipetted onto the top of the protein solution until the guides were immerged in the oil. Both A-W and O-W interfaces were equilibrated for 3 h. Afterwards, the interfacial films were measured over wavelength ranges varying from 499.8 to 793.8 nm of two zones at an angle of incidence of 50° to obtain the ellipsometric parameters phase shift (δ) and amplitude ratio (ψ). The measurements were performed at room temperature, and at least two independently prepared interfacial films were measured. A wavelength scan was also performed on Milli-Q-air and MCT-air interfaces to determine their refractive indices for the model fitting. The output of the protein layers was analyzed with the EPModel v3.6.1. software provided by the supplier. A three layers system was built in the model by combining the air/oil layer, the protein layer, and the Milli-Q layer. The parameters of the protein layer in the model were fitted using a Cauchy model:

$$n(\lambda) = A + \frac{B}{\lambda^2} + \frac{C}{\lambda^4} \qquad \text{Eq. 3.4}$$

Where n is the refractive index; λ is the wavelength of the polarized light; A, B, and C are fitting parameters.

3.2.9. Statistical treatment of the data

All samples were prepared in duplicate, and all tests were performed at least twice. The data in this paper are reported as mean ± standard deviation.

3.3. Results

3.3.1. Size distribution of different fractions of casein micelle dispersion

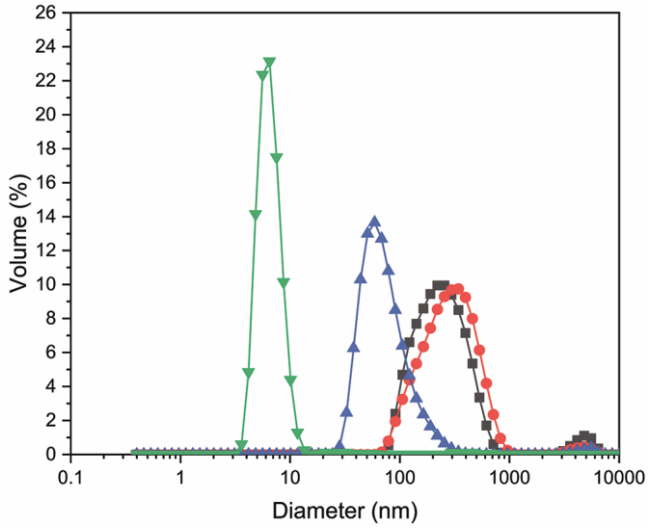

Fig. 3.2. Particle size distribution of the casein micelle dispersion (●), pellet redispersion (■), supernatant (▲) and β-casein solution (▼).

In order to compare the behavior of its different colloidal components at O-W and A-W interfaces, the casein dispersion was ultracentrifuged into two fractions, pellet and supernatant. The efficiency of separation was evaluated by testing the particle size distribution of casein micelle dispersion, pellet redispersion, and supernatant (Fig. 3.2). The size distributions of the pellet redispersion and casein micelle dispersion almost overlapped and presented a main peak at 200-400 nm, which is the typical size of casein micelles (Dalgleish, Spagnuolo, & Douglas Goff, 2004; Fox & McSweeney, 2013; Walstra, 1990). The main peak of the curve of the supernatant was at 40 - 50 nm, i.e. a fraction which in older literature is often referred to as “submicelles” (Qi, 2007; Walstra, 1999). Here, we will refer to this fraction

as “small aggregates”. The particle size distribution of a β-casein solution was analyzed, and showed a main peak around 6 nm. So, we can assume β-casein was mainly present in the solution in monomeric form. Basically, the results clearly show that the pellet redispersion was mainly composed of micellar caseins. The supernatant appeared to consist mainly of small aggregates, but contained undoubtably also monomers of the various casein fractions. The latter could not be detected by the NanoSizer since the scattering was dominated by the small aggregates present in the samples. To confirm the presence of monomers in the supernatant fraction and to obtain an estimate of the amount of β-casein in the supernatant, it was further analyzed with high performance liquid chromatography (HPLC).

3.3.2. Protein species in the supernatant

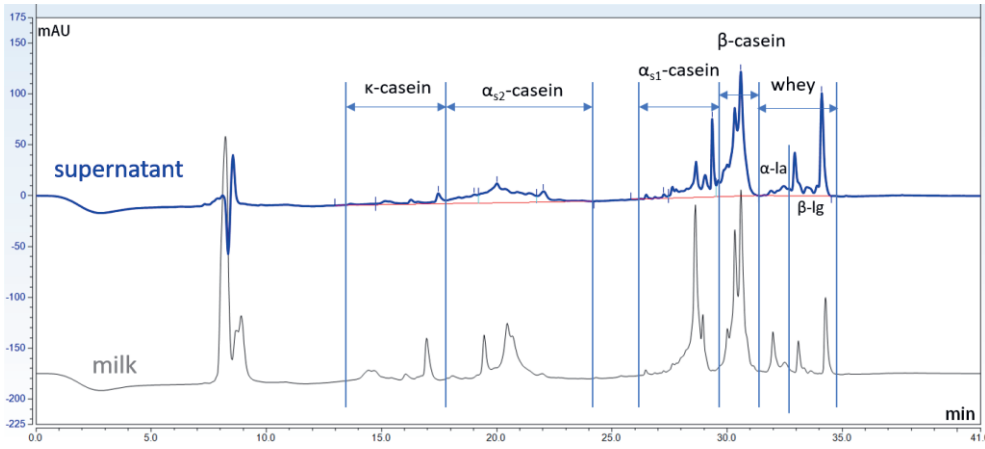

Fig. 3.3. HPLC chromatogram of the supernatant of the casein micelle dispersion after ultracentrifugation and of the milk reference. The peak at 8 min is most likely from the elution buffer.

According to the result of the HPLC analysis of the supernatant (Fig. 3.3), monomers were indeed present in this fraction, the main ones being α_s-casein and β-casein. The proportion of β-casein in the total protein in the supernatant was around 65.5%. Compared with α_s-casein, β-casein is less charged and has more distinct hydrophobic and hydrophilic regions. As a result, it behaves like a low molecular weight surfactant (Dalgleish & Leaver, 1991; Dickinson & Matsumura, 1994), and is more likely to adsorb at interfaces. It was even shown to displace α_s-casein from the interface, and also was dominant at the air-water interface when mixed with β-

lactoglobulin (Mackie, Gunning, Ridout, Wilde, & Morris, 2001; Ridout, Mackie, & Wilde, 2004). Consequently, for the execution of this study, only β-casein was selected as representative to investigate the role of monomers at the O-W and A-W interfaces. As the total protein concentration of supernatant was around 0.31 wt% (see section 3.2.2), the concentration of β-casein in the supernatant was roughly estimated to be 0.20 wt%, which will be the concentration of β-casein solution used in the following phases of this study.

3.3.3. Nonlinear rheology of O-W interfaces

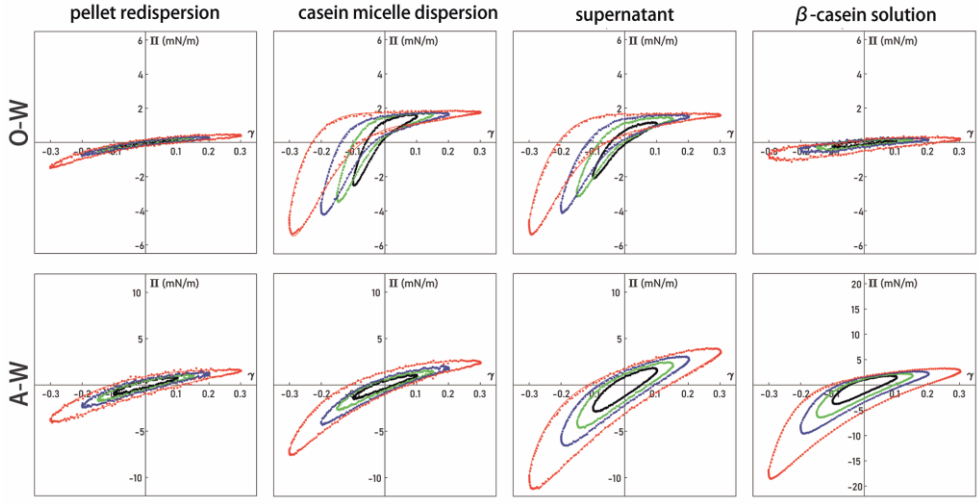

Fig. 3.4. Lissajous plots showing the surface pressure versus deformation for O-W and A-W interfaces stabilized with casein micelles dispersion, supernatant, pellet redispersion, or β-casein. The strain amplitudes were 10% (black), 15% (green), 20% (blue), 30% (red). The frequency was 0.01Hz.

A dilatational amplitude sweep at a frequency of 0.01 Hz was applied for interfaces stabilized with casein dispersion, supernatant or pellet redispersion, to ascertain which fraction of the solution dominated the response. Also, a β-casein solution was analyzed. The Lissajous plots of the O-W interfaces are shown in Fig. 3.4. At an amplitude of 10%, the response of the O-W interfaces stabilized with the casein dispersion was asymmetrical, which meant that at this strain amplitude the response was already in the nonlinear regime. The interfaces showed softening in expansion and hardening in compression. Softening was evidenced by the combination of a rapid increase of surface pressure at the beginning of the expansion (the upper part of the curve from left to right) followed by a decrease in the slope of the curve towards the end of the expansion phase. Hardening was indicated by an increasing slope of the curve in compression (the bottom part of the curve from right to left). With an increase of the amplitude, the gradual softening behavior in expansion turned into yielding, as the slope of the surface pressure abruptly changed during expansion and reached a plateau where the slope of the curve was close to zero. Yielding and

hardening behavior imply changes of the microstructure formed by the proteins at the interfaces. At the start of expansion, this structure was strong enough to resist the deformation and showed a highly stiff response. When the interfaces kept expanding, the structure was disrupted, leading to a significant decrease in stiffness, and a relatively more viscous response. In compression, the disrupted structure was densified, until the proteins reached a jammed (or gelled) state, which resulted in much stronger molecular interactions and an abrupt decrease of the surface pressure.

The same behavior was also found for the O-W interfaces stabilized with the protein species present in the supernatant, namely, expansion softening (or yielding) and compression hardening of the interfaces. As shown in Tab. 3.1, the O-W interfaces stabilized with the casein micelle dispersion or supernatant also had similar elastic and viscous moduli at all amplitudes. However, the interfaces stabilized with the pellet redispersion displayed very weak responses at all amplitudes. No clear softening or hardening behavior was found for these interfaces. The plots are very narrow and show only a mild asymmetry at the highest amplitude. This type of response points either to an interface stabilized with surface active components that are irreversibly adsorbed and display only weak in-plane interactions between the molecules, or to a system in which diffusion between bulk and interface is very fast and (partially) compensates for changes in surface coverage induced by oscillation. The first harmonic based moduli of the O-W interfaces stabilized with the pellet redispersion were much lower than the ones of the interfaces stabilized with the casein micelle dispersion or supernatant (Tab. 3.1). Based on these observations, it appears that micellar caseins did not adsorb at the O-W interfaces, but small aggregates or monomers did.

In order to further distinguish whether the response of the O-W interfaces was dominated by small aggregates or monomers, dilatational oscillatory rheology was also applied on interfaces stabilized with β-casein. If monomers were responsible for the response, we would expect this protein to be dominant, in view of its surface activity. As shown in Fig. 3.4, compared to micellar casein dispersion and supernatant, β-casein stabilized O-W interfaces showed much weaker response during oscillation. β-casein has a highly hydrophilic head and a hydrophobic tail. Therefore, β-casein displays typical water soluble small molecular surfactant properties (Dickinson, 1998), which means that β-casein can adsorb at the interfaces quickly and

spontaneously without forming a network. The in-plane interactions among these molecules are apparently relatively weak, since only low surface pressure values were found in Lissajous plots of O-W interfaces stabilized with β-casein, and the first harmonic based moduli were low (Tab. 3.1).

As micellar caseins were probably not adsorbing at the interfaces, and β-casein stabilized interfaces did not display a strong response during oscillation, the behavior of the O-W interfaces stabilized with casein micelle dispersions appeared to be dominated by small aggregates. Also, in view of the weak response of the redispersed pellet, a situation in which micelles did adsorb but subsequently fell apart seems unlikely.

3.3.4. Nonlinear interfacial rheology of A-W interfaces

Compared with O-W interfaces, A-W interfaces showed higher stiffness during oscillation, which was evidenced by the higher elastic moduli (Tab. 3.1). Similar findings were also reported by (Hinderink, Sagis, Schroën, & Berton-Carabin, 2020). The higher stiffness could be a result of the lower dielectric constant of air, as the dielectric constant of triglycerides is around 3, while the dielectric of air is around 1 (Benjamins, Lyklema, & Lucassen-Reynders, 2006). This will affect the balance between attractive and repulsive interactions among protein molecules at the A-W interface. A relative increase in attractive interactions could lead to stiffer interfaces.

A-W interfaces stabilized with either the casein micelle dispersion or the supernatant showed softening and hardening behaviors similar to those of O-W interfaces. A-W interfaces stabilized with the pellet redispersion displayed the mildest response during oscillation, which was evidenced by the flattest Lissajous plots and the smallest stiffness (Tab. 3.1). Therefore, it can be hypothesized that micellar caseins were not adsorbing at the A-W interfaces either.

In order to estimate the role of individual casein fractions in the behavior of A-W interfaces, systems stabilized with β-casein were studied. As shown in Fig. 3.4, A-W interfaces stabilized with β-casein displayed softening and hardening similar to those observed for the casein micelle dispersion and supernatant. As the properties of interfaces stabilized with β-casein and the supernatant were similar, β-casein may be the dominant protein at the A-W interfaces. The differences among the response of pellet redispersion, casein micelle dispersion, supernatant, and β-casein solution were not as evident

as in the case of the O-W interface. This may be because the amount of β-casein monomers in the samples were different. The pellet was re-dispersed in Milli-Q water, and micellar casein in the pellet may have partially fallen apart. Consequently, β-casein could be present also in the pellet redispersion.

Tab. 3.1. First harmonic based elastic and viscous moduli (mN/m) of O-W or A-W interfaces stabilized with pellet redispersion, casein micelle dispersion, supernatant, or β-casein solution at different strains amplitudes. The frequency of the oscillation was 0.01 Hz.

O-W	pellet redispersion		casein micelle dispersion		supernatant		β-casein solution	
strain	E_1'	E_1''	E_1'	E_1''	E_1'	E_1''	E_1'	E_1''
0.1	1.78±0.25	0.78±0.05	19.21±0.73	5.48±0.41	14.62±0.55	4.23±0.12	1.69±0.08	1.04±0.02
0.15	2.09±0.21	0.75±0.01	15.38±0.86	4.69±0.27	13.55±0.13	3.95±0.18	1.67±0.3	1.1±0.01
0.2	2.31±0.3	0.65±0.01	12.88±0.85	4.04±0.24	12.19±0.08	3.58±0.14	1.8±0.31	1.08±0.06
0.3	2.66±0.39	0.66±0.04	9.41±0.38	3.27±0.18	9.26±0.09	2.9±0.15	1.75±0.09	1.16±0.01
A-W	pellet redispersion		casein micelle dispersion		supernatant		β-casein solution	
strain	E_1'	E_1''	E_1'	E_1''	E_1'	E_1''	E_1'	E_1''
0.1	10.32±2.77	5.25±2.59	12.76±1.22	5.96±2.81	29.74±13.03	16.55±8.45	33.67±14.3	17±4.45
0.15	10.24±2.4	4.85±2.51	13.27±0.41	5.83±2.54	27.38±9.56	15.12±7.09	34.12±13.6	16.23±4.03
0.2	10.04±2.01	4.68±2.26	14±0.59	5.77±2.23	26.14±7.2	14.08±6.18	35.47±13.56	15.67±3.3
0.3	9.87±1.66	4.62±2.03	14.65±0.71	5.88±1.96	25.97±5.94	12.87±5.1	39.25±12.28	14.55±1.83

3.3.5. Visualization of O-W and A-W interfaces

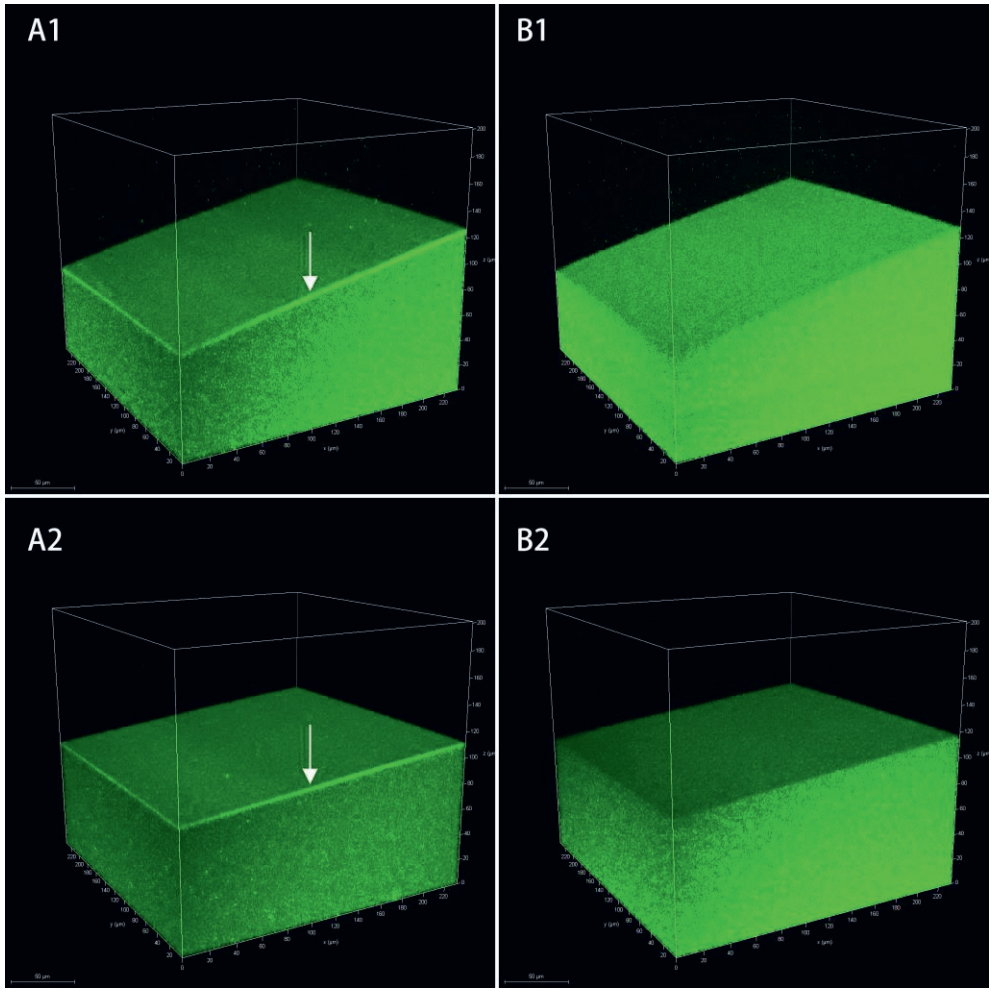

Fig. 3.5. Visualization of O-W (1) and A-W (2) interfaces stabilized with supernatant (A) or pellet redispersion (B). A 3-dimensional region (240*240*200 µm) was scanned by the MPM (see Fig. 3.1). The bottom part of each image is the water phase; the top part is the oil or air phase. The green color represents the proteins. The scale bar in the pictures represents 50 µm.

Based on the surface rheology results, it was hypothesized that micellar caseins do not adsorb at the O-W or the A-W interfaces, and that instead some smaller species such as small aggregates or monomers do. In order to

confirm this hypothesis, O-W and A-W interfaces stabilized with pellet redispersion or supernatant were visualized by multiphoton microscopy (MPM) (Fig. 3.5). Distinct bright interfacial layers were observed for O-W and A-W interfaces stabilized with the supernatant (indicated by arrows). On the other hand, no distinct layers were found for interfaces stabilized with the pellet redispersion. The micelles remained in the bulk phase. The pictures clearly support the hypothesis that micellar caseins adsorb neither at the O-W interface nor at the A-W interface. The protein species from the supernatant were more surface active and could accumulate at the interfaces. The pictures were in line with the rheology results. Further detailed characterizations of O-W and A-W interfaces were carried out by ellipsometry. The A-W interface was also further characterized by atomic force microscopy (AFM).

3.3.6. Thickness of O-W and A-W interfaces

Tab. 3.2. Thickness of interfaces stabilized with casein micelles dispersion, pellet redispersion or supernatant, as measured by ellipsometry.

interface	pellet redispersion (nm)	casein micelle dispersion (nm)	supernatant (nm)
O-W	11.1 ± 1.5	22.2 ± 2.3	27.5 ± 0.1
A-W	4.2 ± 0.1	4.1 ± 0.1	4.4 ± 0.1

The thickness of the studied A-W interfaces or O-W interfaces was characterized using ellipsometry. The thickness of the interfacial layer may also provide additional information on which species preferentially adsorb at the interface. The results are shown in Tab. 3.2. The pellet redispersion formed the thinnest O-W interface, with a thickness around 11 nm. The thickness values of O-W interfaces stabilized with the casein micelle dispersion or supernatant were comparable and were between 20 and 30 nm, which is in the range of the size of small aggregates. This is in line with the results of O-W interfacial rheology, where the dispersion and supernatant had similarly shaped Lissajous plots, and further supports the hypothesis that micellar caseins do not adsorb at the O-W interfaces, but those small aggregates do. The smaller size for the pellet redispersion may be due to adsorption of some residual subunits or monomers (~6 nm) present in that sample.

The thickness of A-W interfaces stabilized with pellet, micelle dispersion and supernatant was roughly the same, i.e. around 4.0 nm, which is close to the size of monomers (O'Connell, Grinberg, & de Kruif, 2003). This also confirms the hypothesis that micellar caseins were not adsorbing on the A-W interfaces.

3.3.7. AFM imaging of A-W interfaces

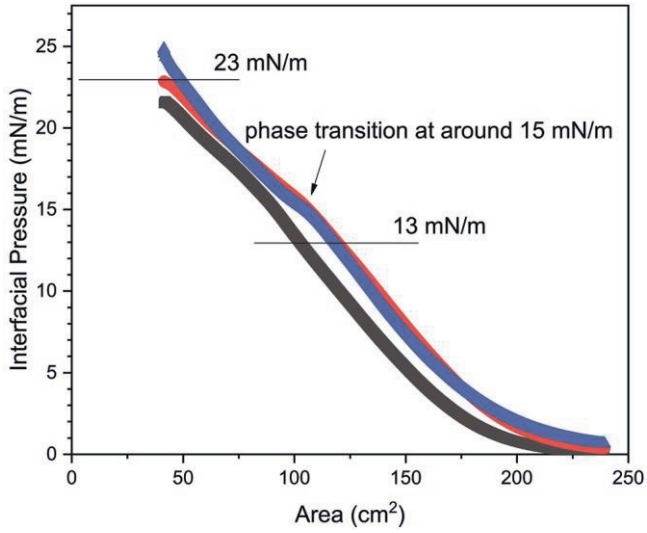

Fig. 3.6. Interfacial pressure isotherms of pellet redispersion (■), casein micelle dispersion (●) and supernatant (▲), obtained using a Langmuir trough.

The microstructure of A-W interfaces was further investigated by creating adsorption-based Langmuir-Blodgett (LB) films, which were analyzed with Atomic Force Microscopy (AFM). The surface pressure isotherms determined using a Langmuir trough are shown in Fig. 3.6. When the surface pressure increased to roughly 15 mN/m, the interfaces stabilized with the casein micelle dispersion, pellet redispersion, or supernatant all showed a change in slope, often associated with a phase transition from a liquid state to a solid state. The isotherm of the micelle dispersion mostly overlapped with the isotherm of the supernatant, which again suggests that the micelle dispersion and supernatant form a similar A-W interface in the liquid regime. To achieve the same surface pressure, the pellet stabilized interface needed to be compressed further, which may indicate a lower amount of material in the pellet redispersion which can adsorb at the interface.

The structure of the A-W interfaces was visualized at a surface pressure of 13 mN/m (Fig. 3.7 A1, B1, C1) and 23 mN/m (Fig. 3.7 A2, B2, C2), so just below and above the liquid-solid transition, respectively. At the lower surface pressure, the microstructures of all three interfaces were remarkably similar. This is in line with the result obtained with ellipsometry, and again indicates that micellar caseins did not adsorb at the A-W interfaces, but only monomers did. At the high surface pressure, all three samples formed dense interfacial films. The supernatant stabilized film formed the densest microstructure, and the pellet formed the least dense one. A lower density of the stabilizer could lead to weaker in-plane interactions among adsorbed proteins, which could contribute to the formation of weaker interfacial layers. The density differences among the samples might explain the A-W interfacial rheology results, where the moduli increased (pellet redispersion < casein micelle dispersion < supernatant, Tab. 3.1) with higher protein density at the A-W interfaces, as shown in the AFM images.

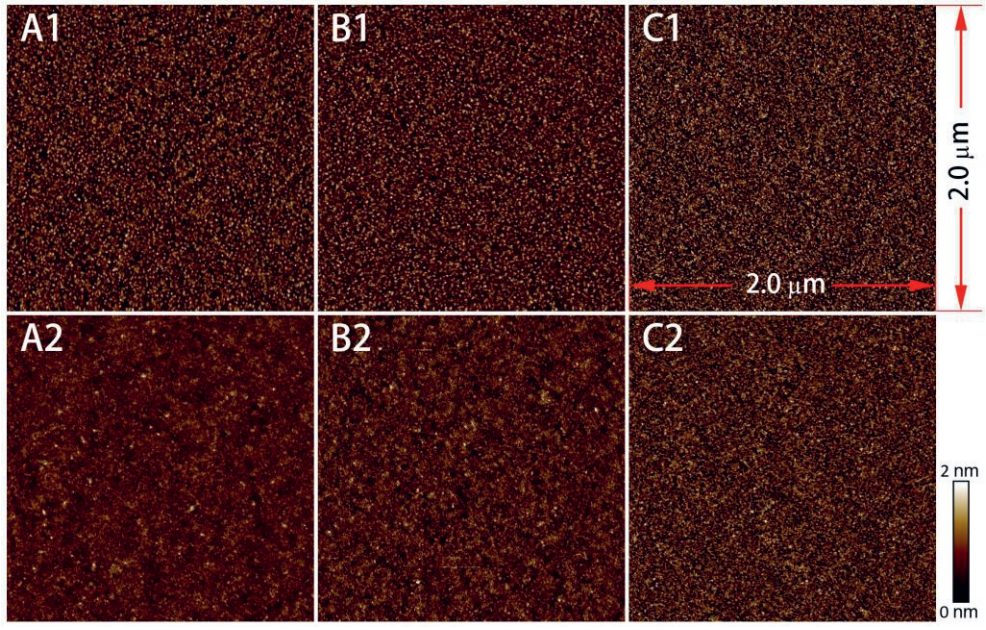

Fig. 3.7. AFM images of A-W interfaces stabilized with pellet redispersion (A), casein micelles dispersion (B) or supernatant (C). The surface pressure values during film sampling were 13 mN/m (1) and 23 mN/m (2). The area of each image represents 2.0 × 2.0 μm^2.

3.4. Conclusion

In this study we comprehensively investigated the role of the different fractions (micelles, small aggregates and casein fraction monomers) present in casein micelle dispersions at O-W and A-W interfaces. The results presented above clearly show that, although casein small aggregates and casein fraction monomers are the minor species in a casein micelle dispersion, they are the main surface-active components. Small aggregates and β-casein determine the mechanical properties of O-W and A-W interfaces, respectively. We did not find any proof that casein micelles stabilize interfaces by a Pickering mechanism (Dickinson, 2015), as micelles adsorb at neither O-W interfaces nor A-W interfaces. A possible reason why the smaller species are dominant at the interface is their faster diffusion towards the interface, in view of their smaller size. There may also be differences in the magnitude of the adsorption barrier energy between micelles and smaller components.

A note we want to make here is that in our study the adsorption of the various fractions was diffusion based. In emulsion and foam preparation there is typically also a convective contribution to the transport of surface active components to the interface. This may be the reason that in some studies in electron microscopy pictures, micelles do appear to be at the oil-water or air-water interfaces (Anderson, et al., 1987; Brooker, 1985; Jensen, 2013). However, their distribution on the surface tends to be sparse, and it is hard to distinguish whether they are actually adsorbed at the interface, or attached to a primary layer of molecules or smaller aggregates. Diffusion can still be a dominant factor in highly turbulent flows, because of the boundary layer that forms close to the bubble or oil droplet interface, in which the flow is laminar and parallel to the interface, and across which the motion of the surface active species towards the interface is mostly diffusive. But we cannot exclude the possibility that some micelles still do adsorb at/to the interface driven by convection.

We also studied only the initial state of the adsorption and did not perform long-term studies. Since emulsions tend to have long shelf lives, proteins may be displaced over time. If this were to happen the most likely scenario would be that the small aggregates are over time displaced by the casein monomer fraction, rather than by the micelles. Further measurements are needed to prove or disprove this scenario.

The approach we have outlined here, based on fractionation of a complex mixture, and on the study of the functionality of the individual fractions using a combination of (nonlinear) surface rheology and microstructural analysis (MPM, ellipsometry, AFM), can help in identifying the most relevant components in the mixture.

References

Anderson, M., Brooker, B., & Needs, E. (1987). Stabilization/Destabilization of Dairy Foams. In Food Emulsions and Foams: Based on the Proceedings of an International Symposium Organised by the Food Chemistry Group of the Royal Society of Chemistry at Leeds from 24th-26th March 1986 (Vol. 58, pp. 100): Royal Society of Chemistry.

Benjamins, J., Lyklema, J., & Lucassen-Reynders, E. H. (2006). Compression/expansion rheology of oil/water interfaces with adsorbed proteins. Comparison with the air/water surface (Vol. 22).

Brooker, B. (1985). Observations on the air-serum interface of milk foams. Food Structure, 4(2), 12.

Carr, A., & Golding, M. (2016). Functional Milk Proteins Production and Utilization: Casein-Based Ingredients. In P. L. H. McSweeney & J. A. O'Mahony (Eds.), Advanced Dairy Chemistry: Volume 1B: Proteins: Applied Aspects (pp. 35-66). New York, NY: Springer New York.

Chen, M., Bleeker, R., Sala, G., Meinders, M. B. J., van Valenberg, H. J. F., van Hooijdonk, A. C. M., & van der Linden, E. (2016). Particle size determines foam stability of casein micelle dispersions. International Dairy Journal, 56, 151-158.

Chen, M., Sala, G., Meinders, M. B. J., van Valenberg, H. J. F., van der Linden, E., & Sagis, L. M. C. (2017). Interfacial properties, thin film stability and foam stability of casein micelle dispersions. Colloids and Surfaces B-Biointerfaces, 149, 56-63.

Courthaudon, J. L., Girardet, J. M., Campagne, S., Rouhier, L. M., Campagna, S., Linden, G., & Lorient, D. (1999). Surface active and emulsifying properties of casein micelles compared to those of sodium caseinate. International Dairy Journal, 9(3-6), 411-412.

Dalgleish, D. G., & Leaver, J. (1991). The possible conformations of milk proteins adsorbed on oilwater interfaces. Journal of colloid and interface science, 141(1), 288-294.

Dalgleish, D. G., Spagnuolo, P. A., & Douglas Goff, H. (2004). A possible structure of the casein micelle based on high-resolution field-emission scanning electron microscopy. International Dairy Journal, 14(12), 1025-1031.

de Vries, R., van Knegsel, A., Johansson, M., Lindmark-Månsson, H., van Hooijdonk, T., Holtenius, K., & Hettinga, K. (2015). Effect of shortening or omitting the dry period of Holstein-Friesian cows on

casein composition of milk. Journal of Dairy Science, 98(12), 8678-8687.

Dickinson, E. (1997). Properties of Emulsions Stabilized with Milk Proteins: Overview of Some Recent Developments. Journal of Dairy Science, 80(10), 2607-2619.

Dickinson, E. (1998). Proteins at interfaces and in emulsions stability, rheology and interactions. Journal of the Chemical Society, Faraday Transactions, 94(12), 1657-1669.

Dickinson, E. (2001). Milk protein interfacial layers and the relationship to emulsion stability and rheology. Colloids and Surfaces B: Biointerfaces, 20(3), 197-210.

Dickinson, E. (2015). Microgels—an alternative colloidal ingredient for stabilization of food emulsions. Trends in Food Science & Technology, 43(2), 178-188.

Dickinson, E., & Matsumura, Y. (1994). Proteins at liquid interfaces: Role of the molten globule state. Colloids and Surfaces B: Biointerfaces, 3(1), 1-17.

Dombrowski, J., Dechau, J., & Kulozik, U. (2016). Multiscale approach to characterize bulk, surface and foaming behavior of casein micelles as a function of alkalinisation. Food Hydrocolloids, 57, 92-102.

Dumpler, J. (2017). Heat stability of concentrated milk systems: Kinetics of the dissociation and aggregation in high heated concentrated milk systems: Springer.

Ewert, J., Claassen, W., Gluck, C., Zeeb, B., Weiss, J., Hinrichs, J., Stressler, T., & Fischer, L. (2016). A non-invasive method for the characterisation of milk protein foams by image analysis. International Dairy Journal, 62, 1-9.

Fox, P. F., & McSweeney, P. L. (2013). Advanced Dairy Chemistry: Volume 1: Proteins, Parts A&B: Springer.

Hinderink, E. B. A., Sagis, L., Schroën, K., & Berton-Carabin, C. C. (2020). Behavior of plant-dairy protein blends at air-water and oil-water interfaces. Colloids and Surfaces B: Biointerfaces, 192, 111015.

Ho, T. M., Bhandari, B. R., & Bansal, N. (2021). Functionality of bovine milk proteins and other factors in foaming properties of milk: a review. Critical reviews in food science and nutrition, 1-21.

Huppertz, T. (2010). Foaming properties of milk: A review of the influence of composition and processing. International Journal of Dairy Technology, 63(4), 477-488.

Jackson, R., & Pallansch, M. (1961). Influence of Milk Proteins on Interfacial Tension between Butter Oil and Various Aqueous Phases. Journal of agricultural and food chemistry, 9(6), 424-427.

Jensen, L. H. S. (2013). Ultrastructure of emulsions - a comparative electron microscopy study.

Lazzaro, F., Saint-Jalmes, A., Violleau, F., Lopez, C., Gaucher-Delmas, M., Madec, M. N., Beaucher, E., & Gaucheron, F. (2017). Gradual disaggregation of the casein micelle improves its emulsifying capacity and decreases the stability of dairy emulsions. Food Hydrocolloids, 63, 189-200.

Leman, J., Kinsella, J., & Kilara, A. (1989). Surface activity, film formation, and emulsifying properties of milk proteins. Critical Reviews in Food Science & Nutrition, 28(2), 115-138.

Li, Y., Li, Y., Yuan, D. D., Wang, Y. N., Li, M. L., & Zhang, L. B. (2020). The effect of caseins on the stability and whipping properties of recombined dairy creams. International Dairy Journal, 105.

Liang, Y. C., Patel, H., Matia-Merino, L., Ye, A. Q., & Golding, M. (2013). Effect of pre- and post-heat treatments on the physicochemical, microstructural and rheological properties of milk protein concentrate-stabilised oil-in-water emulsions. International Dairy Journal, 32(2), 184-191.

Mackie, A. R., Gunning, A. P., Ridout, M. J., Wilde, P. J., & Morris, V. J. (2001). Orogenic Displacement in Mixed β-Lactoglobulin/β-Casein Films at the Air/Water Interface. Langmuir, 17(21), 6593-6598.

O'Connell, J. E., Grinberg, V. Y., & de Kruif, C. G. (2003). Association behavior of β-casein. Journal of colloid and interface science, 258(1), 33-39.

Qi, P. X. (2007). Studies of casein micelle structure: the past and the present. Le Lait, 87(4-5), 363-383.

Ridout, M. J., Mackie, A. R., & Wilde, P. J. (2004). Rheology of Mixed β-Casein/β-Lactoglobulin Films at the Air−Water Interface. Journal of agricultural and food chemistry, 52(12), 3930-3937.

Roman, J. A., & Sgarbieri, V. C. (2006). The hydrophilic, foaming and emulsifying properties of casein concentrates produced by various methods. International Journal of Food Science and Technology, 41(6), 609-617.

Sagis, L. M., & Fischer, P. (2014). Nonlinear rheology of complex fluid–fluid interfaces. Current Opinion in Colloid & Interface Science, 19(6), 520-529.

San Martin-González, M. F., Roach, A., & Harte, F. (2009). Rheological properties of corn oil emulsions stabilized by commercial micellar casein and high pressure homogenization. LWT - Food Science and Technology, 42(1), 307-311.

Scott, L. L., Duncan, S. E., Sumner, S. S., & Waterman, K. M. (2003). Physical properties of cream reformulated with fractionated milk fat and milk-derived components. J Dairy Sci, 86(11), 3395-3404.

Silva, N. F. N., Saint-Jalmes, A., de Carvalho, A. F., & Gaucheron, F. (2014). Development of Casein Microgels from Cross-Linking of Casein Micelles by Genipin. Langmuir, 30(34), 10167-10175.

Tomas, A., Paquet, D., Courthaudon, J. L., & Lorient, D. (1994). Effect of Fat and Protein Contents on Droplet Size and Surface Protein Coverage in Dairy Emulsions. Journal of Dairy Science, 77(2), 413-417.

Walstra, P. (1990). On the stability of casein micelles. Journal of Dairy Science, 73(8), 1965-1979.

Walstra, P. (1999). Casein sub-micelles: do they exist? International Dairy Journal, 9(3-6), 189-192.

Wu, S., Wang, G., Lu, Z., Li, Y., Zhou, X., Chen, L., Cao, J., & Zhang, L. (2016). Effects of glycerol monostearate and Tween 80 on the physical properties and stability of recombined low-fat dairy cream. Dairy Science & Technology, 96(3), 377-390.

Yang, J., Thielen, I., Berton-Carabin, C. C., van der Linden, E., & Sagis, L. M. (2020). Nonlinear interfacial rheology and atomic force microscopy of air-water interfaces stabilized by whey protein beads and their constituents. Food Hydrocolloids, 101, 105466.

Zhang, Z., Dalgleish, D. G., & Goff, H. D. (2004). Effect of pH and ionic strength on competitive protein adsorption to air/water interfaces in aqueous foams made with mixed milk proteins. Colloids and Surfaces B-Biointerfaces, 34(2), 113-121.

Zhang, Z., & Goff, H. D. (2004). Protein distribution at air interfaces in dairy foams and ice cream as affected by casein dissociation and emulsifiers. International Dairy Journal, 14(7), 647-657.

Zhou, X., Chen, L., Han, J., Shi, M., Wang, Y., Zhang, L., Li, Y., & Wu, W. (2016). Stability and physical properties of recombined dairy cream: Effects of soybean lecithin. International Journal of Food Properties, 20(10), 2223-2233.

Zhou, X., Sala, G., & Sagis, L. M. (2020). Bulk and interfacial properties of milk fat emulsions stabilized by whey protein isolate and whey protein aggregates. Food Hydrocolloids, 106100.

Chapter 4

Structure and rheological properties of oil-water and air-water interfaces stabilized with casein and whey protein mixtures

Abstract

The mechanical properties of oil-water (O-W) and air-water (A-W) interfaces stabilized with mixtures of casein and whey protein at different ratios were investigated by interfacial dilatational rheology, at a small (5%) and a large (25%) amplitude. The composition of the layer of proteins adsorbed at the O-W interfaces was investigated by multiphoton excitation microscopy. The structure of A-W interfaces was visualized by atomic force microscopy. The results obtained for O-W interfaces showed that casein preferentially adsorbs and dominates the interface even when present in mixtures in a very low proportion. The interfacial layer formed by casein is weaker and more brittle compared with the one formed by whey proteins. In case of A-W interfaces, casein is more surface active and displays faster diffusion, and leads to a decrease of surface tension to lower values compared with whey protein. Casein will co-adsorb with whey protein at the A-W interface, and the viscoelastic solid-like network normally formed by pure whey proteins at the interface is significantly affected by casein. The interfacial layer becomes more brittle with an increasing proportion of casein in the mixture.

4.1. Introduction

Dairy proteins are naturally amphiphilic and tend to adsorb at oil-water (O-W) and air-water (A-W) interfaces, providing electrostatic and steric repulsions to stabilize oil droplets or air bubbles (Lam & Nickerson, 2013). Because of this behaviour, they are widely used in many food products to stabilize multiphase systems, for example recombined dairy cream, ice-cream, and foamy coffee beverages (Goff, et al., 1989; Scott, et al., 2003; Sharma, et al., 2012; Tomas, et al., 1994; Wu, et al., 2016; Zhou, et al., 2016). Dairy proteins are mainly composed of casein and whey. Quite often, they are used to stabilize emulsions or foams as a mixture, like milk protein concentrate or skimmed milk powder. Quite some research already showed that at interfaces casein and whey can have various interactions, for example, competitive adsorption and displacement (J. M. Brun & D. G. Dalgleish, 1999; Zhang, et al., 2004). Some studies show that casein preferentially adsorbs at O-W interfaces in mixtures of skim milk powder and whey protein isolate (Sourdet, et al., 2002), but can be (partially) displaced by whey proteins at elevated temperatures (> 40^{o}C) (Dalgleish, Goff, Brun,

et al., 2002; Dalgleish, Goff, & Luan, 2002). Preparing formulations with casein and whey protein mixtures to stabilize emulsions or foams is often still done empirically. The relative contributions of casein and whey to emulsion or foam properties are still not completely clear. To mix casein and whey in food emulsions or foam systems can have practical advantages. Some research already showed that to use a mixture of casein and whey proteins can significantly change the heat sensitivity of the emulsions (Chevallier, et al., 2016). Surel, et al. (2014) used different ratios of casein and whey protein to adjust the interfacial composition of emulsions and change their textures. Foam overrun and stability can also be changed by adjusting whey and casein ratios in a system (Borcherding, et al., 2009; Martínez-Padilla, et al., 2014). However, how the proteins in mixtures of casein and whey protein interact at interfaces, thus affecting bulk stability or functionality is not well studied yet. In Chapter 3, we showed that complete micelles adsorb at neither O-W interfaces nor A-W interfaces, and that the smaller fractions present in the dispersion adsorb preferentially at the interface (β-casein for A-W interfaces, and small casein aggregates at O-W interfaces). How this changes when a significant amount of whey protein isolate is added to the dispersion of caseins is not yet completely known.

Some special food products require different stability under different physicochemical conditions, for example whipping cream. This product needs to be statically stable, which will guarantee a long shelf life, but dynamically unstable, i.e. be prone to partial coalescence upon shearing, which is necessary for whipping it into a stable foam (Han, et al., 2018). Correspondingly, the interfaces of the oil droplets present in the cream need to display different properties under static and dynamic conditions. The interface needs to be solid-like under static conditions, which can prevent coalescence. But it needs to become weaker and possibly even show yielding when vigorous shear is applied to the emulsion, which can promote partial coalescence. This large deformation behavior of interfaces can be probed using large amplitude oscillations, either in surface shear or dilatational mode. These test modes are still not widely applied in studies on protein stabilized interfaces. After whipping, the foam needs to be stable and have a long lifetime, so the interfacial structure needs to be able to recover (at least partially) when the deformations stop. Therefore, whether it is possible to use different ratios of casein and whey proteins to tune the mechanical properties of interfaces of emulsions or foams has much practical significance. In recent years, there was increasing attention for the study of

the interfacial properties of plant and dairy protein mixtures (Hinderink, et al., 2020; Yang, et al., 2021). Often, at interfaces plant proteins fail to perform comparably to dairy proteins. To fully characterize the interfacial behavior of mixtures of casein and whey protein can provide a benchmark for research relevant to (partial) dairy protein substitution, and in spite of clear differences between plant and dairy proteins, this may help us to better understand the lower functionality of plant proteins in interface stabilization. A more fundamental understanding of the structure, composition and the mechanical properties of the interfacial layers stabilized with casein and whey protein mixtures can contribute to a more efficient design of formulations or improve the physiochemical properties of related food products (Dickinson, 1999).

In this research, we aimed at understanding the relative contribution of casein and whey protein to the rheological properties of O-W and A-W interfaces stabilized with their mixtures. Small and large amplitude dilatational oscillations were applied to the interfaces to study their mechanical properties. Casein and whey protein were visualized individually at O-W interfaces with a novel method using multiphoton excitation microscopy. The structure of the A-W interfaces stabilized with casein and whey mixtures was visualized by atomic force microscopy.

4.2. Material and methods

4.2.1. Material

Anhydrous milk fat, micellar casein isolate (Refit™, MCI88, 84.15% protein, lactose 3.0%, ash 7.3%, moisture 3.3 %, fat 1.1%) was kindly donated by FrieslandCampina (Netherlands). Whey protein isolate (WPI, Bipro, 88.8% protein content) was purchased from Agropur (Canada). Florisil (60-100 mesh), syringe filters (PVDF, 5.0 µm, d 25 mm; PVDF, 0.45 µm, d 33 mm; PVDF, 0.1 µm, d 33 mm), membrane filters (PVDF, 0.45 µm, d 47 mm) and dimethyl sulfoxide (DMSO) were purchased from Merck (Netherlands). Medium chain triglyceride (MCT) was purchased from IMCD (France). Cyanine 5 NHS ester (Cy5 NHS) and Cyanine 3 NHS ester (Cy3 NHS) were purchased from Lumiprobe (Germany). UV glue, nylon rings (M10) and metal washers (diameter 7 mm) were purchased online (Amazon). Glass slides (#1.5) were purchased from Thermo (Netherlands). Dialysis membranes (3.5kD, #3) were purchased from Spectrum Labs (Greece).

4.2.2. Methods

4.2.2.1. Sample preparation

Whey protein (W) solutions and casein (CA) dispersions were made by stirring whey protein isolate and micellar casein isolate in Milli-Q water overnight. An amount of 0.02 wt% sodium azide was added to prevent spoilage. The obtained whey solution had a protein concentration of 2.0 wt%, and the casein dispersion had a protein concentration of 2.6 wt%. Whey protein solutions were filtered through a syringe filter with a pore size 0.45 µm. Casein dispersions were filtered through syringe filters with a pore size 5 µm and 0.45 µm, successively. The protein content of both the whey protein solution and casein dispersion after filtration was 2.0 wt%, tested by DUMAS (with a coefficient 6.38). The casein dispersion and whey protein solution were subsequently mixed to have different ratios between the two proteins. The mixtures for O-W tests had casein and whey protein ratios of 0:2, 0.05:1.95, 0.1:1.9, 0.2:1.8 and 2:0 (wt%:wt%). The samples for A-W interfaces had ratios of 0:2, 1:1, 1.5:0.5 and 2:0 (wt%:wt%).

4.2.2.2. Oil purification

Anhydrous milk fat (AFM) and medium chain triglyceride (MCT) oil used in this research were first purified. Florisil was desiccated overnight at 105 °C in an oven, then cooled down to room temperature. AMF was melted at 60 °C and mixed with 10 wt% Florisil. The mixture was stirred at 60 °C for at least 2 h. Subsequently, 10 mL of the mixture was sampled and filtered with a syringe filter to remove Florisil particles. The surface tension of the interface between the filtered AMF and Milli-Q water was tested for at least 1 h. If the tension decreased over time, AMF needed to be purified further by repeating the steps described above. Once the surface tension stayed constant, the AMF and Florisil mixture were filtered using vacuum filtration with a filter membrane (PVDF, 0.45 µm, d 47 mm). The filtered AMF was sealed in blue cap bottles and kept in the dark at room temperature. MCT was purified according to the same protocol, but at room temperature.

4.2.2.3. Adsorption kinetics

The surface tension of protein samples against purified anhydrous milk fat or air was monitored over time at 40 °C using a Tracker Automated Droplet Tensiometer (Teclis, France). For O-W interfaces, purified milk fat was transferred to a cuvette and kept at 40 °C. A pendent droplet of the protein

samples with an area of 20 mm^2 was formed at the tip of a needle that was immersed in the milk fat phase. The density of the bulk phase and droplet at 40 °C were 0.90411 and 0.9922 g/mL, respectively. For A-W interfaces, the liquid droplet at the tip of the needle was hanging in an empty cuvette at 20 °C. In order to prevent evaporation of water at the surface of the droplet, a little bit of water was added at the bottom of the cuvette, and the open cuvette was sealed by parafilm. The area of the droplet was set as 15 mm^2. Densities of bulk phase and droplet at 20 °C were 0.0012 and 0.9982 g/mL, respectively. The dynamic interfacial tension over time was monitored for 3 h.

4.2.2.4. Interfacial rheology

After monitoring the tension for 3 h, 5 cycles of oscillation with an amplitude of 5% and a frequency of 0.02 Hz were applied to the droplet interface, followed by 900 s rest to allow for recovery. After recovery, another 5 cycles with an amplitude of 25% and a frequency of 0.02 Hz were applied to the droplet interface. For every round of oscillations, only the middle three cycles were used for constructing Lissajous plots. The construction of Lissajous plots is discussed by Sagis and Fischer (2014), and these are cyclic plots of surface pressure versus strain. The surface pressure (π) and surface strain amplitude (γ) were defined as:

$$\gamma = \frac{A_t - A_0}{A_0} \qquad \text{Eq. 4.1}$$

$$\pi = \sigma_t - \sigma_0 \qquad \text{Eq. 4.2}$$

where A_t and σ_t are interfacial area and interfacial tension at time t; A_0 and σ_0 are the initial interfacial area and interfacial tension of the non-deformed interface.

Apart from the Lissajous plots, we also determined the tangent modulus (E_{dEM}) at zero strain in expansion, as described by van Kempen, et al. (2013).

4.2.2.5. Visualization of the interfaces with multiphoton excitation microscopy (MPM)

In a recent study on the interfacial behavior of aqueous casein micelle dispersions, we showed that complete micelles do not adsorb at either the A-W or O-W interface. We therefore centrifuged the casein micelle

dispersions and performed the visualization of the interfaces with the supernatant only. The latter contains only serum proteins and small micellar aggregates (small fractions of micelles). The method to obtain the supernatant is described below.

4.2.2.5.1. Protein labeling and dialysis

Proteins in the casein supernatant and whey protein solution were labeled individually with fluorescent dyes for visualization. The casein supernatant was made from a casein dispersion, using an ultracentrifuge (Beckman Coulter, US) at 15,000 g for 1 h. The supernatant was collected and filtered with a syringe filter with a pore size of 0.1 µm. The protein content of the supernatant was tested by DUMAS (with a coefficient 6.38) and turned out to be 0.25 ± 0.01 wt%. Both the casein supernatant and whey protein solution were further diluted to a concentration of 0.2 wt% protein. Cy5 NHS and Cy3 NHS were separately dissolved in dimethyl sulfoxide (DMSO) at a concentration of 1 mg/mL. Twenty microliter Cy5 NHS and Cy3 NHS solution were correspondingly added to 1 mL diluted whey protein solution and casein supernatant. The resulting protein dispersions were quickly vortexed for a few seconds and incubated in the dark for 5 min. The labelled whey protein solution and casein supernatant were subsequently dialyzed separately at room temperature in dark, until the conductivity of the surrounding water was constant. The cutoff size of dialysis was 3.5 kDa for both samples. The dialyzed whey protein solution and casein supernatant were mixed to have different casein and whey protein ratios of 0:0.2, 0.002:0.198, 0.01:0.19, 0.02:0.18, 0.04:0.16, and 0.2:0 (wt%:wt%).

4.2.2.5.2. Object slides for MPM

A picture and a schematic of the slides used for MPM are shown in Fig. 4.1. A metal washer and a nylon ring were attached on a glass slide using liquid UV glue. The whole setup was incubated with UV light overnight to solidify the glue.

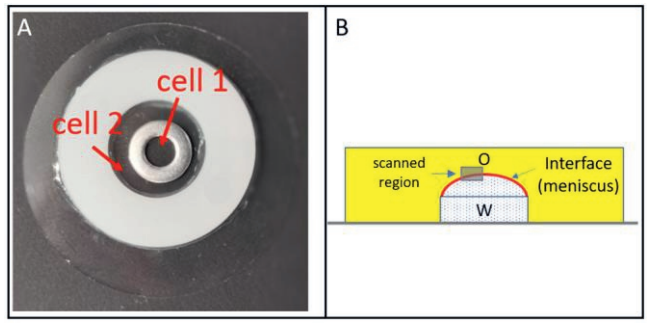

Fig. 4.1. Picture and schematic of the slide used for MPM. (A) top view of the slide; (B) side view of the slide for the O-W interface; 'W' represents the water phase with proteins; 'O' represents oil phase.

4.2.2.5.3. Visualization of the O-W interface

The protein samples made in section 4.2.2.5.1 were slowly pipetted into cell 1 until a meniscus was formed. MCT oil was slowly pipetted into cell 2 until the water droplet in cell 1 was completely immersed. The created interface was equilibrated for 1 h and then visualized by a Leica SP8Dive multiphoton excitation microscope (Leica, Germany), using a HC FLUOTAR L 25×/0.95 W VISIR objective. A three-dimensional region (240 ×240 ×100 µm) was scanned by two channels, individually. One channel was set for Cy3 NHS, with an excitation wavelength of 780 nm and emission wavelength range of 550-600 nm; another one was set for Cy5 NHS, with an excitation wavelength of 840 nm and emission wavelength of 650-700 nm. The Cy3 NHS labelled casein was visualized as green, and Cy5 NHS labelled whey was visualized as red.

4.2.2.6. Interfacial pressure isotherms

Interfacial pressure isotherms (area vs. surface pressure) were made using a Langmuir trough (KSV NIMA/Biolin Scientific Oy, Finland). The trough was first filled with Milli-Q water. Casein dispersion and whey protein solution were diluted to 0.2 wt%. Two hundred microliter of the samples were injected at the bottom of the Langmuir trough using a gas-tight syringe. Afterwards, the system was equilibrated for 3 h, while monitoring the surface pressure using a platinum Wilhelmy plate (perimeter 20 mm, height 10 mm). At last, the interfacial area was reduced by compressing the film with Teflon barriers, moving with a speed of 5 mm/min. The tension was recorded over time.

4.2.2.7. Preparation of Langmuir-Blodgett (LB) films

LB films were also made using a Langmuir trough. The trough was first filled with Milli-Q water. A freshly cleaved mica sheet was fixed vertically with respect to the interface and then immersed in the water phase. Two hundred microliter protein samples were injected at the bottom of the trough, while monitoring the surface pressure using a platinum Wilhelmy plate. After equilibrating for 3 h, the interfacial layer was compressed to a target surface pressure of 13 or 23 mN/m. The interfacial films were deposited on a freshly cleaved mica sheet (Highest Grade V1 Mica, Ted Pella, USA) by pulling the mica sheet upwards at a withdrawal speed of 1 mm/min. During the withdrawing of the mica sheet, the surface pressure was maintained constant by automatic movement of the teflon barriers. All films were produced in duplicate and dried for two days in a desiccator at room temperature.

4.2.2.8. Atomic force microscopy (AFM)

The topography of the LB-films was studied using AFM (MultiMode 8-HR, Bruker, USA). The films were analyzed in tapping mode with a Scanayst-air model non-conductive pyramidal silicon nitride probe (Briker, USA). A normal spring constant of 0.40 N/m and a lateral scan frequency of 0.977 Hz were applied for the analysis. The films were scanned for a 2.0 × 2.0 μm^2 area with a lateral resolution of 512×512 $pixels^2$. To ensure good representativeness, at least two locations of each replicate were scanned. The images were analyzed with Nanoscope Analysis v1.5 software (Bruker, USA).

4.3. Results and discussion

4.3.1. Adsorption kinetics

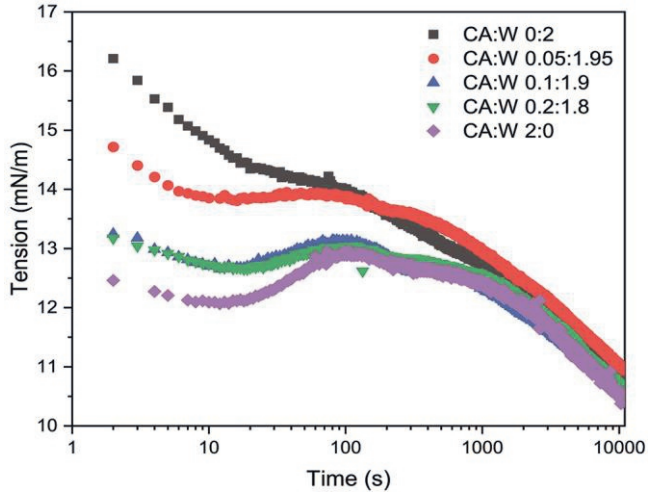

Fig. 4.2. Surface tension as a function of time for mixtures of casein (CA) and whey protein (W) at different ratios at O-W interfaces. The total protein content of each mixture was 2.0 wt%.

The dynamic surface tension of O-W interfaces stabilized with mixtures of casein (CA) and whey protein (W) at different ratios is shown in Fig. 4.2. At a total protein concentration of 2.0 wt%, the surface tension of all the mixtures decreased to a similar extent after 3 h. The main differences between casein and whey protein were visible during the first 10 s and following 10 – 100 s. For the pure whey protein sample, the tension decreased quickly to 14.4 mN/m during the first 10 s. The decrease generally slowed down thereafter. β-lactoglobulin, the main surface active component in whey protein, is a globular protein, and was reported to have a smaller surface tension decrease rate than casein (Dickinson, 1997; Shimizu, 1995). Compared with whey protein, casein decreased the tension to a greater extent to 12 mN/m during the first 10 s, which implies a faster adsorption at the initial stage of the adsorption process. β-casein is one of the most abundant species among the casein fractions in milk (Walstra, 1990). Because of its flexible structure, β-casein can reorient rapidly and adsorb fast at the interfaces (Ho, et al., 2021). Therefore, the fast decrease in tension for casein within the first 10 s may be ascribed to the adsorption

of β-casein. The surface tension of the pure casein sample showed a small increase within the range of 10 – 100 s. In a previous study we showed that casein micelles do not adsorb at the interface and that small casein aggregates are dominant at O-W interfaces. We would expect the free soluble casein proteins present in the dispersion to diffuse faster towards and hence adsorb faster at the interface than small aggregates. A possible explanation of the upswing in surface tension could then be the displacement of serum monomers by aggregates, or the self-assembling of monomers into aggregates at the interface. The mutual displacement between β-casein and α_{s1}-casein at the O-W interface was reported before (Dickinson, et al., 1988). In this research it was not possible to distinguish which of the mentioned mechanisms played a role in the observed increase in tension. For casein and whey protein mixtures, with increasing proportion of casein, the tension decreased to a greater extent during the first 10 s. At a very low ratio CA:W = 0.1:1.9, the dynamic tension beyond 100 s almost completely overlapped with that of the ratio 0.2:1.8 and even with that of pure casein. This may imply that in these mixtures, casein, even at a low proportion, was dominating the interfacial properties. Further evidence is needed to confirm this, which will be shown in later sections (interfacial rheology, section 4.3.2.1, and interface visualization, section 4.3.3).

Concerning A-W interfaces, casein showed a higher surface activity. A higher proportion of casein in the mix led to a lower tension after 3 h adsorption (Fig. 4.3). Based on the surface tension results, no significant synergy between caseins and whey proteins was found. For the pure casein, the upswing in surface tension we observed for O-W interfaces after the first 10 s was also not found. In previous work we showed that at A-W interfaces stabilized with casein dispersions, soluble casein monomers (particularly β-casein) dominated the response. Other studies showed that β-casein preferentially adsorbs at A-W interfaces over other caseins (Mackie, et al., 2001; Zhang, et al., 2004) and is finally dominant at the interfaces (Anand & Damodaran, 1996). Therefore, the displacement among different casein species may happen only to a very limited extent. For mixed casein and whey protein samples, with increasing proportion of casein in the mixture, the dynamic tension curve generally shifted downwards. For A-W interfaces, the dominance of casein even at a low proportion was also not found. At this type of interface, casein and whey are most-likely co-adsorbing.

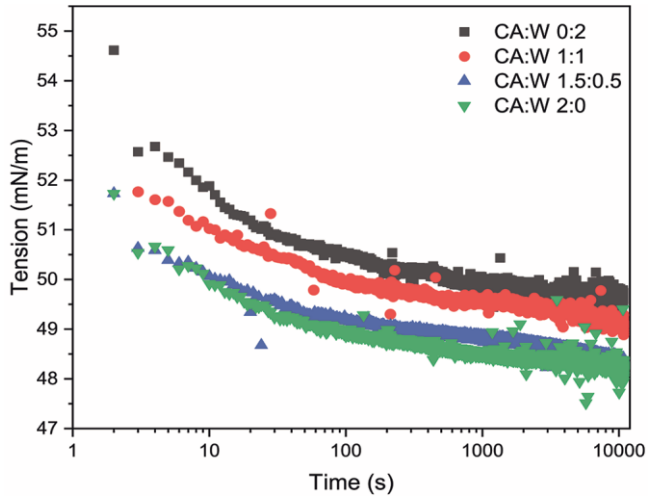

Fig. 4.3. Surface tension as a function of time for casein (CA) and whey protein (W) at different ratios at A-W interfaces. The total protein content of each mixture was 2.0 wt%.

4.3.2. Interfacial rheology

4.3.2.1. O-W interface

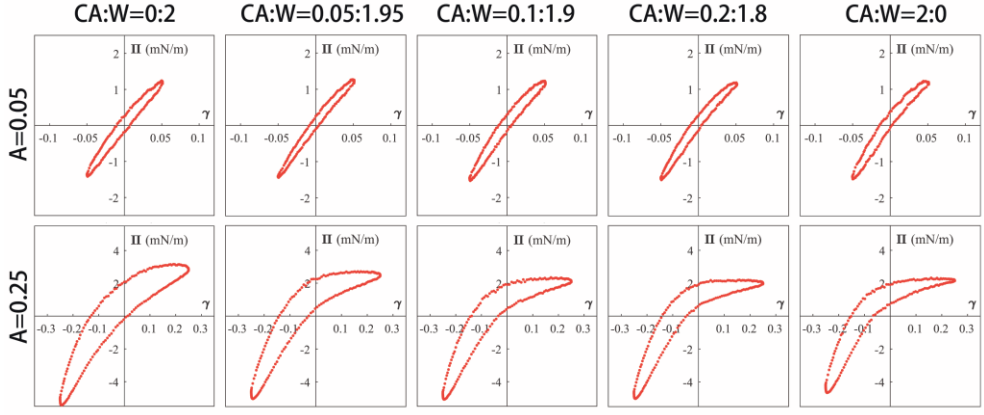

Fig. 4.4. Lissajous plots showing surface pressure versus deformation for O-W interfaces stabilized with mixtures of casein (CA) and whey protein (W) at different ratios. The total protein concentration was 2.0 wt%. The frequency of the oscillation was 0.02 Hz.

Dilatational oscillations were applied to the interfaces stabilized with mixtures of casein and whey protein at different ratios to test their mechanical properties. The Lissajous plots showing surface pressure versus deformation for O-W interfaces are shown in Fig. 4.4. At a small amplitude of 5 %, all the mixture samples showed comparably shaped Lissajous plots which were quite narrow, with limited asymmetry between extension and compression. This shape of the plots indicated a nearly linear response with a dominant elastic component. The elastic and viscous moduli of all the samples were around 25 mN/m and 5 mN/m, respectively (Fig. 4.5). When the amplitude increased to 25%, the response of the interfaces was clearly in the nonlinear regime, as all the Lissajous plots were asymmetrical. For pure whey proteins, clear expansion softening and compression hardening were found. Softening was evidenced by the decrease of the slope of the surface pressure curve in the expansion part of the Lissajous plots (upper part, from left to right), and hardening was evidenced by the increase of the slope of the compression part (lower part, from right to left). Cyclic softening and hardening are normally associated with the (partial) disruption and recovery of interconnected network structures formed by the proteins at the interface (Sagis, et al., 2014; Zhou, et al., 2020). β-lactoglobulin is a relatively small and highly ordered globular protein and was previously reported to construct cohesive networks at interfaces (Rippner Blomqvist, et al., 2004; Torcello-Gómez, et al., 2011), due to strong interactions among molecules by a combination of ionic, hydrophobic and hydrogen bonds (Dickinson, 1998). In the nonlinear regime, the Fourier transform of the stress contains higher harmonics, and the first harmonic alone cannot properly describe the behavior of the interface (Sagis, et al., 2014). As an alternative, to compare the elasticity of the interfaces quantitatively we used here the tangent modulus at minimum expansion (E_{dEM}). As shown in Fig. 4.6, the interface stabilized with whey proteins had the largest E_{dEM}, which is in line with the formation of a strong viscoelastic network for whey proteins, as a result of strong molecular interactions at the interface. When a small amount of casein was present in the mixture (CA:W = 0.05:1.95), the expansion softening tended to be more abrupt, and appeared to turn into expansion yielding, as the slope of the expansion part in Lissajous plots leveled off to almost horizontal. After yielding, the surface pressure was nearly constant, which could be ascribed to mass transfer (diffusion) of β-caseins between the bulk and interface, as observed for some low molecular weight surfactants (Lucassen & Van Den Tempel, 1972; van Kempen, et al., 2013).

Compared with the interface stabilized with pure whey protein, the interface stabilized with a mixture of casein and whey at a ratio 0.05:1.95 had a lower E_{dEM} at the interface. So, the interfacial layer became weaker because of the presence of casein. The network formed by β-lactoglobulin was apparently gradually disrupted by β-casein or small aggregates as their concentration increased, which made the structure more brittle during expansion. At ratios higher than 0.05:1.95, the shape of Lissajous plots and elastic modulus (E_{dEM}) at an amplitude of 25% were quite comparable with those of pure casein. This result was in line with what we observed in the dynamic surface tension test (section 4.3.1), where we saw that casein was dominant at the O-W interface even at a low ratio.

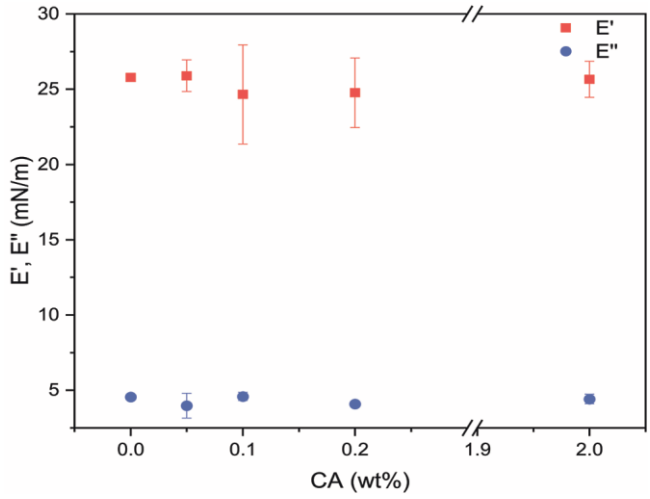

Fig. 4.5. Elastic (*E'*) and viscous modulus (*E''*) of O-W interfaces stabilized with mixtures of casein (CA) and whey protein at different ratios at an oscillation amplitude of 5%. The horizontal axis represents the concentration of CA in the mixture. The total protein concentration was 2.0 wt%.

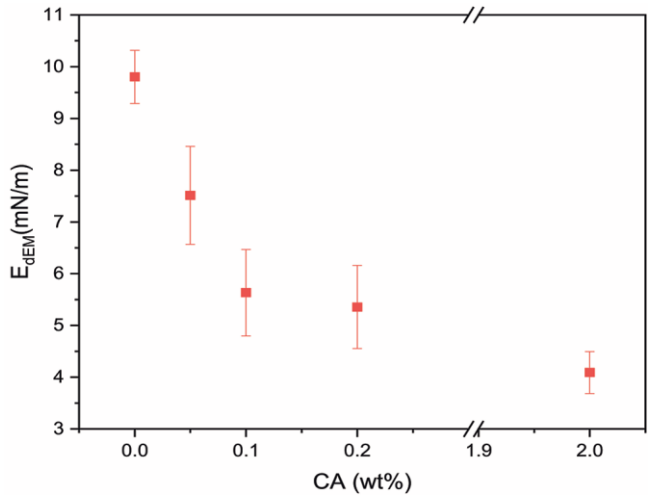

Fig. 4.6. E_{dEM} of O-W interfaces stabilized with mixtures of casein (CA) and whey protein at different ratios at an oscillation amplitude of 25%. The horizontal axis represents the concentration of CA in the mixture. The total protein concentration was 2.0 wt%.

4.3.2.2. A-W interface

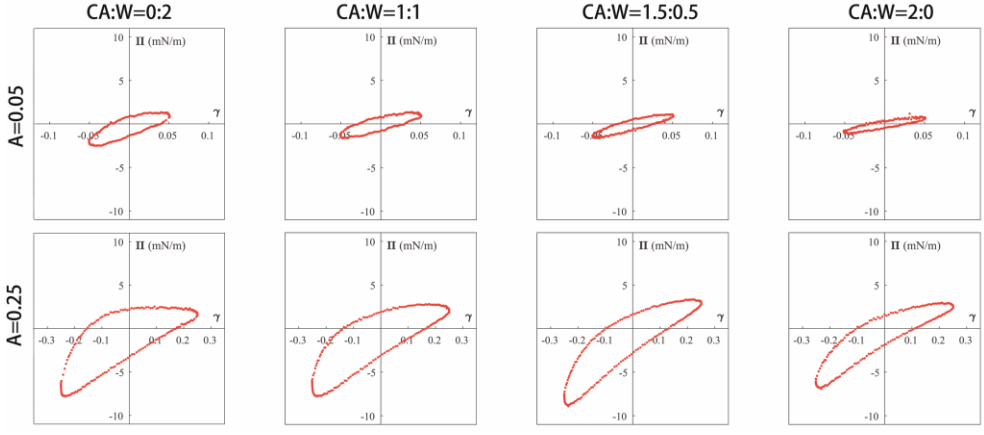

Fig. 4.7. Lissajous plots showing surface pressure versus deformation for A-W interfaces stabilized with mixtures of casein (CA) and whey protein (W) at different ratios. The total protein concentration was 2.0 wt%. The frequency of the oscillation was 0.02 Hz.

A-W interfaces stabilized with mixtures of casein and whey protein at different ratios already showed differences at 5% amplitude of oscillation (Fig. 4.7). With an increasing proportion of casein, the plots became narrower and the slope of Lissajous plots with respect to the horizontal axis became smaller. *E'* and *E''* generally decreased with increasing proportion of casein in the mixture (Fig. 4.8), which implies that at the A-W interface, the interactions among casein molecules were weaker than those among whey protein molecules. At 25% amplitude, pure whey protein showed a very wide Lissajous plot with yielding behavior in expansion, and pure casein showed a more gradual softening behavior. Whey protein showed a steep increase of the stress at the beginning of the expansion, which indicates a stiff structure formed at the interface as a result of strong in-plane interactions between the whey proteins. With an increasing proportion of casein, the structure formed at the interface became weaker, as indicated by the decreasing slope of the initial expansion part of Lissajous plots. This could be because when casein coexisted with whey proteins at the interface, the network formed by β-lactoglobulin was disrupted by casein. These results are similar to the findings of the paper of Petkov, et al. (2000), where the entangled protein network constructed by β-lactoglobulin was disrupted by a more surface active surfactant, Tween 20.

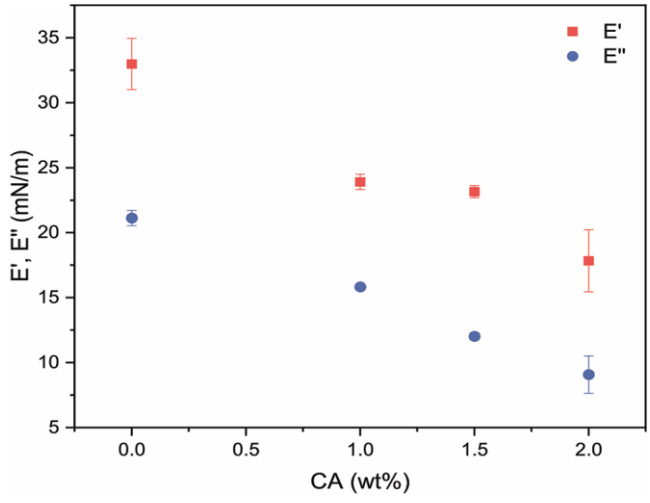

Fig. 4.8. Elastic (*E'*) and viscous modulus (*E''*) of A-W interfaces stabilized with mixtures of casein (CA) and whey protein at different ratios at an oscillation amplitude of 5%. The total protein concentration was 2.0 wt%.

4.3.3. MPM of O-W interfaces

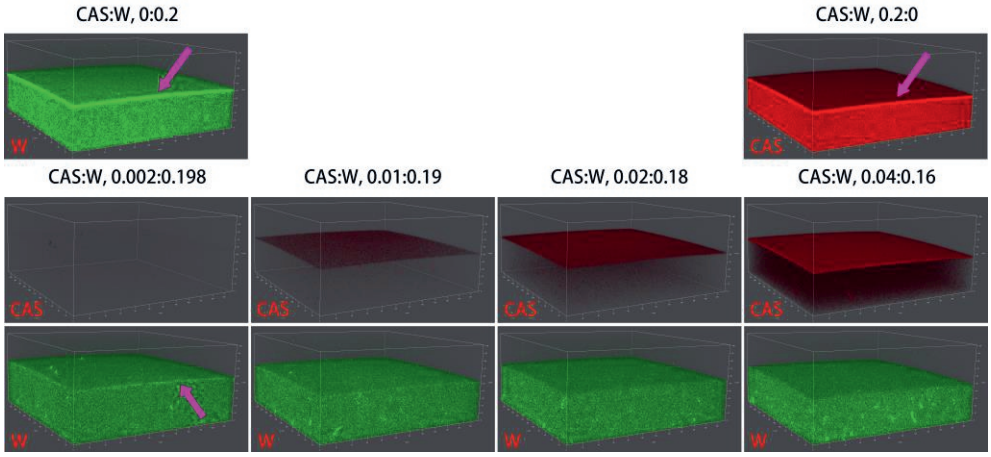

Fig. 4.9. Multiphoton excitation microscopy pictures illustrating protein layers adsorbed at O-W interfaces stabilized with mixtures of casein supernatant (CAS) and whey protein (W) at different ratios. The total protein concentration was 0.2 wt%. For each casein and whey protein mixture, the visualization of casein is shown in the middle row, and the visualization of whey protein is shown in the bottom row.

MPM has already been shown to be a useful technique to identify the protein species at interfaces in the previous chapter. In this experiment, meant to study the competitive adsorption of casein and whey protein at O-W interfaces, instead of a casein dispersion, we used its supernatant obtained by ultracentrifugation. As a matter of fact, in Chapter 3 we already convincingly proved that micellar caseins do not adsorb at the O-W interface, and the main surface-active components, casein fraction monomers and small aggregates thereof, dominate at the interface. So, we assumed that results obtained for casein supernatant can be representative for the entire casein dispersion. As shown in Fig. 4.9, a densely bright protein layer (indicated by an arrow) could be observed at O-W interfaces stabilized solely with casein or whey protein. When a small amount of casein was present in the mixture (CAS:W = 0.002:0.198), the signal at the interface from whey protein became much weaker, but was still distinguishable. The signal from caseins was not detectable. If the casein and whey protein ratio increased to 0.01:0.19, a casein layer was clearly visible, and the whey protein signal at the interface completely disappeared. When the concentration of casein

increased further, the interfacial layer became denser and thicker, and more casein could also be observed in the bulk phase. The results indicated that casein preferably adsorbed at the O-W interface and would be dominant even at a very low concentration. The results proved the hypothesis mentioned in section 4.3.1 and 4.3.2.1. These results diverge from the findings of the research of Dalgleish, Goff, and Luan (2002), where whey protein was reported to displace casein at the O-W interface. The main reason could be because these authors performed the displacement tests at 80 °C. Considerable amounts of casein de-adsorb from the interface to the bulk phase at a higher temperature (Jacqueline M. Brun & Douglas G. Dalgleish, 1999), due to a higher desorption rate of protein from the O-W interface (Fainerman, et al., 2006) and a higher solubility of casein in bulk phase at a higher temperature (Bajpai & Sachdeva, 2000). Our tests were performed at room temperature. Temperature is another important factor that affects the composition of interfaces. These effects were out of the scope of this study, but are an important topic for future research.

4.3.4. Interfacial pressure isotherm

The surface pressure isotherms of the studied samples are shown in Fig. 4.10. The isotherm curve of casein was much lower than the one of whey protein. This could be caused by the concentration difference of surface active species in casein dispersion and whey solution. As mentioned before, micellar caseins will not adsorb at the interfaces, only some monomers or small aggregates are surface active and will do so. The proportion of the surface active species in casein dispersions only accounts for around 16% of the total protein content (based on the data from chapter 3). Consequently, although the total protein content of the two systems was the same, the real content of surface active proteins in the casein dispersion was much lower than the ones in the whey protein solution. Upon compression, whey protein showed the highest surface pressure and two clear phase transitions were observed. For the pure casein, phase transitions were much less evident. This difference could be due to the fact that whey protein mainly consists of globular proteins, which are more rigid than caseins. The interfacial layer formed by casein was consequently more compressible. For casein and whey mixtures, casein and whey proteins may co-adsorb at the interfaces, as shown by the fact that the pressure curves were between those of pure casein and whey protein. Also, phase transitions could not be clearly

observed in the isotherms of mixed samples. These results support the co-adsorption statement in section 4.3.2.2.

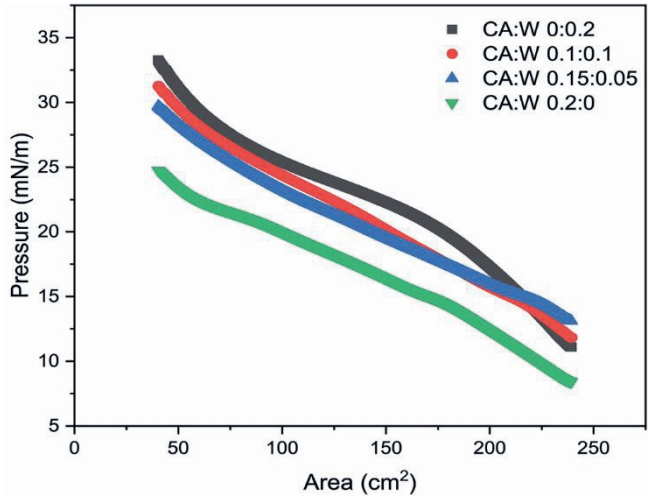

Fig. 4.10. Interfacial pressure isotherms of mixtures of casein (CA) and whey protein (W) at different ratios. The total protein content was 0.2 wt%.

4.3.5. AFM of A-W interface

The microstructure of the A-W interface stabilized with casein and whey protein mixtures at a surface pressure of 13 mN/m and 23 mN/m were visualized by AFM (Fig. 4.11). At 13 mN/m, the interface stabilized with casein and whey mixtures with ratios 1:1 and 1.5:0.5 had a much denser structure compared to the interface stabilized with pure whey protein, which is again an indication of the co-adsorption of casein and whey protein at A-W interfaces.

When the interfaces were further compressed to achieve a higher pressure, 23 mN/m, the whey protein stabilized interface became much denser, and the casein stabilized interface became more heterogenous. Casein molecules were probably pushed together and formed some clusters. A similar structure for casein at the A-W interface was also observed in another study (Gunning, et al., 1996). The heterogenous clustered structure formed after compression could explain the weaker response of the interface stabilized with casein in the Lissajous plots (Fig. 4.7). For interfaces stabilized with casein and whey protein mixtures, no clustered structures were found. When the casein and whey protein ratio was 1:1, the structure

of the interfacial layer was comparable with the one formed by pure whey protein, which implies that at this ratio, although the intermolecular connections may be partially broken by caseins, as described in section 4.3.2.2, whey proteins can still form network structures at the interface. When the casein and whey protein ratio increased to 1.5:0.5, the interface became flatter and smoother. This could be caused by the fact that the interface was already dominated by caseins, and was thus more compressible.

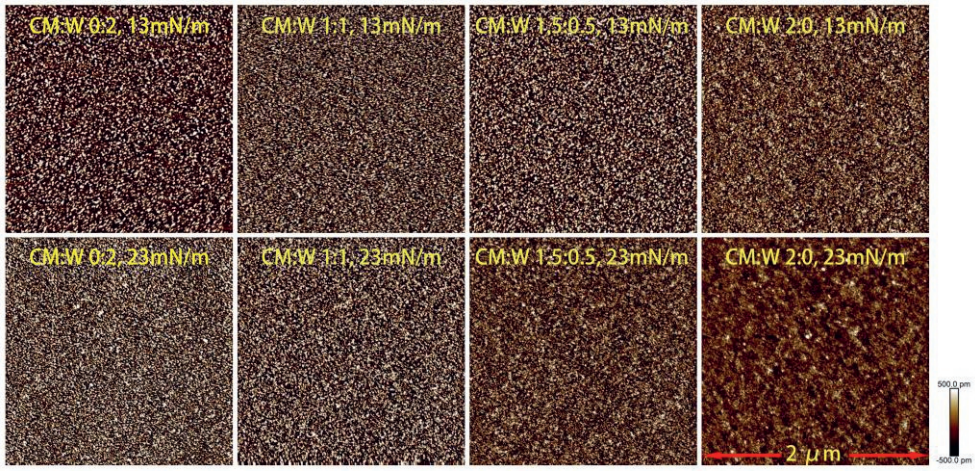

Fig. 4.11. AFM images of A-W interfaces stabilized with mixtures of casein (CA) and whey protein (W) at different ratios.

4.4. Discussion

The findings of this research clearly support the fact that in emulsions stabilized by mixtures of casein and whey protein, the latter protein contributes little to emulsion stability in terms of interfacial composition and mechanical properties. However, adding whey protein may improve foam stability as at the A-W interface it can co-adsorb with casein and form a stiffer interfacial layer with an increasing W:CA ratio. For some special emulsions, vigorous stirring and aeration are applied during processing, for example whipping cream or ice-cream, and casein and whey protein mixtures could be advantageous in these formulations. Our results show that at small amplitude, casein can provide similar mechanical strength to O-W interfaces as whey protein. Therefore, under static conditions cream

made with casein is expected to be as stable against coalescence as one made with whey protein. However, casein stabilized O-W interfaces yield more easily at large deformations, and the interfacial layer becomes weaker afterwards. This is an advantage during whipping, because a weaker interface is beneficial for partial coalescence. After whipping, tiny and stable air bubbles are desired. Although casein can quickly adsorb at the A-W interface, it cannot form a stiff interfacial layer. The stability of the air bubbles can be improved by using whey protein in the formulation. So, adding whey protein to the formulation will not change the properties of O-W interfaces stabilized with casein, but can improve stiffness of A-W interfaces, as whey protein can co-adsorb with casein there. More emulsion and foam stability tests are needed to confirm this.

4.5. Conclusion

The structure and mechanical proprieties of A-W and O-W interfaces stabilized with casein and whey protein mixtures were investigated. At O-W interfaces, casein adsorbs faster and decreases the surface tension to a greater extent at the beginning of the adsorption. However, subsequent displacement (by small casein aggregates) or self-assembling of monomers can happen at the O-W interface, which results in a small upswing of the surface tension, followed by a decrease at longer times. When casein is mixed with whey protein, even at a very low proportion, it will preferably absorb and be dominant at the O-W interface. At a small deformation, O-W interfaces stabilized with whey protein, casein, or mixtures thereof have similar viscoelasticity. However, at a large deformation, whey protein shows stronger intermolecular interactions than casein. At A-W interfaces, casein has higher surface activity than whey protein and displays faster diffusion towards the interface. When casein and whey protein are mixed, they can co-adsorb at the interface, but the network formed by whey protein at the interface will be partially disrupted by casein. The results gained in this research not only improved our understanding on the relative contribution of casein and whey in a mixed system, but also provided some guidance for tailoring the mechanical properties of A-W interface by adjusting the casein-whey protein ratio.

References

Anand, K., & Damodaran, S. (1996). Dynamics of Exchange between αS1-Casein and β-Casein during Adsorption at Air− Water Interface. Journal of agricultural and food chemistry, 44(4), 1022-1028.

Bajpai, A., & Sachdeva, R. (2000). Adsorption of casein onto alkali treated bentonite. Journal of Applied Polymer Science, 78(9), 1656-1663.

Borcherding, K., Chrlorenzen, P., & Hoffmann, W. (2009). Effect of protein content, casein-whey protein ratio and pH value on the foaming properties of skimmed milk. International Journal of Dairy Technology, 62(2), 161-169.

Brun, J. M., & Dalgleish, D. G. (1999). Some effects of heat on the competitive adsorption of caseins and whey proteins in oil-in-water emulsions. International Dairy Journal, 9(3-6), 323-327.

Brun, J. M., & Dalgleish, D. G. (1999). Some effects of heat on the competitive adsorption of caseins and whey proteins in oil-in-water emulsions. International Dairy Journal, 9(3), 323-327.

Chevallier, M., Riaublanc, A., Lopez, C., Hamon, P., Rousseau, F., & Croguennec, T. (2016). Aggregated whey proteins and trace of caseins synergistically improve the heat stability of whey protein-rich emulsions. Food Hydrocolloids, 61, 487-495.

Dalgleish, D. G., Goff, H. D., Brun, J. M., & Luan, B. B. (2002). Exchange reactions between whey proteins and caseins in heated soya oil-in-water emulsion systems - overall aspects of the reaction. Food Hydrocolloids, 16(4), 303-311.

Dalgleish, D. G., Goff, H. D., & Luan, B. B. (2002). Exchange reactions between whey proteins and caseins in heated soya oil-in-water emulsion systems - behavior of individual proteins. Food Hydrocolloids, 16(4), 295-302.

Dickinson, E. (1997). Properties of Emulsions Stabilized with Milk Proteins: Overview of Some Recent Developments. Journal of Dairy Science, 80(10), 2607-2619.

Dickinson, E. (1998). Proteins at interfaces and in emulsions stability, rheology and interactions. Journal of the Chemical Society, Faraday Transactions, 94(12), 1657-1669.

Dickinson, E. (1999). Adsorbed protein layers at fluid interfaces: interactions, structure and surface rheology. Colloids and Surfaces B-Biointerfaces, 15(2), 161-176.

Dickinson, E., Rolfe, S. E., & Dalgleish, D. G. (1988). Competitive adsorption of αs1-casein and β-casein in oil-in-water emulsions. Food Hydrocolloids, 2(5), 397-405.

Fainerman, V. B., Miller, R., Ferri, J. K., Watzke, H., Leser, M. E., & Michel, M. (2006). Reversibility and irreversibility of adsorption of surfactants and proteins at liquid interfaces. Adv Colloid Interface Sci, 123-126, 163-171.

Goff, H. D., Kinsella, J. E., & Jordan, W. K. (1989). Influence of Various Milk Protein Isolates on Ice Cream Emulsion Stability. Journal of Dairy Science, 72(2), 385-397.

Gunning, A. P., Wilde, P. J., Clark, D. C., Morris, V. J., Parker, M. L., & Gunning, P. A. (1996). Atomic Force Microscopy of Interfacial Protein Films. Journal of colloid and interface science, 183(2), 600-602.

Han, J., Zhou, X., Cao, J., Wang, Y., Sun, B., Li, Y., & Zhang, L. (2018). Microstructural evolution of whipped cream in whipping process observed by confocal laser scanning microscopy. International Journal of Food Properties, 21(1), 593-605.

Hinderink, E. B. A., Sagis, L., Schroën, K., & Berton-Carabin, C. C. (2020). Behavior of plant-dairy protein blends at air-water and oil-water interfaces. Colloids and Surfaces B: Biointerfaces, 192, 111015.

Ho, T. M., Bhandari, B. R., & Bansal, N. (2021). Functionality of bovine milk proteins and other factors in foaming properties of milk: a review. Critical reviews in food science and nutrition, 1-21.

Lam, R. S., & Nickerson, M. T. (2013). Food proteins: a review on their emulsifying properties using a structure-function approach. Food Chem, 141(2), 975-984.

Lucassen, J., & Van Den Tempel, M. (1972). Dynamic measurements of dilational properties of a liquid interface. Chemical Engineering Science, 27(6), 1283-1291.

Mackie, A. R., Gunning, A. P., Ridout, M. J., Wilde, P. J., & Morris, V. J. (2001). Orogenic Displacement in Mixed β-Lactoglobulin/β-Casein Films at the Air/Water Interface. Langmuir, 17(21), 6593-6598.

Martínez-Padilla, L. P., García-Mena, V., Casas-Alencáster, N. B., & Sosa-Herrera, M. G. (2014). Foaming properties of skim milk powder fortified with milk proteins. International Dairy Journal, 36(1), 21-28.

Petkov, J. T., Gurkov, T. D., Campbell, B. E., & Borwankar, R. P. (2000). Dilatational and shear elasticity of gel-like protein layers on air/water interface. Langmuir, 16(8), 3703-3711.

Rippner Blomqvist, B., Ridout, M., Mackie, A., Wärnheim, T., Claesson, P. M., & Wilde, P. (2004). Disruption of Viscoelastic β-Lactoglobulin Surface Layers at the Air− Water Interface by Nonionic Polymeric Surfactants. Langmuir, 20(23), 10150-10158.

Sagis, L. M., & Fischer, P. (2014). Nonlinear rheology of complex fluid–fluid interfaces. Current Opinion in Colloid & Interface Science, 19(6), 520-529.

Scott, L. L., Duncan, S. E., Sumner, S. S., & Waterman, K. M. (2003). Physical properties of cream reformulated with fractionated milk fat and milk-derived components. J Dairy Sci, 86(11), 3395-3404.

Sharma, A., Jana, A. H., & Chavan, R. S. (2012). Functionality of milk powders and milk-based powders for end use applications—a review. Comprehensive Reviews in Food Science and Food Safety, 11(5), 518-528.

Shimizu, M. (1995). Structure of proteins adsorbed at an emulsified oil surface. Food macromolecules and colloids, 34-42.

Sourdet, S., Relkin, P., Fosseux, P. Y., & Aubry, V. (2002). Composition of fat protein layer in complex food emulsions at various weight ratios of casein-to-whey proteins. Lait, 82(5), 567-578.

Surel, C., Foucquier, J., Perrot, N., Mackie, A., Garnier, C., Riaublanc, A., & Anton, M. (2014). Composition and structure of interface impacts texture of O/W emulsions. Food Hydrocolloids, 34, 3-9.

Tomas, A., Paquet, D., Courthaudon, J. L., & Lorient, D. (1994). Effect of Fat and Protein Contents on Droplet Size and Surface Protein Coverage in Dairy Emulsions. Journal of Dairy Science, 77(2), 413-417.

Torcello-Gómez, A., Maldonado-Valderrama, J., Gálvez-Ruiz, M. J., Martín-Rodríguez, A., Cabrerizo-Vílchez, M. A., & de Vicente, J. (2011). Surface rheology of sorbitan tristearate and β-lactoglobulin: Shear and dilatational behavior. Journal of Non-Newtonian Fluid Mechanics, 166(12), 713-722.

van Kempen, S. E., Schols, H. A., van der Linden, E., & Sagis, L. M. (2013). Non-linear surface dilatational rheology as a tool for understanding microstructures of air/water interfaces stabilized by oligofructose fatty acid esters. Soft Matter, 9(40), 9579-9592.

Walstra, P. (1990). On the stability of casein micelles. Journal of Dairy Science, 73(8), 1965-1979.

Wu, S., Wang, G., Lu, Z., Li, Y., Zhou, X., Chen, L., Cao, J., & Zhang, L. (2016). Effects of glycerol monostearate and Tween 80 on the physical

properties and stability of recombined low-fat dairy cream. Dairy Science & Technology, 96(3), 377-390.

Yang, J., Waardenburg, L. C., Berton-Carabin, C. C., Nikiforidis, C. V., van der Linden, E., & Sagis, L. M. C. (2021). Air-water interfacial behaviour of whey protein and rapeseed oleosome mixtures. Journal of colloid and interface science, 602, 207-221.

Zhang, Z., Dalgleish, D., & Goff, H. (2004). Effect of pH and ionic strength on competitive protein adsorption to air/water interfaces in aqueous foams made with mixed milk proteins. Colloids and Surfaces B: Biointerfaces, 34(2), 113-121.

Zhou, X., Chen, L., Han, J., Shi, M., Wang, Y., Zhang, L., Li, Y., & Wu, W. (2016). Stability and physical properties of recombined dairy cream: Effects of soybean lecithin. International Journal of Food Properties, 20(10), 2223-2233.

Zhou, X., Sala, G., & Sagis, L. M. (2020). Bulk and interfacial properties of milk fat emulsions stabilized by whey protein isolate and whey protein aggregates. Food Hydrocolloids, 106100.

Chapter 5

Emulsifier crystal formation and its role in repeated deformation-relaxation of emulsion droplets upon cooling

Abstract

When an emulsion is stabilized by monoglyceride stearate (MAG-S), which has a high melting point, and is cooled down to a temperature below the melting point of the emulsifier, an intriguing phenomenon can sometimes be observed. During steady cooling, the emulsion droplets show repeated shape deformation, followed by relaxation back to a spherical shape.

Our hypothesis is that this is an interfacial phenomenon, attributable to two factors: the formation of brittle crystalline solid interfacial layers by the emulsifier, and the stress build-up in these layers due to shrinkage of the oil phase upon cooling. Because of the high stiffness of the interfacial crystal layers, shrinkage of the oil phase leads to wrinkling of the interface, resulting in shape deformations. This continues until the interfacial structure ruptures. The drop subsequently relaxes back to a spherical shape. Upon further cooling, the process repeats itself multiple times, leading to a sequence of shape-deformation - relaxation events, which in this research we refer to as repeated deformation-relaxation (RDR) phenomenon.

Emulsions made with MAG-S or monoglyceride oleate, which will not crystallize above 0 °C, were compared to confirm MAG-S crystallization plays a role in RDR. Two additional types of emulsions were compared to determine the location of crystals responsible for RDR. One was made with medium chain triglyceride oil and MAG-S, in which crystals form at both the interface and in the bulk of the droplet; another one was made with palm kernel oil, in which crystals are formed in the bulk phase of the droplet only. The crystallization process of monoglyceride stearate at the interface was monitored and confirmed by multiphoton excitation microscopy. The effects of MAG-S concentration and cooling rate on the onset temperature (T_w) of RDR were evaluated. The mechanism of the buckling of the interface was illustrated by droplet compression tests in a tensiometer, and finally proved by exposing the emulsion made with MAG-S to stepwise cooling.

The results prove that the formation of emulsifier crystals at the surface of droplets and a continuous cooling process are essential for the RDR to occur. The emulsifiers crystallize at the oil-water interface and form a compact heterogenous layer. In general, the process has a higher onset temperature at higher emulsifier concentration and a lower cooling rate. The results prove our hypothesis and confirm the mechanism how MAG-S stabilizes oil-

in-water emulsions. Namely, they form compact interfacial layers at the surface of oil droplets thus preventing (partial) coalescence.

5.1. Introduction

Emulsion-based food products are ubiquitous in our daily life, for example margarine, mayonnaise, coffee cream and whipping cream. They normally require a long shelf life of several months or even years. However, emulsions are thermodynamically unstable systems, in which several instability phenomena can occur, for example (partial) coalescence and creaming (Fredrick, et al., 2010). Proteins and small molecular weight emulsifiers are widely used as stabilizers in food emulsions. Owning to the amphiphilicity of proteins, they adsorb at the oil-water (O-W) interface to form a stiff viscoelastic layer, which in addition induces steric and electrostatic repulsions between droplets (Amagliani, et al., 2017; Mitropoulos, et al., 2014). However, a disadvantage of protein-stabilized emulsions is that they are sometimes sensitive to other instability phenomena, for example coagulation after heat treatment (Euston, et al., 2000; Liang, et al., 2017), or flocculation (Dickinson, 2019). Small molecular weight emulsifiers lower the O-W interfacial tension significantly to produce smaller droplets upon processing, and typically prevent droplet coalescence by the Marangoni effect (Tadros, et al., 2004). Their disadvantage is that they cannot stabilize emulsions against coalescence as efficiently as proteins, due to the fact that they do not form stiff viscoelastic layers at the interface. Besides proteins and small molecular weight emulsifiers, crystals are also reported to be able to stabilize emulsions. In water-in-oil emulsion, lipid or emulsifier crystals exist in the continuous oil phase and are claimed to stabilize emulsions by a Pickering mechanism (Yang, et al., 2020). In this mode of stabilization, crystals in the oil phase cover the interfaces and form compact layers, thereby hindering water droplet coalescence (Ghosh, et al., 2011; Rousseau, 2000). The stabilization efficiency of crystals largely depends on the position of the crystals in the interface (Johansson, et al., 1995). Conversely, in oil-in-water emulsion, crystals in the dispersed phase are normally reported to result in partial coalescence (Fuller, Considine, Golding, Matia-Merino, & MacGibbon, 2015; Fuller, Considine, Golding, Matia-Merino, MacGibbon, et al., 2015; Moens, et al., 2018). However, some recent research reported that crystals of oil soluble emulsifier in the dispersed phase can stabilize oil-in-water emulsions. Fredrick, et al. (2013) made milk fat cream with

monoglyceride stearate (MAG-S) or monoglyceride oleate (MAG-O) and compared the sensitivity of the two creams to shear-induced partial coalescence. They found that the cream made with MGA-S, which can crystallize inside droplets, was more resistant to partial coalescence. A similar finding was also observed in the research of Goibier, et al. (2017). Both Fredrick, et al. (2013) and Goibier, et al. (2017) ascribed the protective function of MAG-S to its crystals. They proposed two mechanisms. The first one is that MAG-S crystals provide numerous small particles serving as templates for further milk fat crystallization, which results in a faster nucleation rate of milk fat. More and smaller milk fat crystals are subsequently formed inside the droplets (Basso, et al., 2010). Consequently, fat crystals pierce through the interfaces only over small distances. The extent of partial coalescence is subsequently reduced. The second mechanism involves the formation of rigid barriers by MAG-S crystals at the interfaces, that prevent the piercing of milk fat crystals through the membrane. A similar mechanism was also mentioned in the research of Munk, et al. (2014), but there was proposed to be by Pickering stabilization. However, so far, neither the templating effect nor the rigid barrier (or Pickering) mechanism is well supported by evidence in oil-in-water emulsion. Research on how MAG-S forms layers at the O-W interface, is still inconclusive. Crystals could form in the bulk and could move to the interface (Carrillo-Navas, et al., 2013), or the MAG-S could crystallize directly at the interface itself. These two processes are difficult to distinguish because the most frequently used techniques to study crystal formation in multiphase systems, like nuclear magnetic resonance (Fredrick, et al., 2011), differential scanning calorimetry (Derkach, et al., 2018; Neumann, et al., 2018), X-ray diffraction (Mao, et al., 2014) and ultrasound (Mei, et al., 2010; Povey, 2017), cannot discriminate very well between signals of the interface and the bulk phase.

In this research, we aimed at confirming the mechanism according to which MAG-S crystals stabilize oil-in-water emulsion against (partial) coalescence, specifically the formation of MAG-S compact solid layers at the surface of droplets. We studied the crystallization process of MAG-S at a planar O-W interface using multi photon excitation microscopy. The crystallization process of MAG-S in oil-in-water emulsions was monitored by normal optical microscopy. An intriguing phenomenon, repeated deformation-relaxation (RDR) of oil droplets upon cooling was observed during those experiments. A series of experiments was designed to figure out the cause of this new

phenomenon, including (i) comparing emulsions made with different emulsifiers (MAG-S or monoglyceride oleate) or oils (medium chain triglyceride or palm kernel oil); (ii) evaluating the effect of MAG-S concentration and cooling rate on this phenomenon; (iii) performing oil droplet compression tests with a tensiometer, and (iv) subjecting emulsion droplets to stepwise cooling.

5.2. Materials and methods

5.2.1. Materials

Medium chain triglyceride oil was purchased from Cremer Olea GmbH & Co. KG (Germany). Refined palm kernel (PK) oil was kindly provided by Sime Darby Oils (the Netherlands). Florisil adsorbent (60-100 mesh), syringe filters (PVDF, 5.0 µm, d 25 mm; PVDF, 0.45 µm, d 33 mm), filter membrane (PVDF, 0.45 µm, d47 mm) and Tween 80 were purchased from Merck (the Netherlands). Monoglycerides stearate (MAG-S, Palsgaard® DMG 0091), containing 86.0-96.0% C18:0, and monoglycerides oleate (MAG-O, Palsgaard® DMG 0298), containing 79.0-90.7% C18:1 cis were provided by Palsgaard (Denmark). UV glue, nylon rings (M10) and metal washers (7 mm diameter) were purchased online (Amazon). Hermetic aluminium pans (T210701) and lids (T210416) used for differential scanning calorimetry were purchased from TA (The Netherlands). Gene frames (25 µL, adhesives) were purchased from Thermal Fischer (UK).

5.2.2. Methods

5.2.2.1. Oil purification

In order to avoid the effect of surface-active contaminants present in the oil on our results, MCT and PK oil were purified. Florisil was desiccated overnight at 105 °C in an oven, then cooled down to room temperature. MCT oil was mixed with 10 wt% Florisil and was stirred at room temperature for at least 2 h. 10 mL of the mixture was sampled to check whether purification was completed. The sample was firstly filtered with a syringe filter to remove Florisil particles and then used for testing the surface tension against Milli-Q water. If the surface tension decreased over time, the oil was further purified by repeating the steps described above. After achieving a constant surface tension for 1 h, the oil and Florisil mixture was filtered using vacuum

filtration with a filter membrane (PVDF, 0.45 µm, d 47 mm). The filtered oil was sealed in bottles and kept in the dark at room temperature.

5.2.2.2. Emulsion preparation

MCT and PK oil-in-water emulsions with different MAG-S or MAG-O concentrations were prepared. A weight fraction of 0 wt%, 0.1 wt%, 0.5 wt%, 1.5 wt%, 2.5 wt% or 3.5 wt% (oil mass based) MAG-S or MAG-O was added to 20 g MCT or melted PK oil. The oil was preheated in a water bath at 80 °C for at least 10 min. The oil was mixed with 80 g Milli-Q water containing 0.1 wt% (water mass based) Tween® 80. Tween® 80 was used for preventing immediate phase separation (prior to crystal layer formation). The oil water mixture was kept in a water bath at 80 °C for 15 min, then homogenized by Ultra Turrax (IKA T25, Germany) at 10,000 rpm for 5 min. Samples were sealed in blue cap bottles and cooled down quickly to room temperature by tap water. All samples were analysed on the same day they were prepared.

5.2.2.3. Differential scanning calorimetry (DSC)

The crystallization profile of MAG-S and MAG-O, and their crystallization profile in the oil phase were determined with a discovery DSC25 calorimeter (TA instruments, USA). An amount of 10 ± 1 mg samples was put in hermetically sealed aluminium pans with a capacity of 0.7 mL. The MAG-S (or MAG-O) and oil mixtures were kept at 80 °C for 10 min to clear all crystal memory. Subsequently, the sample was cooled to 5 °C with a cooling rate of -5 °C/min, then the temperature was kept constant at 5 °C for 10 min.

5.2.2.4. Optical microscopy

The emulsion droplets were visualized during cooling using a bright field microscope (Axioskop 2 Plus, Zeiss, Germany) equipped with a ×50 long distance objective and a hot stage with temperature control (Linkam, UK). The emulsions were diluted 10 times with Milli-Q water to be able to visualise individual droplets. The diluted emulsion was placed on a microscope slide with a gene frame and sealed with a glass cover. The formation of air bubbles was avoided. Prior to the analysis, sample slides were heated to 80 °C and kept for 10 min. Then, videos were recorded during cooling to 5 °C using different cooling rates: -1 °C/min, -5 °C/min and -10 °C/min. Additionally, a stepwise cooling instead of continuous cooling was performed. The cooling profile vs. time is shown in Fig. 5.1. Each cooling

step had a same cooling rate of -5 °C/min. The duration of each isothermal stage at 30, 25, 20, 15, 10, 5 °C was 2 min.

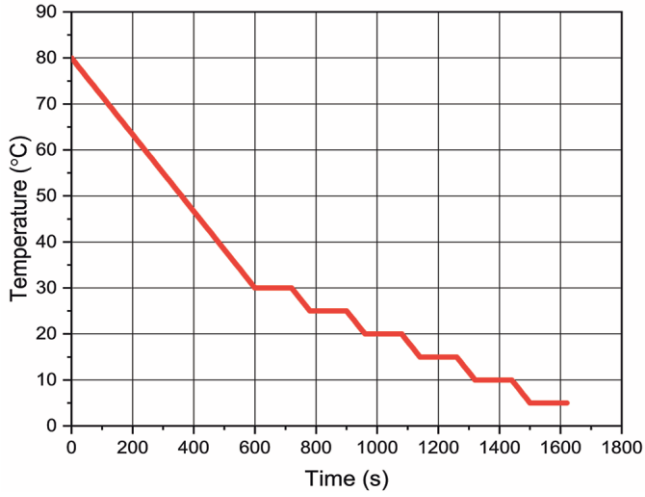

Fig. 5.1. Illustration of the temperature change upon step cooling.

5.2.2.5. Multiphoton excitation microscopy

Multiphoton excitation microscopy (MPM) was used to visualize the crystallization of MAG-S on the interface of a water droplet in MCT oil. For this, a custom-made sample holder was built using UV glue to fix a 7 mm metal washer and a nylon ring to a glass slide (Fig. 5.2A). The glue was solidified by exposing the whole setup to UV light overnight. A little Milli-Q water was slowly pipetted inside the metal washer (cell 1) until a relatively flat surface was obtained. A solution of 1.0% MAG-S in MCT oil at about 80 °C was pipetted inside the nylon ring (cell 2) until the water layer was fully covered. The central region of the O-W interface formed was visualized using a Leica SP8Dive multiphoton excitation microscope (Leica, Germany) with a HC FLUOTAR L 25×/0.95 W VISIR objective. The laser excitation wavelength was set at 552 nm, and the emission range of the detector was set at 549-554 nm. Horizontal 2-dimensional (2D) scans were recorded at different heights to locate the central region of the interface (region shown in grey in Fig. 5.2B). 2D scans of this region were continuously recorded while the sample was allowed to cool at room temperature. The focus of the laser had to be adjusted slightly during the experiment, probably due to volume changes during cooling. In addition to these 2D scans, a surrounding 3-

dimensional region (240*240*200 µm) was scanned after the detection of crystals on the interface.

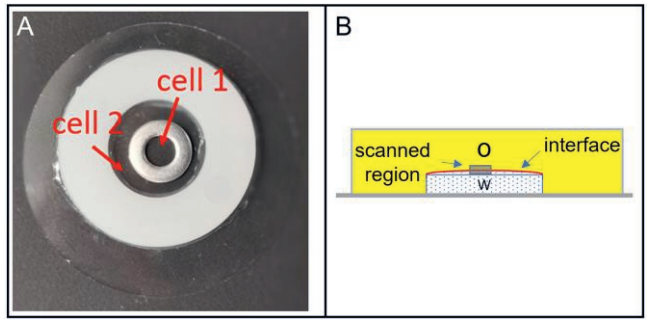

Fig. 5.2. Picture and schematic of slides for MPM. (A) Top view of the slide; (b) Side view of the slide for visualizing the O-W interface. 'W' represents water phase; 'O' represents the oil phase with MAG-S.

5.2.2.6. Droplet compression test

A droplet compression test was carried out with an automated droplet tensiometer (Teclis, France) using a "rising drop" configuration. The syringe of the tensiometer was filled with a 1.0 wt% MAG-S solution in MCT oil. The temperature of the syringe holder and the cuvette holder were controlled with an external water bath. The temperature was initially set at 80 °C for at least 10 min to be sure there was no crystallization in the syringe. A rising droplet was formed at the tip of a 'U' shape needle, which was connected with the syringe and was immersed in Milli-Q water inside a cuvette. The surface area of the droplet was 10 mm^2. Subsequently, the temperature of the water bath was decreased to 20 °C by adding ice and then kept at that temperature for 10 min. The area of the droplet was compressed by withdrawing the inner liquid from the droplet. As the automatic withdrawing speed of the equipment was too fast to monitor shape changes accurately, the compression was performed manually by quick clicks on the controller.

5.3. Results

5.3.1. Crystallization profiles

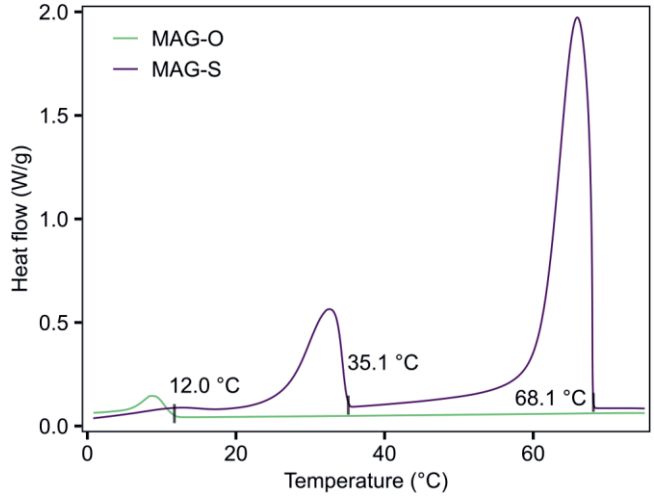

Fig. 5.3. Crystallization profiles of MAG-S and MAG-O upon cooling.

In order to find out the cooling range within which MAG-S and MAG-O show different physical states (liquid or solid), the crystallization profile of pure MAG-O and MAG-S (Fig. 5.3), and their crystallization process in MCT oil (Fig. 5.4) were characterized by DSC. For MAG-S, two exothermic peaks with onset temperatures of 68 °C and 36 °C were recorded. It is well known that these peaks correspond to the formation of two types of crystals, α- and sub-α- polymorphs (Vereecken, et al., 2009). For pure MAG-O, only one exothermic peak with a low onset temperature of 12 °C was recorded during cooling. This peak corresponds to the formation of β-polymorph crystals (Vereecken, et al., 2009). When the monoglycerides were dissolved in MCT oil, the crystallization temperature of MAG-S decreased to 25.7 °C, and MAG-O did not show any crystallization between 0 to 80 °C (Fig. 5.4). When the emulsifiers were dissolved and diluted in the oil phase, the crystallization temperature of the oil shifted to a lower temperature because of mixing entropy. MCT oil crystallized at temperatures lower than -10 °C in both mixtures. As a result, it was possible to use MCT oil with 1.5 wt% MAG-S to make emulsions and adjust the physical state of MAG-S via cooling from 60 to 5 °C. The emulsions made with MAG-O were used for comparison, since

from the above results no crystal formation in emulsions containing MAG-O could be expected within the temperature range of 5-60 °C.

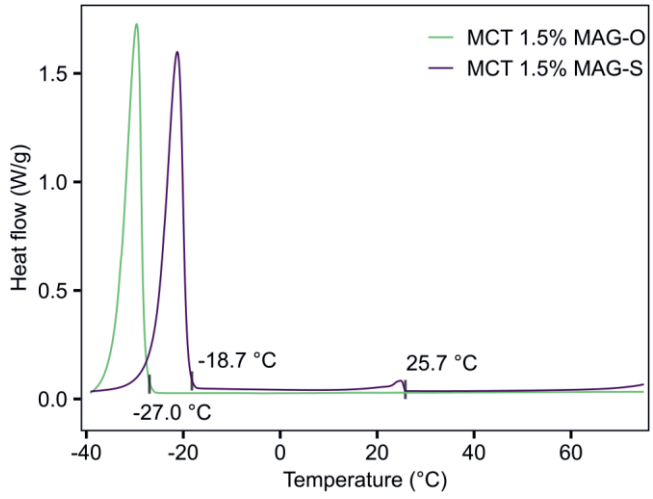

Fig. 5.4. Crystallization profiles of MAG-S and MAG-O in MCT oil upon cooling.

5.3.2. Visualization of emulsifier crystals at the O-W interface

So far, the crystallization of emulsifiers at the O-W interface has not been convincingly confirmed, because it is difficult to clearly identify the location of the crystals (i.e. whether they are formed inside the bulk phase of droplets or at the interfaces) with a normal optical microscope. Here, the growth of the crystals was monitored using multiphoton excitation microscopy. Initially, no structure was formed at the interface (Fig. 5.5A). While the temperature of the sample slowly cooled down to room temperature, after 15 s, several areas with a size of 2-5 µm could be observed where crystals were forming at the interface (Fig. 5.5C). At 25 s, crystalline regions showed a petal shape and kept expanding (Fig. 5.5D). After 35 s (Fig. 5.5E and Fig. 5.5F), every crystalline region had a size over 50 µm and stayed still at the interface. Some regions showed a typical dendritic pattern, which is normally observed in supercooled melts and supersaturated solutions (Alexandrov, et al., 2021; Mullin, 2001). The crystalline regions kept growing until they touched each other (Fig. 5.5G). When all the crystal regions were connected, a compact solid layer was formed at the interface (Fig. 5.5H). The layer was heterogenous, where some parts were thicker and denser, while others were thinner. When the sample was completely cooled down, a 3D

zone was scanned again. As shown in Fig. 5.5B, crystal particles could also be observed in the oil phase (upper layer), but crystallization was most evident at the O-W interface.

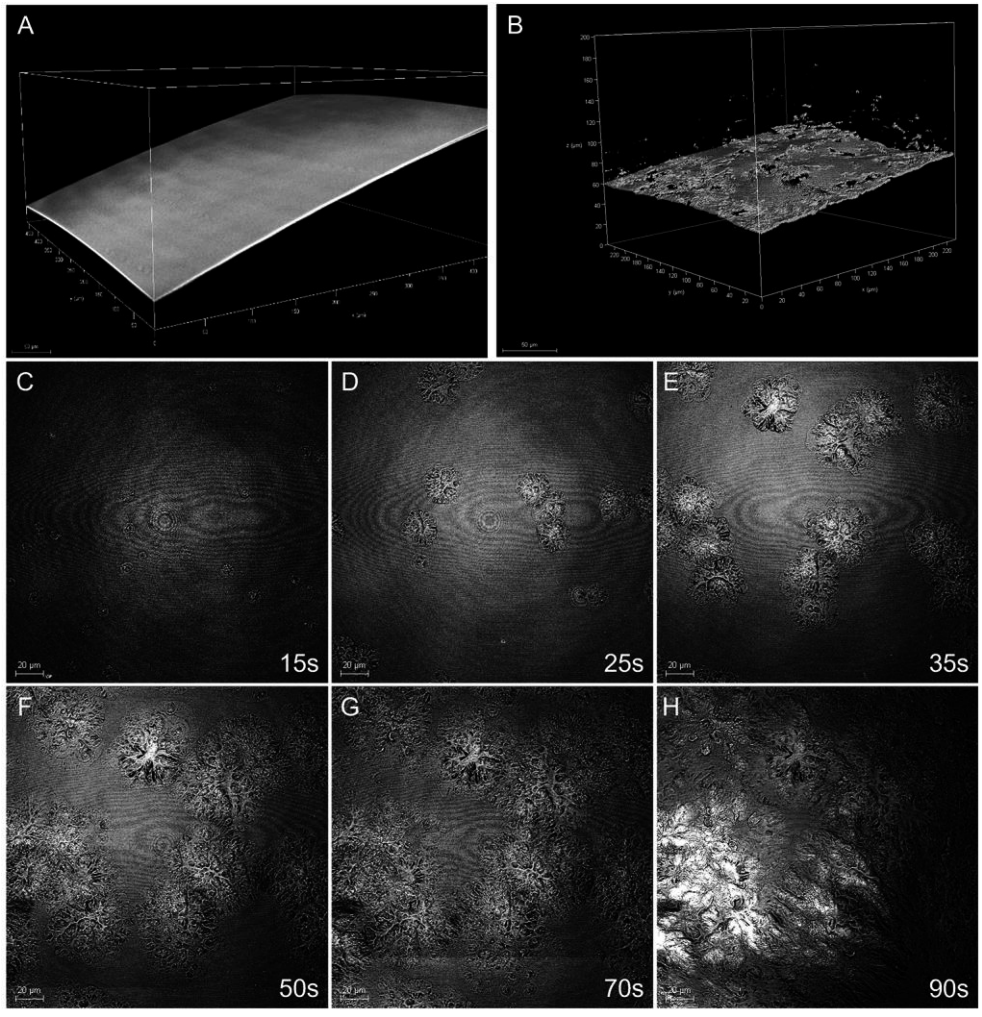

Fig. 5.5. Growth of MAG-S crystals at the O-W interface over time. Pictures were obtained using multiphoton excitation microscopy. A: 3D scan of the sample before crystallization of emulsifiers. The bright layer is the O-W interface, with the oil phase (with 1.0 wt% MAG-S) on top, and the water phase at the bottom. B: 3D scan of the sample after crystallization. C-H: growth of MAG-S crystals at the O-W interface at different times (15, 25, 35, 50, 70, 90 s).

5.3.3. Visualization of emulsion droplets

The crystallization process of the MAG-S in emulsions upon cooling was monitored by means of microscopy analysis (Fig. 5.6). Initially, all the droplets stayed liquid and spherical. When the temperature decreased to 22 °C, wrinkles could be observed at the surface of some droplets, and those droplets started to deform, as indicated by the red arrows in Fig. 5.6B. However, most of the droplets remained spherical at 22 °C. When the temperature further decreased to 19 °C, almost all the droplets deformed and the wrinkles at the surface of the droplet were more evident. After the sample was cooled to 10 °C, the winkling and buckling phenomenon of droplets was no longer observed. Most of the droplets showed a cone-like shape and that shape remained till the end of cooling (5 °C). We took the emulsion made with 2.5 wt% MAG-O as a comparison, and the droplets remained spherical during the whole cooling process (Fig. S 5.1). Therefore, we concluded that the deformation of droplets and appearance of the wrinkles at the surface of the droplets were the result of the formation of MAG-S crystals. Interestingly, when we looked in detail at the buckling of a single droplet, an intriguing phenomenon was observed, and the phenomenon actually happened on most of the other droplets.

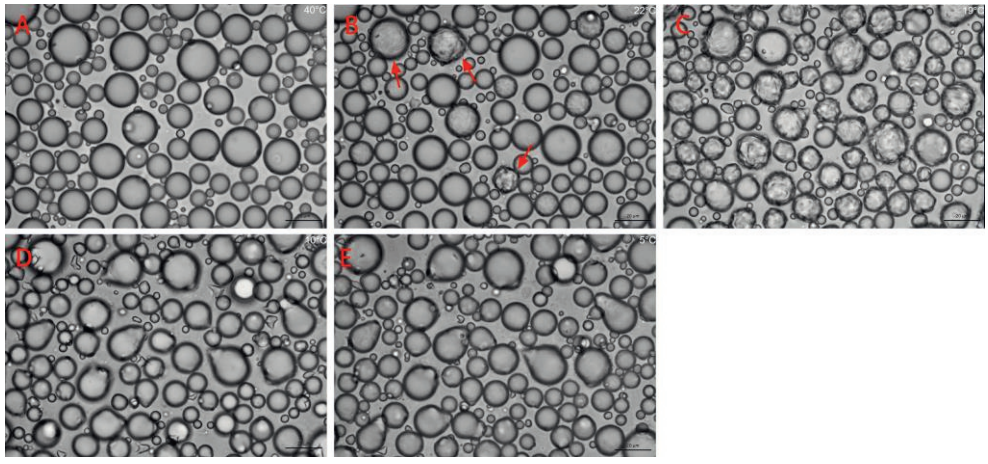

Fig. 5.6. Change in morphology of emulsion droplets stabilized with MAG-S (1.5 wt%) upon cooling (40 °C – 5 °C). The cooling rate was -10 °C/min. A-E are the views of the emulsion at 40, 23, 19, 10 and 5 °C, respectively. The scale bar represents 20 µm.

A schematic representation of the dynamic evolution of this phenomenon is shown in Fig. 5.7. As in the aforementioned observation, the droplet was initially spherical, and the interface was smooth (Fig. 5.7.1). As a result of cooling, some wrinkles formed at the interface, and the shape of the droplets gradually became less non-spherical (Fig. 5.7.2-Fig. 5.7.3). The droplet kept deforming until its shape was completely irregular, and its surface became much rougher (Fig. 5.7.4). Apparently, during this step, some defects and wrinkles were formed at the surface of the droplet. However, these defects or wrinkles subsequently disappeared, and the droplet quickly relaxed back to a nearly spherical shape (Fig. 5.7.5-Fig. 5.7.7). Several sequences of these deformation-relaxation events were observed on most droplets. They repeated steps 1-7 once or more times, so they showed RDR. After RDR, a solid grain was observed at the surface of the droplet, and it generally grew (Fig. 5.7.8-5.7.9). Finally, the droplet displayed a cone-like shape and did not change anymore.

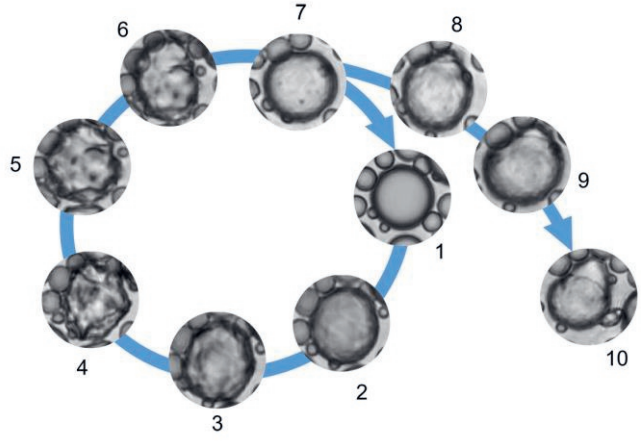

Fig. 5.7. Schematic of repeated deformation-relaxation phenomenon of emulsion droplets upon cooling. The pictures were obtained from an emulsion made with 1.5 wt% MAG-S; the cooling rate was -15 °C/min.

The cone-like shape formation was also found in the research of Spicer, et al. (2005). They suggest this is the result of the de-wetting of the emulsifier crystals by the oil phase. Emulsifier crystals formed at the surface or inside the droplet were being expelled from the oil droplet (Sato, 2018; Spicer, et al., 2005). To our knowledge, the RDR has not been reported before, and is clearly induced by MAG-S crystallization. In the following sections, we

further investigated the mechanisms how MAG-S crystals induce RDR. Effects of the type of oil, emulsifier concentration and cooling process parameters on RDR were evaluated.

5.3.4. Effects of type of oil

Comparing emulsions made with MAG-S and MAG-O suggested that MAG-S crystals were responsible for the RDR. As shown in section 5.3.2, MAG-S crystallized not only at the O-W interface, but also in the oil phase. To further distinguish which fraction of crystals was playing a role in RDR, emulsions made with MCT oil or PK oil were compared. It is known that PK oil crystallizes in a range 0-10 °C (see Appendix, Fig. S 5.5), and the crystals are expected to be formed in the bulk phase of the droplet, and not at the O-W interface (Fredrick, et al., 2013; Van Boekel, 1980). The crystallization process of emulsion droplets made with PK oil but without MAG-S was recorded and is shown in Fig. S 5.2. During crystallization, PK oil droplets were elongated into an oval shape, but did not show further deformation or relaxation. At the end of the cooling process, the droplets were entirely solidified, and the oval shape was maintained. However, when MAG-S was added back to the PK oil emulsion, the deformation-relaxation phenomenon could be observed again (Fig. S 5.3). It was noticeable that the droplets deformed much more slowly than the droplets made with MCT and MAG-S, and the deformation-relaxation was repeated fewer times. This may be ascribed to the high viscosity and low flowability of PK oil droplets when crystals are formed inside. PK oil crystals increased the solid content of the droplet, which would increase viscosity (Konijn, et al., 2014). The PK oil droplet was thus more solid like and resistant to deformation. These results proved that the MAG-S crystals are an essential factor for the repeated buckling of droplets upon cooling, and the phenomenon is clearly an interfacial one, and not caused by bulk crystallization.

5.3.5. Effects of cooling rate and emulsifier concentration on RDR

Since emulsifier crystals formed at the interface appeared to be essential for the deformation-relaxation phenomenon to occur, emulsifier concentration and cooling process parameters would be key factors that affect the phenomenon, because they affect the crystallization of emulsifiers. Emulsions made with different MAG-S concentrations were tested with different cooling rates. The results are shown in Fig. 5.8. The temperature at which more than 10 droplets in the view field of the optical microscopy

started to show wrinkles (Fig. 5.7.2) was referred to as T_w, and was chosen as an indicator for the onset temperature of the RDR.

The RDR was not observed in emulsions made with 0.1 wt% MAG-S at any of the cooling rates. Clearly, there was a minimum MAG-S concentration for this phenomenon, and below this concentration probably insufficient MAG-S molecules were present in the system to form a sufficiently rigid film at the interface. As seen in Fig. 5.8, with an increasing cooling rate, the T_w of emulsions slightly decreased for all MAG-S concentrations. Compared with cooling rate, the effect of MAG-S concentration was more prominent. At a cooling rate of -5 °C/min, when the concentration increased from 0.5 wt% to 1.5 wt%, the T_w increased from 14.0 °C to 22.1 °C and then stayed constant until the concentration increased to 2.5 wt%. As the concentration increased further from 2.5 wt% to 3.5 wt%, T_w increased again to a value of 39.4 °C. The effect of emulsifier concentration on T_w was also observed for other cooling rates. At the cooling rate of -20 °C/min, the T_w for 1.5 wt% MAG-S emulsion was a bit lower than the one for 2.5 wt% MAG-S emulsion, but the difference was small and within the margin of error.

The results discussed in section 5.3.2 showed that upon cooling a compact solid interfacial layer can be formed by MAG-S at the O-W interface, and the insights of section 5.3.4 proved that the RDR is an interfacial phenomenon. Combined with the results in this section, we could deduce that the phenomenon was linked to the formation of a compact shell at the O-W interface.

When the emulsion had a concentration of 0.1 wt% MAG-S, the deformation-relaxation phenomenon was not observed because concentration was not high enough to form a compact interfacial layer. When the concentration increased to 0.5 wt%, more crystals could be formed upon cooling, and the RDR could be observed. At concentrations between 1.5 wt% and 2.5 wt%, the emulsions had similar T_w. This could be because at the lower concentration the interfaces were already saturated, thus the local concentrations at the interface were comparable. A possible explanation for the higher T_w at the concentration of 3.5 wt%, is that reverse micelles could have formed in the bulk oil phase (Gaonkar, et al., 1991) and promoted bulk nucleation. When some crystals from the bulk phase attached at the interface, crystallization at the interface could happen earlier due to heterogeneous nucleation. In terms of the effect of cooling rate, a faster cooling rate was coupled with a lower T_w (Fig. 5.8). This could

be because it took time for crystals to grow and cover the interface. A faster cooling rate means the temperature decreased more when the interface was completely covered. As a result, a lower T_w was observed.

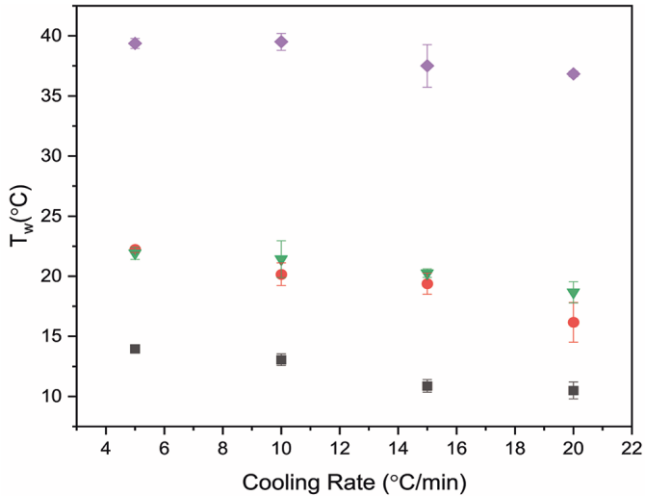

Fig. 5.8. Effects of cooling rate and MAG-S concentration on the T_w of RDR. The chosen MAG-S concentrations were 0.5 wt% (■), 1.5 wt% (●),2.5 wt% (▼), 3.5 wt% (◆).

5.3.6. Droplet compression test and stepwise cooling

Based on the evidence discussed above, it is reasonable to assume the RDR phenomenon to be related to the formation of a compact crystalline solid interfacial layer, but such a layer by itself is not enough to drive the buckling of the interface. Stress buildup in the layer is needed to cause it to buckle and rupture. The shrinkage of the bulk phase of the oil droplet induced by cooling could be a possible cause of the stress buildup. To prove this, we created a droplet of MCT oil containing 1.0 wt% MAG-S at the tip of a syringe in a tensiometer, immersed in Milli-Q water, as illustrated in Fig. 5.9. Before compression, a solid layer was allowed to form at the interface via cooling (Fig. 5.9A), and the obtained interface was smooth. Upon compression, wrinkles appeared almost instantaneously (Fig. 5.9B). When the droplet was further compressed, it became distorted and showed an irregular shape (Fig. 5.9C), which was similar to the observation for emulsion droplets upon cooling. In the emulsions, the shrinkage of the bulk phase of the oil droplets was caused by the decrease of temperature, and thus a stepwise cooling test

was performed to prove this hypothesis, of which pictures are shown in Fig. S 5.4.

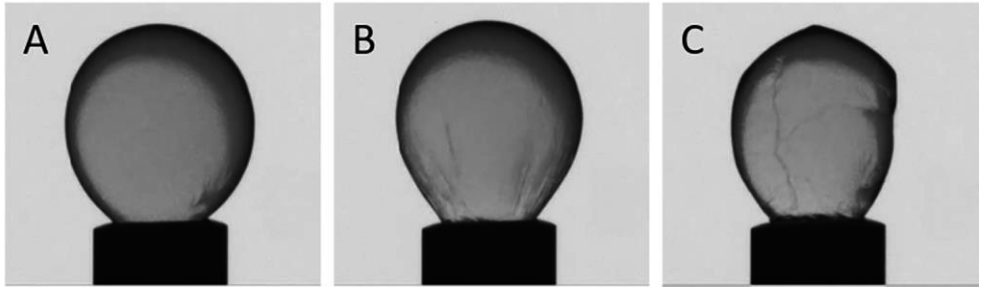

Fig. 5.9. MCT droplet (10 mm^2) with 1.0 wt% MAG-S formed at the tip of the needle in a droplet tensiometer. The droplet was immersed in Milli-Q water and was kept for 10 min at an ambient temperature of 22 °C. Subsequently, the interface was compressed by withdrawing fluid from the bulk phase. A, the droplet before compression; B, the droplet upon compression; C, the droplet after compression.

The images clearly illustrated that the deformation-relaxation phenomenon only happened when the temperature decreased. During the isothermal stages, the droplets did not deform any further and retained their shape. Consequently, we can conclude that the formation of emulsifier crystals at the surface of oil droplets is not the only essential factor inducing the deformation-relaxation phenomenon. A continuous cooling process is also required, which results in the shrinkage of the bulk phase of the droplets. This shrinkage results in stress buildup in the interface, and when a critical stress is exceeded, the interface buckles and eventually ruptures. Some of the crystals are then most likely ejected from the interface into the bulk oil, and the droplet restores its spherical shape due to surface tension. MAG-S further crystallizes at the interface and forms a new interfacial layer, and the deformation-relaxation phenomenon is repeated. The role of MAG-S crystals in the RDR is illustrated in the schematic in Fig. 5.10.

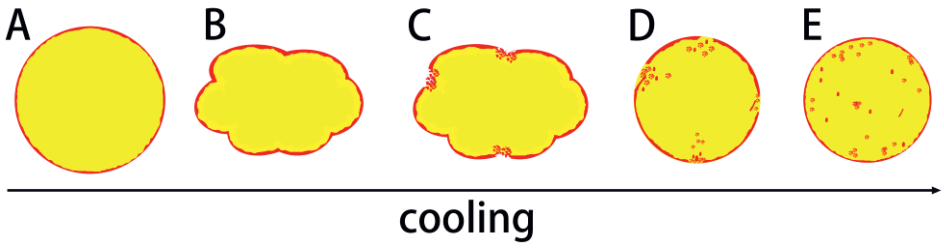

Fig. 5.10. Schematic of the various sequences of the mechanism of deformation-relaxation phenomenon described in this paper. Yellow and red parts represent oil phase and MAG-S crystals, respectively. A: a heterogenous solid layer is formed at the surface of the droplet. B: shrinkage of the droplet and appearance of wrinkles at the interface. C: breakage of the solid interfacial layer. D: relaxation of the droplet. E: a new solid layer is formed at the interface.

5.4. Conclusion

In this research, we aimed at confirming the mechanism how MAG-S stabilizes emulsions against (partial) coalescence, specifically, whether MAG-S crystallizes and forms solid barriers at the O-W interface. We investigated the crystallization process of MAG-S at a planar O-W interface and in emulsions. Results clearly confirmed that MAG-S can crystallize at the O-W interface and form a compact heterogenous interfacial layer, but it also crystallizes inside the bulk droplet. In emulsions, droplets show repeated shape deformation, followed by relaxation back to a spherical shape, during steady cooling. Emulsifier crystals create a compact solid layer at the O-W interface of the droplets. Because of the volume shrinkage of oil droplets upon cooling, stresses build up in the interfacial layer until the interface buckles and the droplets become deformed. When the stress in the interfacial layer reaches the fracture point, the solid layer partially breaks, and the droplet relaxes back to a spherical shape. Subsequently, a new solid layer can be formed upon cooling and the deformation-relaxation will be repeated. The sensitivity of the compact solid interfacial layer to temperature changes may diminish the protective function of MAG-S.

Appendix

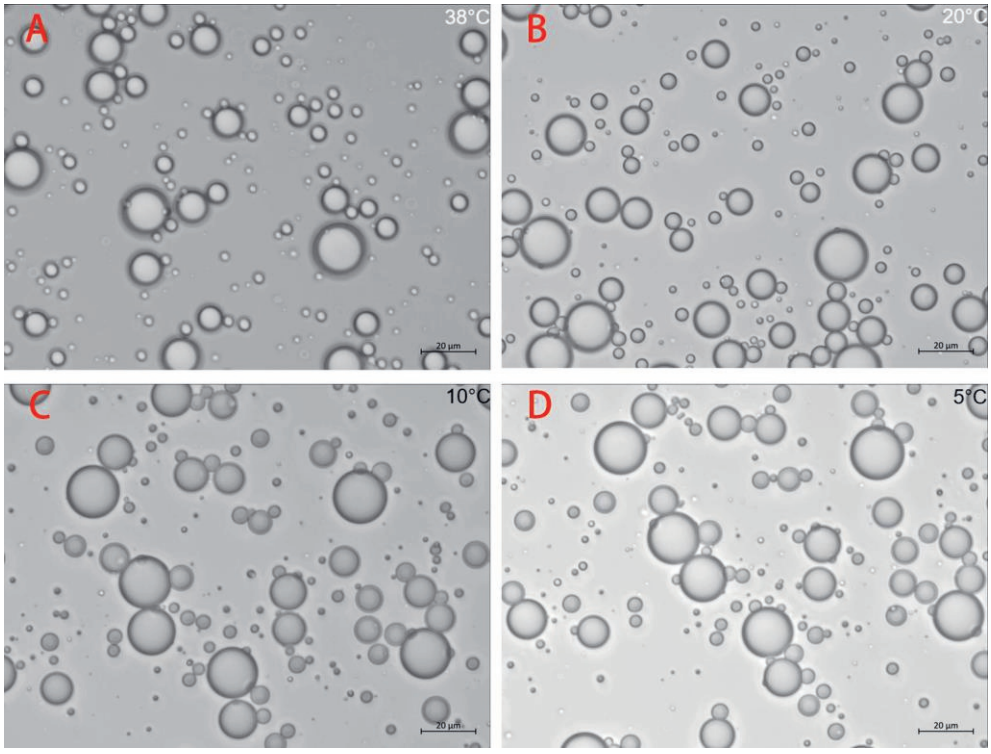

Fig. S 5.1. Change in morphology of emulsion droplets stabilized with MAG-O (2.5 wt%) upon cooling (35 °C - 5 °C). The cooling rate was -10 °C/min. A-D are the views of the emulsion at 38, 20, 10, and 5 °C, respectively. The scale bar represents 20 µm.

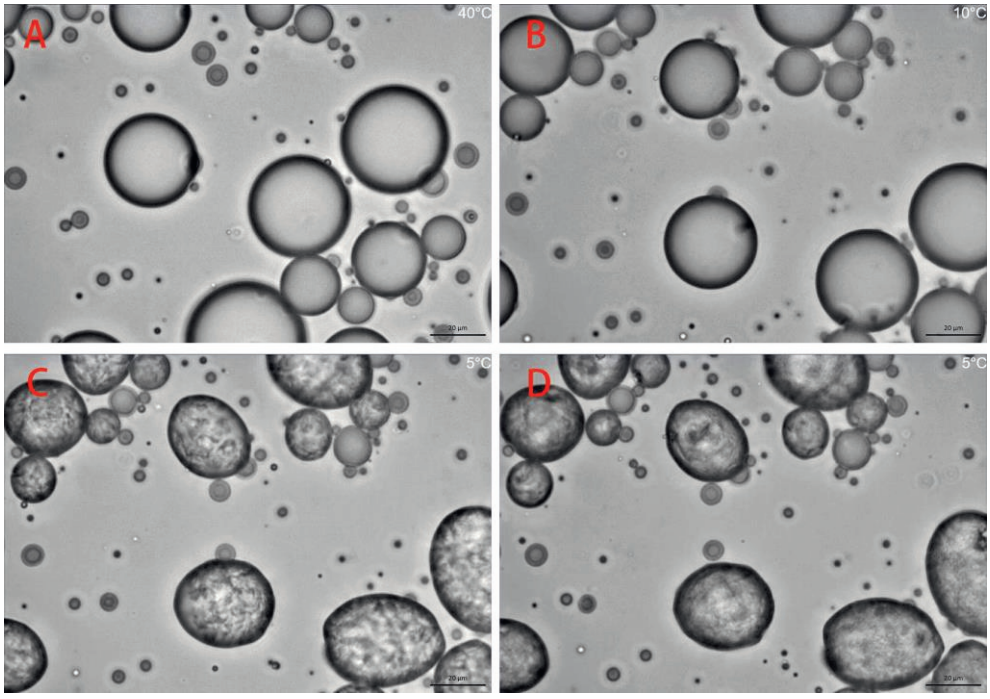

Fig. S 5.2. Change in morphology of emulsion droplets made with PK oil upon cooling (40 °C - 5 °C). The cooling rate was -10 °C/min. A-D are the views of the emulsion at 40, 10, 5 °C, and the end of cooling, respectively. The scale bar represents 20 µm.

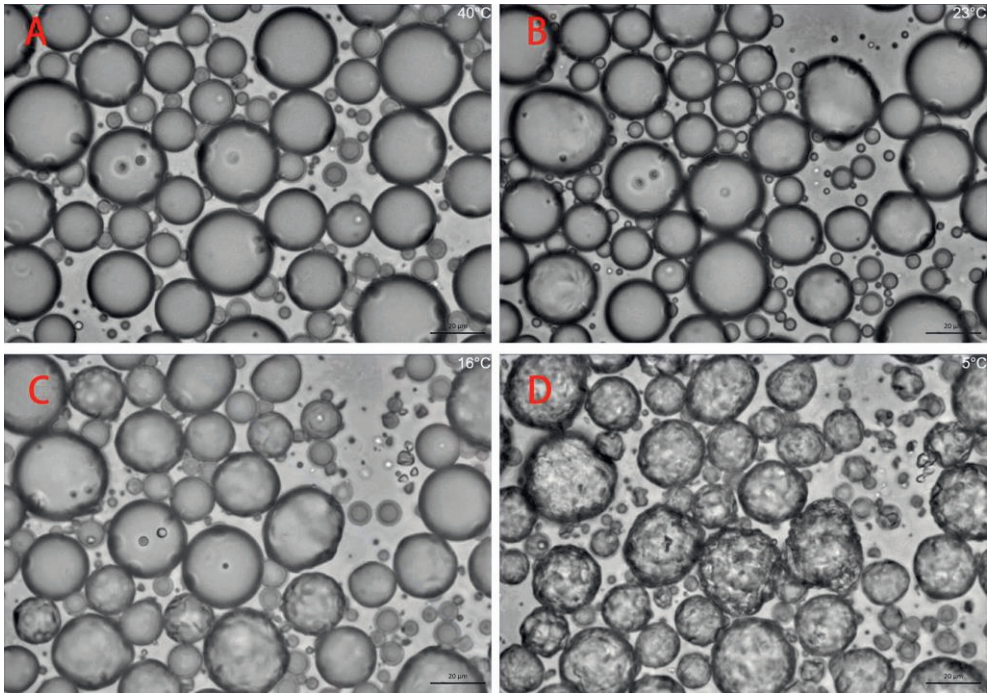

Fig. S 5.3. Change in morphology of emulsion made with palm kernel (PK) oil and 1.5 wt% MAG-S upon cooling (35 °C - 5 °C). The cooling rate was -10 °C/min. A-D are the views of the emulsion at 40, 23, 16, and 5 °C, respectively. The scale bar represents 20 µm.

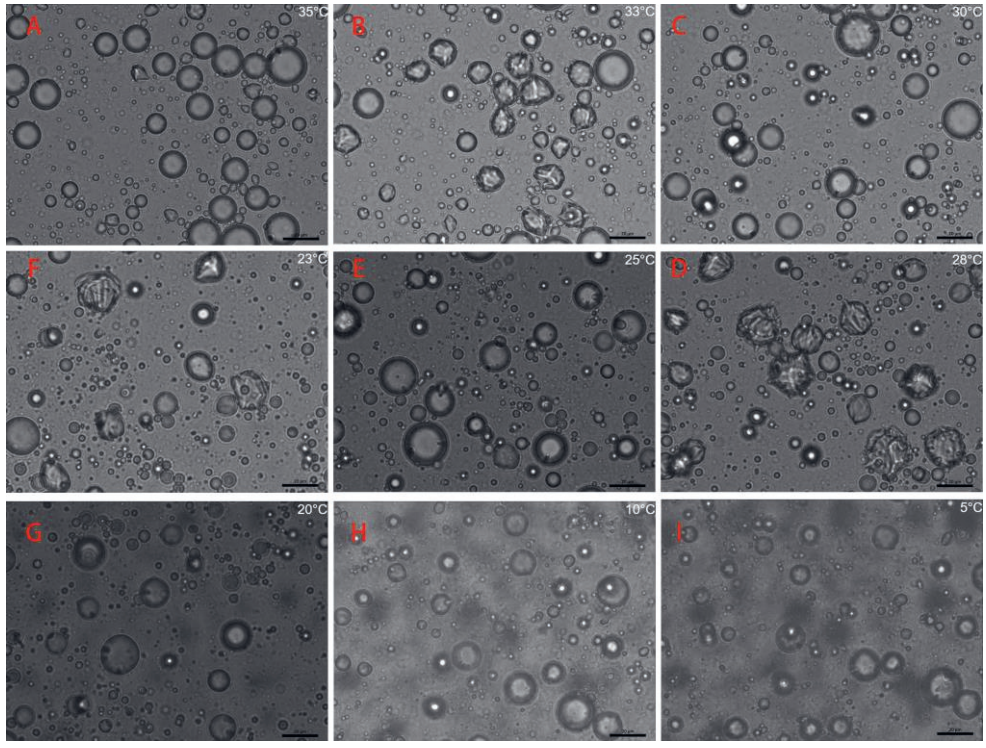

Fig. S 5.4. Evolution of emulsion droplets upon step cooling. The emulsion was made with 1.5 wt% MAG-S. A-I are the views of the emulsion at 35, 33↓, 30, 28↓, 25, 23↓, 20, 10 and 5 °C, respectively. The scale bar represents 20 µm. The downwards arrow represents the sample was under a continuous cooling.

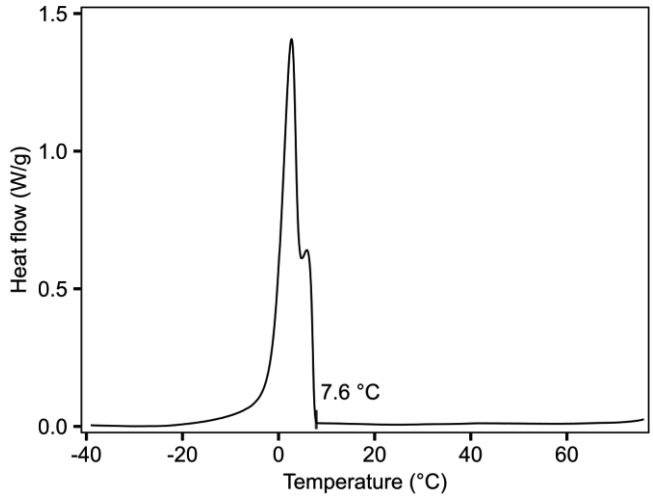

Fig. S 5.5. Crystallization profiles of PK oil upon cooling.

References

Alexandrov, D. V., & Galenko, P. K. (2021). A review on the theory of stable dendritic growth. Philosophical Transactions of the Royal Society A, 379(2205), 20200325.

Amagliani, L., & Schmitt, C. (2017). Globular plant protein aggregates for stabilization of food foams and emulsions. Trends in Food Science & Technology, 67, 248-259.

Basso, R. C., Ribeiro, A. P. B., Masuchi, M. H., Gioielli, L. A., Gonçalves, L. A. G., Santos, A. O. d., Cardoso, L. P., & Grimaldi, R. (2010). Tripalmitin and monoacylglycerols as modifiers in the crystallisation of palm oil. Food Chem, 122(4), 1185-1192.

Carrillo-Navas, H., Fouconnier, B., Vernon-Carter, E. J., & Alvarez-Ramirez, J. (2013). Shear rheology of water/glycerol monostearate crystals in canola oil dispersions interfaces. Colloids and Surfaces a-Physicochemical and Engineering Aspects, 436, 215-224.

Derkach, S. R., Kolotova, D. S., Simonsen, G., Simon, S. C., Sjöblom, J., Andrianov, A. V., & Malkin, A. Y. (2018). Kinetics of crystallization of aqueous droplets in water-in-crude oil emulsions at low temperatures. Energy & Fuels, 32(2), 2197-2202.

Dickinson, E. (2019). Strategies to control and inhibit the flocculation of protein-stabilized oil-in-water emulsions. Food Hydrocolloids, 96, 209-223.

Euston, S. R., Finnigan, S., & Hirst, R. (2000). Aggregation kinetics of heated whey protein-stabilized emulsions. Food Hydrocolloids, 14(2), 155-161.

Fredrick, E., Heyman, B., Moens, K., Fischer, S., Verwijlen, T., Moldenaers, P., Van der Meeren, P., & Dewettinck, K. (2013). Monoacylglycerols in dairy recombined cream: II. The effect on partial coalescence and whipping properties. Food Research International, 51(2), 936-945.

Fredrick, E., Van de Walle, D., Walstra, P., Zijtveld, J., Fischer, S., Van der Meeren, P., & Dewettinck, K. (2011). Isothermal crystallization behaviour of milk fat in bulk and emulsified state. International Dairy Journal, 21(9), 685-695.

Fredrick, E., Walstra, P., & Dewettinck, K. (2010). Factors governing partial coalescence in oil-in-water emulsions. Adv Colloid Interface Sci, 153(1-2), 30-42.

Fuller, G. T., Considine, T., Golding, M., Matia-Merino, L., & MacGibbon, A. (2015). Aggregation behavior of partially crystalline oil-in-water emulsions: Part II–Effect of solid fat content and interfacial film composition on quiescent and shear stability. Food Hydrocolloids, 51, 23-32.

Fuller, G. T., Considine, T., Golding, M., Matia-Merino, L., MacGibbon, A., & Gillies, G. (2015). Aggregation behavior of partially crystalline oil-in-water emulsions: Part I–Characterization under steady shear. Food Hydrocolloids, 43, 521-528.

Gaonkar, A. G., & Borwankar, R. P. (1991). Adsorption behavior of monoglycerides at the vegetable oil/water interface. Journal of colloid and interface science, 146(2), 525-532.

Ghosh, S., & Rousseau, D. (2011). Fat crystals and water-in-oil emulsion stability. Current Opinion in Colloid & Interface Science, 16(5), 421-431.

Goibier, L., Lecomte, S., Leal-Calderon, F., & Faure, C. (2017). The effect of surfactant crystallization on partial coalescence in O/W emulsions. Journal of colloid and interface science, 500, 304-314.

Johansson, D., Bergenståhl, B., & Lundgren, E. (1995). Wetting of fat crystals by triglyceride oil and water. 1. The effect of additives. Journal of the American Oil Chemists' Society, 72(8), 921-931.

Konijn, B. J., Sanderink, O. B. J., & Kruyt, N. P. (2014). Experimental study of the viscosity of suspensions: Effect of solid fraction, particle size and suspending liquid. Powder Technology, 266, 61-69.

Liang, Y., Matia-Merino, L., Gillies, G., Patel, H., Ye, A., & Golding, M. (2017). The Heat Stability of Milk Protein-stabilized Oil-in-water Emulsions: A Review. Current Opinion in Colloid & Interface Science.

Mao, L., Calligaris, S., Barba, L., & Miao, S. (2014). Monoglyceride self-assembled structure in O/W emulsion: formation, characterization and its effect on emulsion properties. Food Research International, 58, 81-88.

Mei, L., Choi, S. J., Alamed, J., Henson, L., Popplewell, M., McClements, D. J., & Decker, E. A. (2010). Citral stability in oil-in-water emulsions with solid or liquid octadecane. Journal of agricultural and food chemistry, 58(1), 533-536.

Mitropoulos, V., Mutze, A., & Fischer, P. (2014). Mechanical properties of protein adsorption layers at the air/water and oil/water interface: a

comparison in light of the thermodynamical stability of proteins. Adv Colloid Interface Sci, 206, 195-206.

Moens, K., Tavernier, I., & Dewettinck, K. (2018). Crystallization behavior of emulsified fats influences shear-induced partial coalescence. Food Research International, 113, 362-370.

Mullin, J. W. (2001). Crystallization: Elsevier.

Munk, M. B., Larsen, F. H., Van Den Berg, F., Knudsen, J. C., & Andersen, M. L. (2014). Competitive displacement of sodium caseinate by low-molecular-weight emulsifiers and the effects on emulsion texture and rheology. Langmuir, 30(29), 8687-8696.

Neumann, S. M., van der Schaaf, U. S., & Karbstein, H. P. (2018). Structure stability and crystallization behavior of water in oil in water (WOW) double emulsions during their characterization by differential scanning calorimetry (DSC). Journal of Thermal Analysis and Calorimetry, 133(3), 1499-1508.

Povey, M. J. (2017). Applications of ultrasonics in food science-novel control of fat crystallization and structuring. Current Opinion in Colloid & Interface Science, 28, 1-6.

Rousseau, D. (2000). Fat crystals and emulsion stability - a review. Food Research International, 33(1), 3-14.

Sato, K. (2018). Crystallization of Lipids: Fundamentals and Applications in Food, Cosmetics, and Pharmaceuticals: John Wiley & Sons.

Spicer, P. T., & Hartel, R. W. (2005). Crystal comets: dewetting during emulsion droplet crystallization. Australian Journal of Chemistry, 58(9), 655-659.

Tadros, T., Izquierdo, P., Esquena, J., & Solans, C. (2004). Formation and stability of nano-emulsions. Adv Colloid Interface Sci, 108, 303-318.

Van Boekel, M. A. (1980). Influence of fat crystals in the oil phase on stability of oil-in-water emulsions: Pudoc.

Vereecken, J., Meeussen, W., Foubert, I., Lesaffer, A., Wouters, J., & Dewettinck, K. (2009). Comparing the crystallization and polymorphic behaviour of saturated and unsaturated monoglycerides. Food Research International, 42(10), 1415-1425.

Yang, J., Qiu, C. Y., Li, G. H., Lee, W. J., Tan, C. P., Lai, O. M., & Wang, Y. (2020). Effect of diacylglycerol interfacial crystallization on the physical stability of water-in-oil emulsions. Food Chem, 327.

Chapter 6

General discussion

6.1. Introduction

In the food industry, surface-active components are often mixed to stabilize emulsions or foams. A detailed understanding on which protein species from the mixture are preferentially adsorbing at the oil-water (O-W) or air-water (A-W) interface in such a complex system is in most cases missing. But this knowledge is important for designing the formulation and improving the functionality of emulsion or foam products. In this thesis, we aimed at improving our understanding of the composition and mechanical properties of interfacial layers at O-W or A-W interfaces for mixtures of dairy proteins. More specifically, we used interfacial rheology to test the mechanical properties of the interfaces and interface visualization technics to identify the dominant protein species at the interfaces. In the previous chapter, we also confirmed the mechanism how high melting point emulsifiers stabilize O-W interfaces. In this chapter, all results of the previous chapters will be summarized briefly, and a general discussion will be provided by combining these results and comparing them to results from recent literature.

6.2. Main results of this thesis

In chapter 2, we compared the interfacial properties of whey protein isolate (WPI) and whey protein aggregate (WPA) in terms of adsorption kinetics and rheological properties at the oil-water (O-W) interface, at a low (0.1 wt%) and a high concentration (4.0 wt%), respectively. The results revealed that at the low concentration, WPI was more surface-active than WPA. WPI decreased the surface tension faster and to a greater extent than WPA. The interfacial layer formed by WPI or WPA were both displaying solid-like viscoelastic behavior, in which the elastic contribution to the surface stress was dominant. At the high concentration, the emulsion made with WPA was more stable than the one made from whey protein at static conditions. This is ascribed to the higher bulk viscosity WPA conferred on the continuous phase due to its larger particle size. At dynamic conditions, where vigorous stirring was involved, the emulsion made with WPA was less stable against coalescence than the one made with WPI. In chapter 2 we argued that WPI and WPA impart different interfacial properties to an O-W interface at a high concentration. WPI appeared to form stiffer interfacial layers. When large deformations were applied, the interfacial structure may (partially) break up

and start to flow at the interface, which can protect the lipid droplets by a mechanism similar to the Marangoni effect. On the other hand, WPA formed a more coarse and thicker interfacial layer. Although the layer had a larger maximum linear strain, once it broke up, due to the larger size of protein aggregates, they were less mobile than whey protein monomers. Consequently, some parts of the interface might become exposed at a large deformation, and this could result in more coalescence.

Whether micellar caseins actually adsorb at interfaces has been extensively debated in literature, and is an important question for understanding the function of full dairy protein based products in emulsions or foams, e.g., milk protein concentrate or skimmed milk power. In **Chapter 3**, we ultracentrifuged casein micelle dispersions to separate micellar caseins from the soluble casein fractions (small casein aggregates and some monomers). We investigated the rheological properties of these fractions at the interfaces separately, and visualized the interfaces stabilized with different fractions. Results convincingly proved that micellar casein adsorbed at neither O-W nor A-W interfaces, but some of the smaller protein species did. To be more specific, the O-W interface was dominated by small casein aggregates, while the layers at A-W interfaces were mainly formed by monomers, most likely β-casein.

After recognizing the roles of individual whey protein or casein at the O-W and A-W interfaces, we mixed casein and whey protein in the system to better replicate the real application of dairy proteins in emulsions or foams. In **Chapter 4**, we aimed at understanding the synergistic or antagonistic interactions among casein and whey proteins when they are mixed, and their relative contributions to the mechanical properties of O-W and A-W interfaces at different ratios. Results showed that after 1 h adsorption, casein would be the main species at the O-W interface even at a very low casein to whey ratio (casein : whey = 0.1 wt% : 1.9 wt%). At the A-W interface, casein co-adsorbed with whey protein. With an increasing proportion of casein in the mixture, casein would disrupt the stiff solid-like structure of the interfacial layer formed by whey protein, and as a result the layer became less stiff.

In **chapter 5**, we used glycerol monostearate (MAG-S) as a high melting point emulsifier, to study the mechanism by which crystallizable emulsifier stabilizes O-W interfaces (i.e. bulk versus interfacial stabilization). We confirmed the growth of MAG-S crystals at the oil-water interface, using

multiphoton excitation microscopy. Subsequently, we monitored the crystallization process of emulsifiers in a complete emulsion system. A repeated shape deformation-relaxation phenomenon of emulsion droplets was observed during continuous cooling of the emulsion. This turned out to be an interfacial phenomenon and was attributable to two factors: the formation of brittle solid interfacial layers by the emulsifiers, and the stress build-up in these layers due to shrinkage of the oil bulk phase upon cooling. Because of the high stiffness of the interfacial layers formed by the emulsifier crystals, bulk phase shrinkage led to buckling of the interface, resulting in shape deformations. This continued until the interfacial structure ruptured. The droplet shape subsequently relaxed back to a spherical shape. Upon further cooling, the process repeated itself multiple times, leading to a sequence of shape-deformation - relaxation events.

6.3. Molecular characteristics of proteins and adsorption kinetics

To put the results we summarized in the previous section in a broader context, in particular the results on preferential adsorption of specific fractions from casein micelle dispersions, or specific species from casein-whey protein mixtures, we will discuss some of the factors that control adsorption kinetics of proteins. When proteins adsorb at interfaces, they will decrease the surface-tension, and monitoring the surface-tension as a function of time will provide information on the adsorption kinetics. According to Beverung, et al. (1999), typically three regimes can be observed in the decrease of surface tension with time as a result of protein adsorption, and they identify these as: (i) the diffusion-controlled regime, followed by (ii) continued rearrangement of protein structures, and finally, (iii) formation of a cohesive network. Here we will focus primarily on the first two regimes. Combined with results in chapter 2 - 4, how molecular properties of dairy proteins affect diffusion and rearrangement of proteins will be discussed.

6.3.1. Diffusion-controlled regime

The diffusion process determines how fast proteins or particles can approach an interface. The rate of diffusion directly affects the induction time, which is defined as the time necessary to reach the minimum coverage, at which interfacial tension starts to decrease (Miller, et al., 2000). Normally small molecules have larger diffusion coefficients and a smaller energy

barrier for adsorption, which make them move faster towards interfaces (Beverung, et al., 1999; Jung, et al., 2010). This may partially explain the results in chapter 3, why complete casein micelles adsorb at neither O-W interfaces nor A-W interfaces. When casein micelles reach the interface, it is likely the interface is already substantially covered by smaller aggregates or molecules present in the dispersion, as illustrated in the electron microscopy pictures obtained by Brooker (1985). The same reason can also explain why at a low concentration, WPA has a longer induction time than WPI (Fig.2.7). Compared with the aggregates in WPA, smaller whey protein monomers in WPI can approach the interface faster, resulting in an earlier onset and faster decrease of surface tension. The induction time of whey protein monomers was even too short to be observed at a concentration 0.1 wt%. At a higher concentration, both WPI and WPA can decrease the interfacial tension quickly and to a similar extent, to around 14 mN/m (Fig.2.7). The difference in rate of diffusion is clearly less of a factor at a high bulk protein concentration. In WPA not all protein is present in the form of aggregates. Some of the proteins are still in a monomeric form, and some most-likely also in the form of peptides (formed by heat-induced hydrolysis) (Bolder, et al., 2007). This is similar to the casein micelle dispersion in chapter 3 containing micelles, small aggregates, and monomers at the same time. Results in chapter 3 illustrated that small protein molecules take advantage of faster diffusion and can preferentially adsorb at the interfaces. Therefore, the disappearance of the surface activity difference between WPI and WPA at a high concentration, could be the result of the fast adsorption of small whey protein molecules in WPA solution.

6.3.2. Protein-rearrangement regime

When globular proteins approach an interface, they will (partially) rearrange their structure to expose some of the hydrophobic groups buried in the interior of that structure to the air or oil phase (Dickinson, 1999). The unfolding of globular proteins at interfaces was hypothesized based on the observation that some enzymes lose their activity after adsorbing at A-W interfaces (Donaldson, et al., 1980). Further confirmation of this hypothesis was provided by Corredig and Dalgleish (1995), who showed that compared with non-absorbed proteins, proteins adsorbed at the O-W interface had a reduced amount of heat adsorption in the region 30 -110 °C, using differential scanning microcalorimetry. Unfolding of the protein molecule at the interface is largely affected by the structural stability of the protein itself.

The protein β-casein is a linear molecule with one side of the chain more hydrophobic and the other side more hydrophilic. It has little secondary structure and no intramolecular covalent crosslinks. All these facts make β-casein a very flexible protein which behaves similar to a small molecular weight surfactant at interfaces (Dickinson, 1998, 2001). The whey protein β-lactoglobulin has high level of secondary and tertiary structure, and is regarded as a globular protein held together by intramolecular disulfide bonds (McKenzie, et al., 1972; Papiz, et al., 1986). The molecular structure differences between β-casein and β-lactoglobulin, allow β-casein to rearrange their structure much faster than β-lactoglobulin at the interface. It explains why casein can decrease the tension to a greater extent and much faster than whey proteins at the O-W interfaces (Fig. 6.1).

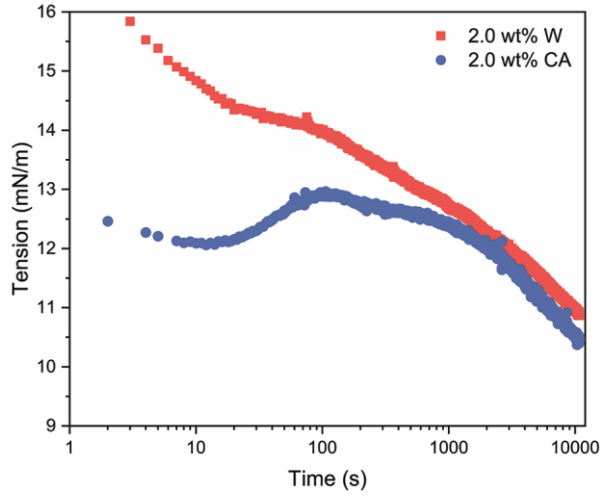

Fig. 6.1. Surface tension of casein (CA) and whey (W) at the milk fat and Milli-Q interface. The protein concentration was 2.0 wt%.

The structural stability difference of WPI and WPA may also contribute to the difference in the rate of surface tension decrease at the O-W, at a low concentration (Fig.2.7). During the heat treatment used to prepare WPA, whey proteins were denatured. The hydrophobic parts and thiol groups of whey protein were exposed, and sulfhydryl/disulfide interchange reactions occurred (Iametti, et al., 1995; Iametti, et al., 1996; Sawyer, 1968). Whey proteins then self-assembled to form aggregates by a combination of covalent bonds and hydrophobic interactions (Galani & Owusu Apenten*, 1999). The larger particle size and rigid structure may take WPA longer time

to unfold and expose hydrophobic groups towards the interface. Consequently, for WPA, the decrease in surface tension is much slower.

For complete casein micelles in micellar casein dispersions, we speculated that a lower diffusion rate resulted in the interfaces being dominated by the smaller species in the dispersion. But also, for that system the structural stability of the micelles may have been another reason why we did not observe complete micelles adsorbing at the interfaces. Casein micelles are relatively large assemblies stabilized by hydrophobic interactions, hydrogen bonds and interactions with colloidal calcium phosphates. The outer surface of the micelle is covered by a dense layer of κ-casein (Walstra, 1990). Such a protein-assembly may not easily rearrange the structure to expose its hydrophobic groups to the interfaces.

6.4. Protein species at interfaces in a mixed system

6.4.1. Mixtures of casein monomers, small aggregates, and micelles

The composition of the layer formed at an interface is largely dependent on the initial adsorption kinetics of the proteins and their interactions after adsorption, at least on a relatively short time scale. On a longer time scale, the structure may also be affected by slow displacement of one species by another. In chapter 3, the casein micelle dispersion was composed of monomers, small casein aggregates and micellar caseins. Micelles were already shown not to adsorb at the O-W or A-W interface. This could be because micelles have a large particle size, which makes them slowly diffuse to interfaces, and their structure may also be slow to rearrange to expose buried hydrophobic groups towards interfaces. The protein β-casein has a small molecular size and flexible structure, and when it is mixed with other larger or more structured proteins, it will preferentially adsorb at the interface, which is also found in other research (Mackie, et al., 2001; Zhang, et al., 2004). However, the results in chapter 3 indicate that when monomers and small casein aggregates coexist in the bulk phase, monomers are not the main species at the O-W interface. This may imply that at the beginning, small casein aggregates co-adsorbed with β-casein, but β-casein was subsequently displaced by the small aggregates.

Co-adsorption of protein species at the interfaces is driven not only by adsorption kinetics, but also by overall bulk concentrations and ratios of the

species (Dickinson, 1992; Hinderink, et al., 2019; Hunt & Dalgleish, 1994; Srinivasan, et al., 1996). It appears that the concentration we used in chapter 3 was in a regime where both monomers and aggregates ended up at the interface. Small proteins can adsorb faster at interfaces compared to larger ones, but can in some cases be displaced by other proteins, for example β-lactoglobulin was reported to be able to displace β-casein. Dalgleish, Goff, Brun, et al. (2002) studied the competitive adsorption of caseins and whey proteins at the O-W interfaces in emulsions. They found both α_{s1} and β-casein can be displaced by β-lactoglobulin and α-lactalbumin, and the displacement is temperature dependent. At a higher temperature, the displacement is faster. For mixtures of β-casein and β-lactoglobulin, Ridout, et al. (2004) also reported that initially β-casein adsorbed at the A-W interface, but was subsequently displaced by β-lactoglobulin. Protein molecules with ordered structures which can unfold at the interface appear to displace β-casein which has a random coil structure. This is also supported by research of Hinderink, et al. (2019), where they found that casein will be displaced by pea protein at the O-W interface in emulsions. When globular proteins unfold at interfaces, hydrophobic groups are exposed which can result in stronger interactions with the oil phase than β-casein. During the unfolding process of globular proteins, adjacent β-caseins may be pushed aside to the gaps between unfolded globular proteins. When the local gaps are saturated with β-casein, further compression of gaps could push them out of the interfaces. This process is sometimes referred to as the orogenic displacement (Damodaran, 2005). Similarly, small casein aggregates could be displacing β-casein from the interfaces. Actually, this could explain the slight increase in surface tension in the first 10-100 s we observed for the O-W interface stabilized by casein micelle dispersion (Fig. 6.1). In view of the above, the most likely scenario in the adsorption of casein micelle dispersion at the O-W interface is the initial co-adsorption of β-casein and small aggregates, followed by the displacement of the former by the aggregates.

6.4.2. Casein and whey protein mixtures

Some research studied the competitive adsorption of β-casein and globular proteins (Brun & Dalgleish, 1999; Cao & Damodaran, 1995; Xu & Damodaran, 1994), and in all studied cases the results showed that flexible casein molecules could not displace globular protein molecules (Dickinson, 2011). This observation appears to be different from the results in Chapter 4, as we found at the O-W interface, when casein and whey are mixed, casein is

dominant at the interface even at a very low proportion of casein in the mixture. The difference of these findings can be the consequence of different experimental designs: β-casein can be introduced in the mixture at the same time as the globular protein, or after the initial adsorption of the globular protein (e.g., by subphase exchange). If globular proteins adsorb initially at the interfaces and reorganize their structures, the resulting network formation can render adsorption more irreversible. After a certain time, once a compact structure is formed at the interfaces, the sequentially added β-casein will not adsorb at the interface to displace the globular proteins. However, in chapter 4, we studied adsorption with a system mixed prior to adsorption. Casein monomers or small aggregates may then dominate the interface as a result of their faster diffusion or easier unfolding during the adsorption.

At the A-W interface, the competitive adsorption among whey protein, casein monomers, and small casein aggregates is different from the O-W interface. As proved in chapter 4, at the O-W interface casein aggregates were dominant, while the A-W interface was occupied by mixtures of casein monomer and whey protein. The difference in protein species at the O-W and A-W interface may be the result of differences between the two types of interfaces. The adsorption dynamics of proteins at O-W and A-W interfaces was compared in several studies (Beverung, et al., 1999; Sengupta & Damodaran, 1998). It was found that for the same protein, the A-W interface has a longer induction time than the O-W interface (which was not found in our research, as the concentration we used for adsorption was too high to clearly observe the induction period). Both Sengupta, et al. (1998) and Beverung, et al. (1999) proposed this was because repulsive dispersion interactions are the dominant force at the A-W interface. The effect of the diffusion rate of proteins will therefore be magnified at the A-W interface. This explains why whey protein and casein monomer were found co-adsorbing at the A-W interface, but small casein aggregates that had a larger size (50-60 nm) and may diffuse slower were not. Furthermore, at the O-W interface, proteins have a stronger affinity to the oil phase, and are proved to be partially immersed in the oil phase (Bergfreund, Diener, et al., 2021). Oil molecules can penetrate into the hydrophobic core of proteins and result in a faster and greater protein unfolding (Bergfreund, et al., 2018). At the A-W interface, without the oil solvent to interact with the hydrophobic residues of proteins, the structure rearrangement and special orientations are limited to a certain extent (Bergfreund, Bertsch, et al., 2021). The

statement is also supported with the findings that β-lactoglobulin loses more tertiary and secondary structure at the O-W interface than at the A-W interface (Drusch, et al., 2021; Meinders & De Jongh, 2002; Zhai, et al., 2010). Consequently, when casein monomer and whey proteins co-adsorb at the A-W interface, the displacement of casein monomers by whey protein will be limited.

6.4.3. Proteins and surface-active lipids

As mentioned in the chapter 1 (1.2.3), several surface active lipids like mono- or diglycerides, or phospholipids are present in milk fat. Different from mixing proteins and water soluble surfactants in the water phase, protein and oil soluble emulsifiers adsorb at the interface from two different phases, which can prevent formation of protein-emulsifier complexes in the bulk phase (Lech, et al., 2015). Even though, oil soluble emulsifiers are widely reported to have interactions with proteins, including displacement or co-adsorption with proteins at the interfaces (Dickinson & Hong, 1994; He, et al., 2008; McSweeney, et al., 2008; Munk, et al., 2014; Pelan, et al., 1997; Rahman & Sherman, 1982). How these surface-active lipids (emulsifiers) affect the composition at the interfaces is often not completely clear.

These emulsifiers can significantly change the interfacial tension of an O-W interface over time, as illustrated in Fig. 6.2. When we carried out a measurement of the surface tension of an O-W interface between an unpurified oil (containing surface-active impurities) against a protein solution, the droplet fell off the needle of the tensiometer, even at a very low protein concentration (0.1 wt%), during the oscillation. This happened as the interfacial tension was too low to maintain the shape of the droplet. In chapter 2, we characterized both emulsions made with purified and unpurified milk fat. Results turned out that the emulsions made with unpurified milk fat had slightly smaller droplet size, creaming rate and lower ζ-potential (results can be seen in the appendix of that chapter). The effects of protein concentrations on emulsions made with purified milk fat were still valid for the emulsions made with unpurified milk fat. All of these results are supporting that the naturally existing surface-active lipids in the oil phase appear to co-adsorb with proteins at the interfaces. The effect of co-adsorption is more prominent in surface tension tests in a drop tensiometer, but is relatively small for macroscopic stability of emulsions. The main reason is that the specific area of the interface is much larger in emulsions than in tensiometer tests: typical drop size in an emulsion is ~ 1 μm, whereas

droplet size in a tensiometer is ~ 1mm. The ratio of the number of surface-active lipid molecules to interfacial area is significantly higher in a tensiometer droplet than the one in an emulsion. As a result, in oil-in-water emulsions, although these surface-active lipids will adsorb at the interface, their effect is largely dominated by the abundant proteins in the aqueous bulk phase.

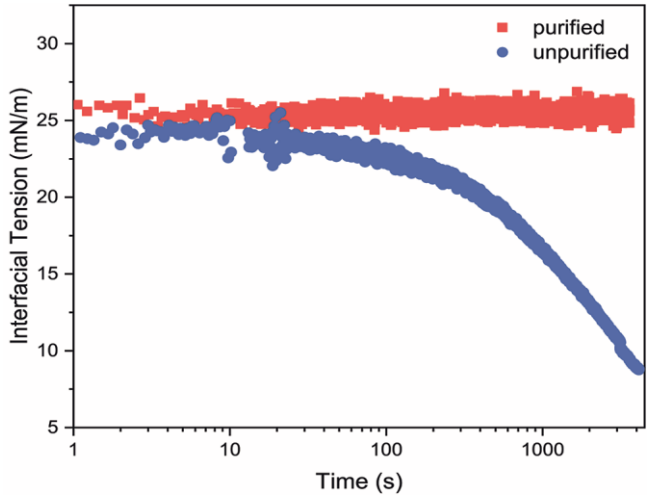

Fig. 6.2. Surface tension of the interface between Milli-Q water and purified milk fat or unpurified milk fat. the temperature was 40 °C.

6.5. Rheological properties of interfaces in a mixed system

In chapter 2, we compared the rheological properties of WPI and WPA at the O-W interface. WPI was shown to form a viscoelastic solid interface, which is stiff but brittle. The interfacial layer formed by WPA was more stretchable, as evident from a larger maximum linear strain. The same finding also holds for the A-W interface, which is not investigated in this thesis, but can be found in the study of Yang, et al. (2020). In chapter 4, we further compared the rheological properties of whey protein, casein, and their mixtures at interfaces. Results showed that whey protein can form a much stiffer layer than casein at both O-W and A-W interfaces. For the casein and whey mixtures, the O-W interface is weak because the interface is dominated by casein. The stiffness of the A-W interface decreases with an increasing proportion of casein in the mixture, as casein and whey co-adsorb at the

interfaces. These results illustrate the well-known fact that the rheological properties of interfaces depend strongly on the composition at the interfaces and of course the intermolecular interactions among the adsorbed components.

Some globular proteins containing thiol groups, like whey protein, can unfold at the interfaces and have strong intermolecular interactions by hydrophobic attraction and sulfhydryl/disulfide interchange reactions. When they exist as monomers and adsorb at interfaces, they may form an interconnected network structure. The formed interfacial layer will normally be stiff and more solid-like. When these monomers form aggregates, the resulting interfacial layer can be thicker, coarser and have fewer connections (as illustrated in Fig. 2.10), as most hydrophobic groups are buried inside the aggregates. The interfacial layer could have a more open structure, which can result in higher stretchability and lower brittleness. Both types of interfaces were shown to protect emulsion droplets against coalescence efficiently. However, when the emulsion was exposed to vigorous shear, the emulsion stabilized with aggregates was slightly more sensitive to coalescence. One potential reason is that those aggregates may have lower mobility, both in the bulk and at the interface. Once the interfacial structure has yielded and starts to flow, they cannot protect the new exposed interface as efficiently as smaller protein molecules, which may show a higher rate of surface diffusion, protecting the droplet with a mechanism similar to the Marangoni effect. Exposed interface can also lead to additional adsorption, and this process too will be faster for smaller proteins than for aggregates.

Small and flexible proteins like casein monomers, cannot form a strong interface due to the weaker intermolecular interactions at the interfaces. When they are mixed with other proteins, they can easily adsorb at the interface quickly at the beginning of the adsorption, because they can diffuse faster towards the interface. The interface will also display a weak response in deformation. However, at the O-W interface, those flexible proteins may be displaced with other more structured proteins, like what we discussed in section 6.4.1 that β-casein can be displaced by small casein aggregates at the O-W interface. The interface is therefore expected to be stiffer after a certain time, as the elasticity of the O-W interface stabilized with small casein aggregates was 10 times larger than the one stabilized with β-casein (chapter 3). At the A-W interface, the story can be quite different.

As discussed in section 6.4.2, smaller molecules preferentially adsorb at the A-W interface, and displacement among proteins is not as evident. The composition and the rheological properties are more governed by relative ratios between molecules in the mixture, as indicated in chapter 4.

6.6. Interfacial properties of plant proteins

Nowadays there is a growing interest in alternatives to animal proteins, including plant-based emulsifiers. Several plant proteins have been reported as potential emulsifiers, for example, soy proteins, pea proteins, lupin, cowpea, wheat gluten, rice glutelin and oilseed proteins (Burger & Zhang, 2019; Kim, et al., 2020; Tang, 2017). However, the stabilizing functionality of these plant proteins is often not comparable to that of dairy proteins, and whether these alternatives can suitably replace dairy proteins is still questionable (Hinderink, et al., 2020; Kim, et al., 2020). Often, these plant proteins particularly fail to perform as well as dairy proteins in terms of interfacial properties. The main plant protein fraction in commercial extracts are the globulins (Sari, et al., 2015). Due to their large size and deeply buried hydrophobic residues (Chéreau, et al., 2016; Rasheed, et al., 2020), they cannot quickly adsorb to the interface or unfold easily to induce strong in-plane interactions, which are essential for the formation of a stiff interfacial layer. To acquire a better interfacial activity and stability, the molecular properties of plant proteins could be modified chemically or physically. Considering the results we obtained for dairy proteins in this thesis, several strategies can be formulated: (i) breaking protein particles or aggregates into smaller fragments can make proteins diffuse faster to the interface. This could be done by physical means, for example, high pressure homogenization, ultrasound (F. Wang, et al., 2020), or by hydrolysis (García-Moreno, et al., 2021; Rodríguez Patino, et al., 2007). However, a reduction that is too extensive, will result in the formation of small peptides, which should be avoided, as they may have weaker intermolecular interactions, and thus cannot construct a stiff interfacial layer; (ii) the surface hydrophobicity of proteins can be modified by controlled heat treatment (J.-M. Wang, et al., 2012), or chemically attaching saccharides (Peng, et al., 2020). Heat treatment can break tertiary and secondary structure of proteins, and expose the buried hydrophobic groups, which is beneficial for the unfolding of proteins at the interface. But heat treatment may normally also induce protein aggregation. A combination of heat treatment and size

reduction methods, for example hydrolysis can be optimal for improving surface activity of plant proteins (Liang, et al., 2020).

Although in structure and behavior plant proteins generally deviate significantly from the dairy proteins we studied here, commercial plant protein extracts show at least one common feature, in the sense that they are never very pure, and are in fact complex mixtures. They normally contain various proteins, either in the form of peptides, native protein, or aggregates, and several non-protein components (Chéreau, et al., 2016; Kornet, et al., 2021; Wanasundara, et al., 2016). When we study the surface-activity of plant protein extracts, it is difficult to identify which ingredients in such a complex mixture are dominating the response. In chapter 3, we convincingly proved that casein micelles, which are the main ingredient in micellar casein isolate, will adsorb at neither O-W interface nor A-W interface. It turns out the real functional fractions which confer viscoelasticity on the interfaces are the casein monomers (A-W) or small aggregates (O-W), which are actually minor components in the mixture. The approach we outlined in chapter 3, based on fractionation of a complex mixture, and studying the functionality of the individual fractions using a combination of (nonlinear) interfacial rheology and visualization analysis (multiphoton excitation microscopy, MPM), can help in identifying the most relevant components in the mixture. This can give potential guidance for determining the most relevant plant protein extraction and modification routes to improve the emulsifying activity or the interfacial activity of plant protein extracts.

6.7. Pickering stabilization

In the early 20th century, Pickering (1907) found that solid particles can be used as stabilizers to stabilize emulsions. Pickering emulsions have several advantages over normal emulsions stabilized with surfactants or proteins, for example, high stability against coalescence and effective drug encapsulation and release (Xiao, et al., 2016). Nowadays, with the increasing health consciousness of consumers, and some frequently used emulsifiers like carboxymethylcellulose and polysorbate-80 proving to be harmful to health (Chassaing, et al., 2015), there is a growing interest in natural or non-synthetic emulsifiers in the food industry. Food-grade material based Pickering emulsions have received significant interest in recent years.

Numerous studies have appeared, devoted to constructing protein particles to stabilize emulsions. The most widely used method is using heat treatment on proteins to produce protein aggregates or so-called protein microgels (Burgos-Díaz, et al., 2019; Gao, et al., 2017; Ning, et al., 2019; Torres, et al., 2017). However, after heat treatment, a protein dispersion will contain not only aggregates, but also monomers and some heat induced peptides (Amagliani & Schmitt, 2017). The compositions in protein aggregate dispersions are comparable with casein micelle dispersion in chapter 3 in terms of protein size. As big particles are not likely to adsorb at the interfaces, the so-called Pickering mechanism at a protein aggregate stabilized interface is questionable. Even though convection during homogenization or vigorous stirring may bring particles to the interfaces, the interfaces are most likely to be covered by small surface active components, for example monomers or peptides. Similar doubts about the stabilization mechanism can be raised for MAG-S stabilized emulsions. Some researchers believe MAG-S would stabilize emulsions by a Pickering stabilization mechanism (Munk, et al., 2014). These researchers hypothesized that MAG-S crystallizes in the bulk phase, and that the crystals are surface-active and can subsequently adsorb at the O-W interface (Carrillo-Navas, et al., 2013). However, our results in Chapter 5 suggest a different mechanism. MAG-S adsorbs at the interface prior to crystallization, and subsequently crystallizes predominantly at the interface, forming a solid shell at the interface, which (although polycrystalline) appears to be continuous and compact. Clearly, the claims that emulsions stabilized by protein aggregates or MAG-S crystals are Pickering emulsions, are highly doubtful.

6.8. Conclusions and outlook

In this thesis, we studied the interfacial properties of dairy proteins, including whey protein, WPA, casein micelles, casein monomers, and small casein aggregates, separately or in a complex mixture. We identified the dominant protein species at the O-W or A-W interfaces, with a combined approach of interfacial rheology and interface visualization techniques. We aimed at providing a detailed understanding of which component is responsible for the functionality at the O-W or A-W interfaces when dairy proteins are mixed to stabilize emulsions or foams. By understanding the links among the molecular characteristics of the selected dairy proteins, their adsorption kinetics, and their rheological properties at the interfaces,

some general findings can be summarized. Small and flexible proteins, for example β-casein, can diffuse and expose hydrophobic groups fast to both A-W and O-W interfaces. Although they can adsorb to the interface quickly, the interfacial layer formed by these small and flexible proteins is normally less stiff due to the weak in-plane intermolecular interactions at the O-W or A-W interfaces. Small globular proteins like β-lactoglobulin, can also diffuse fast to the interfaces but unfold more slowly. As a result, they decrease the interfacial tension slower than small and flexible proteins but will form a stiffer interfacial layer due to strong hydrophobic interactions or covalent bonds. This interfacial layer may yield at large deformations. When these rigid proteins are further made into aggregates, they diffuse slower to the interface and cannot unfold as easily as monomers. They will have a longer induction time at the beginning of adsorption. The interfacial layer will be more stretchable because of fewer connections among aggregates. When mixed proteins are used as a stabilizer of emulsion or foam, the small species which can diffuse fastest to the interface are most likely to adsorb at the interface (at least on the short term), especially at the A-W interface. At the O-W interface, the oil phase can be a solvent for the hydrophobic groups of protein residues and have a stronger affinity to proteins. With a stronger hydrophobic interaction between oil molecules and proteins, proteins can unfold their structure faster and to a greater extent. Consequently, the displacement of proteins may be more evident at the O-W interface, for example, the displacement of casein monomers by small casein aggregates. Recent research showed that the unfolding of proteins is also affected by the polarity of oil phase (Bergfreund, Diener, et al., 2021). With an increasing oil polarity, proteins can unfold to a less extent at the O-W interface, then the displacement effect may be less evident. With a deeper understanding on the links among molecular properties of proteins, adsorption kinetics and rheological properties of protein layers, dairy proteins can be used as a benchmark for plant proteins. The interfacial properties of plant proteins can be improved by some physicochemical methods to have a smaller size and greater surface hydrophobicity. The Pickering mechanism was found neither in mixed protein systems studied in this thesis nor in MAG-S stabilized emulsion. Small surface active proteins or emulsifiers are playing more important roles stabilizing interfaces in these complex systems.

The methodology we used in this thesis to identify protein species at the interfaces can also be applied in other complex systems with mixed components. The first step is to fractionate different species from the

mixture, followed by (nonlinear) interfacial rheology tests on the individual fractions. According to the similarity or distinctive differences in rheological properties among fractions, we can have a preliminary inference which fraction is playing a role at the interfaces. However, it is important to realize, different compositions or structures of interfacial layer may have similar rheological properties. So, more evidence on which component is dominant at the interface needs to be provided by some interface visualization techniques.

In this research, although we mixed casein and whey proteins to replicate the real application of dairy protein materials in stabilizing emulsions or foams, extra efforts can be devoted to make the replication more realistic. In food industry, heat sterilization is often inevitable to guarantee a long shelf life of the emulsion products. Some research already disclosed that whey and casein can have complicated chemical interactions in the bulk phase (Dumpler, 2017). Displacement among proteins at interfaces can also happen during heat treatment (Dalgleish, Goff, & Luan, 2002). The composition change and denaturation of proteins at O-W interfaces upon heat treatment may affect the microstructure they formed at the O-W interface thus affecting the rheological properties of the layer, but this yet to be quantified. With respect to Chapter 5, although the stabilization mechanism of MAG-S crystals in oil-in-water emulsion is well demonstrated in this thesis, the mechanical properties of the solid shell, which strongly affect the dynamic stability of emulsions, are not tested in this research. Drop tensiometer measurements are not easily performed on these interfaces, in view of their high brittleness and propensity to show buckling even at small deformations. Furthermore, in a more complex system, for example when MAG-S co-exists with proteins in the aqueous bulk phase, how the proteins affect the crystallization process and what their effects on the mechanical properties of the solid layer are, still need to be further investigated.

In terms of the new method we developed to visualize proteins at the interfaces using MPM and a lab made setup, additional work could be done to make the method applicable for the quantification of protein load at the interfaces. By using some standard proteins, e.g., bovine serum albumin with given concentrations, we can construct a standard curve of concentration versus fluorescent density. Subsequently, by testing the intensity of the protein layers at the interface, we can have an estimation

how much proteins adsorb at the interfaces. Compared with the classic exclusion method to do protein load quantification using centrifugation, which is affected by protein load and droplet size (Hunt, et al., 1994; Van der Meeren, et al., 2005), this method will be more direct and accurate, as there is no need to break the sample.

Reference

Amagliani, L., & Schmitt, C. (2017). Globular plant protein aggregates for stabilization of food foams and emulsions. Trends in Food Science & Technology, 67, 248-259.

Bergfreund, J., Bertsch, P., & Fischer, P. (2021). Adsorption of proteins to fluid interfaces: Role of the hydrophobic subphase. Journal of colloid and interface science, 584, 411-417.

Bergfreund, J., Bertsch, P., Kuster, S., & Fischer, P. (2018). Effect of Oil Hydrophobicity on the Adsorption and Rheology of β-Lactoglobulin at Oil–Water Interfaces. Langmuir, 34(16), 4929-4936.

Bergfreund, J., Diener, M., Geue, T., Nussbaum, N., Kummer, N., Bertsch, P., Nyström, G., & Fischer, P. (2021). Globular protein assembly and network formation at fluid interfaces: effect of oil. Soft Matter, 17(6), 1692-1700.

Beverung, C., Radke, C. J., & Blanch, H. W. (1999). Protein adsorption at the oil/water interface: characterization of adsorption kinetics by dynamic interfacial tension measurements. Biophysical chemistry, 81(1), 59-80.

Bolder, S. G., Sagis, L. M. C., Venema, P., & van der Linden, E. (2007). Effect of Stirring and Seeding on Whey Protein Fibril Formation. Journal of agricultural and food chemistry, 55(14), 5661-5669.

Brooker, B. (1985). Observations on the air-serum interface of milk foams. Food Structure, 4(2), 12.

Brun, J. M., & Dalgleish, D. G. (1999). Some effects of heat on the competitive adsorption of caseins and whey proteins in oil-in-water emulsions. International Dairy Journal, 9(3-6), 323-327.

Burger, T. G., & Zhang, Y. (2019). Recent progress in the utilization of pea protein as an emulsifier for food applications. Trends in Food Science & Technology, 86, 25-33.

Burgos-Díaz, C., Wandersleben, T., Olivos, M., Lichtin, N., Bustamante, M., & Solans, C. (2019). Food-grade Pickering stabilizers obtained from a protein-rich lupin cultivar (AluProt-CGNA®): Chemical characterization and emulsifying properties. Food Hydrocolloids, 87, 847-857.

Cao, Y., & Damodaran, S. (1995). Coadsorption of. beta.-Casein and Bovine Serum Albumin at the Air-Water Interface from a Binary Mixture. Journal of agricultural and food chemistry, 43(10), 2567-2573.

Carrillo-Navas, H., Fouconnier, B., Vernon-Carter, E. J., & Alvarez-Ramirez, J. (2013). Shear rheology of water/glycerol monostearate crystals in canola oil dispersions interfaces. Colloids and Surfaces a-Physicochemical and Engineering Aspects, 436, 215-224.

Chassaing, B., Koren, O., Goodrich, J. K., Poole, A. C., Srinivasan, S., Ley, R. E., & Gewirtz, A. T. (2015). Dietary emulsifiers impact the mouse gut microbiota promoting colitis and metabolic syndrome. Nature, 519(7541), 92-96.

Chéreau, D., Videcoq, P., Ruffieux, C., Pichon, L., Motte, J.-C., Belaid, S., Ventureira, J., & Lopez, M. (2016). Combination of existing and alternative technologies to promote oilseeds and pulses proteins in food applications. OCL, 23(4), D406.

Corredig, M., & Dalgleish, D. G. (1995). A differential microcalorimetric study of whey proteins and their behaviour in oil-in-water emulsions. Colloids and Surfaces B: Biointerfaces, 4(6), 411-422.

Dalgleish, D. G., Goff, H. D., Brun, J. M., & Luan, B. B. (2002). Exchange reactions between whey proteins and caseins in heated soya oil-in-water emulsion systems - overall aspects of the reaction. Food Hydrocolloids, 16(4), 303-311.

Dalgleish, D. G., Goff, H. D., & Luan, B. B. (2002). Exchange reactions between whey proteins and caseins in heated soya oil-in-water emulsion systems - behavior of individual proteins. Food Hydrocolloids, 16(4), 295-302.

Damodaran, S. (2005). Protein stabilization of emulsions and foams. Journal of Food Science, 70(3), R54-R66.

Dickinson, E. (1992). Adsorption of sticky hard spheres: relevance to protein competitive adsorption. Journal of the Chemical Society, Faraday Transactions, 88(24), 3561-3565.

Dickinson, E. (1998). Proteins at interfaces and in emulsions stability, rheology and interactions. Journal of the Chemical Society, Faraday Transactions, 94(12), 1657-1669.

Dickinson, E. (1999). Adsorbed protein layers at fluid interfaces: interactions, structure and surface rheology. Colloids and Surfaces B-Biointerfaces, 15(2), 161-176.

Dickinson, E. (2001). Milk protein interfacial layers and the relationship to emulsion stability and rheology. Colloids and Surfaces B: Biointerfaces, 20(3), 197-210.

Dickinson, E. (2011). Mixed biopolymers at interfaces: Competitive adsorption and multilayer structures. Food Hydrocolloids, 25(8), 1966-1983.

Dickinson, E., & Hong, S.-T. (1994). Surface Coverage of. beta.-Lactoglobulin at the Oil-Water Interface: Influence of Protein Heat Treatment and Various Emulsifiers. Journal of agricultural and food chemistry, 42(8), 1602-1606.

Donaldson, T. L., Boonstra, E. F., & Hammond, J. M. (1980). Kinetics of protein denaturation at gas—liquid interfaces. Journal of colloid and interface science, 74(2), 441-450.

Drusch, S., Klost, M., & Kieserling, H. (2021). Current knowledge on the interfacial behaviour limits our understanding of plant protein functionality in emulsions. Current Opinion in Colloid & Interface Science, 56, 101503.

Dumpler, J. (2017). Heat stability of concentrated milk systems: Kinetics of the dissociation and aggregation in high heated concentrated milk systems: Springer.

Galani, D., & Owusu Apenten*, R. K. (1999). Heat-induced denaturation and aggregation of β-Lactoglobulin: kinetics of formation of hydrophobic and disulphide-linked aggregates. International journal of food science & technology, 34(5-6), 467-476.

Gao, Z., Zhao, J., Huang, Y., Yao, X., Zhang, K., Fang, Y., Nishinari, K., Phillips, G. O., Jiang, F., & Yang, H. (2017). Edible Pickering emulsion stabilized by protein fibrils. Part 1: Effects of pH and fibrils concentration. LWT - Food Science and Technology, 76, 1-8.

García-Moreno, P. J., Yang, J., Gregersen, S., Jones, N. C., Berton-Carabin, C. C., Sagis, L. M. C., Hoffmann, S. V., Marcatili, P., Overgaard, M. T., Hansen, E. B., & Jacobsen, C. (2021). The structure, viscoelasticity and charge of potato peptides adsorbed at the oil-water interface determine the physicochemical stability of fish oil-in-water emulsions. Food Hydrocolloids, 115, 106605.

He, Q., Zhang, Y., Lu, G., Miller, R., Möhwald, H., & Li, J. (2008). Dynamic adsorption and characterization of phospholipid and mixed phospholipid/protein layers at liquid/liquid interfaces. Adv Colloid Interface Sci, 140(2), 67-76.

Hinderink, E. B., Münch, K., Sagis, L., Schroën, K., & Berton-Carabin, C. C. (2019). Synergistic stabilisation of emulsions by blends of dairy and

soluble pea proteins: Contribution of the interfacial composition. Food Hydrocolloids, 97, 105206.

Hinderink, E. B. A., Kaade, W., Sagis, L., Schroën, K., & Berton-Carabin, C. C. (2020). Microfluidic investigation of the coalescence susceptibility of pea protein-stabilised emulsions: Effect of protein oxidation level. Food Hydrocolloids, 102, 105610.

Hunt, J. A., & Dalgleish, D. G. (1994). Adsorption behaviour of whey protein isolate and caseinate in soya oil-in-water emulsions. Food Hydrocolloids, 8(2), 175-187.

Iametti, S., Cairoli, S., De Gregori, B., & Bonomi, F. (1995). Modifications of High-Order Structures upon Heating of. beta.-Lactoglobulin: Dependence on the Protein Concentration. Journal of agricultural and food chemistry, 43(1), 53-58.

Iametti, S., De Gregori, B., Vecchio, G., & Bonomi, F. (1996). Modifications occur at different structural levels during the heat denaturation of β-lactoglobulin. European Journal of Biochemistry, 237(1), 106-112.

Jung, J.-M., Gunes, D. Z., & Mezzenga, R. (2010). Interfacial activity and interfacial shear rheology of native β-lactoglobulin monomers and their heat-induced fibers. Langmuir, 26(19), 15366-15375.

Kim, W., Wang, Y., & Selomulya, C. (2020). Dairy and plant proteins as natural food emulsifiers. Trends in Food Science & Technology, 105, 261-272.

Kornet, R., Shek, C., Venema, P., Jan van der Goot, A., Meinders, M., & van der Linden, E. (2021). Substitution of whey protein by pea protein is facilitated by specific fractionation routes. Food Hydrocolloids, 117, 106691.

Lech, F. J., Meinders, M. B. J., Wierenga, P. A., & Gruppen, H. (2015). Comparing foam and interfacial properties of similarly charged protein–surfactant mixtures. Colloids and Surfaces A: Physicochemical and Engineering Aspects, 473, 18-23.

Liang, G., Chen, W., Qie, X., Zeng, M., Qin, F., He, Z., & Chen, J. (2020). Modification of soy protein isolates using combined pre-heat treatment and controlled enzymatic hydrolysis for improving foaming properties. Food Hydrocolloids, 105, 105764.

Mackie, A. R., Gunning, A. P., Ridout, M. J., Wilde, P. J., & Morris, V. J. (2001). Orogenic Displacement in Mixed β-Lactoglobulin/β-Casein Films at the Air/Water Interface. Langmuir, 17(21), 6593-6598.

McKenzie, H., Ralston, G., & Shaw, D. (1972). Location of sulfhydryl and disulfide groups in bovine. beta.-lactoglobulins and effects of urea. Biochemistry, 11(24), 4539-4547.

McSweeney, S. L., Healy, R., & Mulvihill, D. M. (2008). Effect of lecithin and monoglycerides on the heat stability of a model infant formula emulsion. Food Hydrocolloids, 22(5), 888-898.

Meinders, M. B. J., & De Jongh, H. H. J. (2002). Limited conformational change of β-lactoglobulin when adsorbed at the air-water interface. Biopolymers - Biospectroscopy Section, 67(4-5), 319-322.

Miller, R., Fainerman, V. B., Makievski, A. V., Krägel, J., Grigoriev, D. O., Kazakov, V. N., & Sinyachenko, O. V. (2000). Dynamics of protein and mixed protein/surfactant adsorption layers at the water/fluid interface. Adv Colloid Interface Sci, 86(1), 39-82.

Munk, M. B., Larsen, F. H., Van Den Berg, F., Knudsen, J. C., & Andersen, M. L. (2014). Competitive displacement of sodium caseinate by low-molecular-weight emulsifiers and the effects on emulsion texture and rheology. Langmuir, 30(29), 8687-8696.

Ning, F., Wang, X., Zheng, H., Zhang, K., Bai, C., Peng, H., Huang, Q., & Xiong, H. (2019). Improving the bioaccessibility and in vitro absorption of 5-demethylnobiletin from chenpi by se-enriched peanut protein nanoparticles-stabilized pickering emulsion. Journal of Functional Foods, 55, 76-85.

Papiz, M., Sawyer, L., Eliopoulos, E., North, A., Findlay, J., Sivaprasadarao, R., Jones, T., Newcomer, M., & Kraulis, P. (1986). The structure of β-lactoglobulin and its similarity to plasma retinol-binding protein. Nature, 324(6095), 383-385.

Pelan, B. M. C., Watts, K. M., Campbell, I. J., & Lips, A. (1997). The Stability of Aerated Milk Protein Emulsions in the Presence of Small Molecule Surfactants. Journal of Dairy Science, 80(10), 2631-2638.

Peng, D., Jin, W., Arts, M., Yang, J., Li, B., & Sagis, L. M. C. (2020). Effect of CMC degree of substitution and gliadin/CMC ratio on surface rheology and foaming behavior of gliadin/CMC nanoparticles. Food Hydrocolloids, 107, 105955.

Pickering, S. U. (1907). Cxcvi.—emulsions. Journal of the Chemical Society, Transactions, 91, 2001-2021.

Rahman, A., & Sherman, P. (1982). Interaction of milk proteins with monoglycerides and diglycerides. Colloid and Polymer Science, 260(11), 1035-1041.

Rasheed, F., Markgren, J., Hedenqvist, M., & Johansson, E. (2020). Modeling to understand plant protein structure-function relationships—implications for seed storage proteins. Molecules, 25(4), 873.

Ridout, M. J., Mackie, A. R., & Wilde, P. J. (2004). Rheology of Mixed β-Casein/β-Lactoglobulin Films at the Air−Water Interface. Journal of agricultural and food chemistry, 52(12), 3930-3937.

Rodríguez Patino, J. M., Miñones Conde, J., Linares, H. M., Pedroche Jiménez, J. J., Carrera Sánchez, C., Pizones, V., & Rodríguez, F. M. (2007). Interfacial and foaming properties of enzyme-induced hydrolysis of sunflower protein isolate. Food Hydrocolloids, 21(5), 782-793.

Sari, Y. W., Mulder, W. J., Sanders, J. P., & Bruins, M. E. (2015). Towards plant protein refinery: review on protein extraction using alkali and potential enzymatic assistance. Biotechnology Journal, 10(8), 1138-1157.

Sawyer, W. (1968). Heat denaturation of bovine β-lactoglobulins and relevance of disulfide aggregation. Journal of Dairy Science, 51(3), 323-329.

Sengupta, T., & Damodaran, S. (1998). A New Methodology for Studying Protein Adsorption at Oil–Water Interfaces. Journal of colloid and interface science, 206(2), 407-415.

Srinivasan, M., Singh, H., & Munro, P. A. (1996). Sodium Caseinate-Stabilized Emulsions: Factors Affecting Coverage and Composition of Surface Proteins. Journal of agricultural and food chemistry, 44(12), 3807-3811.

Tang, C.-H. (2017). Emulsifying properties of soy proteins: A critical review with emphasis on the role of conformational flexibility. Critical reviews in food science and nutrition, 57(12), 2636-2679.

Torres, O., Murray, B., & Sarkar, A. (2017). Design of novel emulsion microgel particles of tuneable size. Food Hydrocolloids, 71, 47-59.

Van der Meeren, P., El-Bakry, M., Neirynck, N., & Noppe, P. (2005). Influence of hydrolysed lecithin addition on protein adsorption and heat stability of a sterilised coffee cream simulant. International Dairy Journal, 15(12), 1235-1243.

Walstra, P. (1990). On the stability of casein micelles. Journal of Dairy Science, 73(8), 1965-1979.

Wanasundara, J. P., McIntosh, T. C., Perera, S. P., Withana-Gamage, T. S., & Mitra, P. (2016). Canola/rapeseed protein-functionality and nutrition. OCL, 23(4), D407.

Wang, F., Zhang, Y., Xu, L., & Ma, H. (2020). An efficient ultrasound-assisted extraction method of pea protein and its effect on protein functional properties and biological activities. LWT, 127, 109348.

Wang, J.-M., Xia, N., Yang, X.-Q., Yin, S.-W., Qi, J.-R., He, X.-T., Yuan, D.-B., & Wang, L.-J. (2012). Adsorption and Dilatational Rheology of Heat-Treated Soy Protein at the Oil–Water Interface: Relationship to Structural Properties. Journal of agricultural and food chemistry, 60(12), 3302-3310.

Xiao, J., Li, Y., & Huang, Q. (2016). Recent advances on food-grade particles stabilized Pickering emulsions: Fabrication, characterization and research trends. Trends in Food Science & Technology, 55, 48-60.

Xu, S., & Damodaran, S. (1994). Kinetics of adsorption of proteins at the air-water interface from a binary mixture. Langmuir, 10(2), 472-480.

Yang, J., Thielen, I., Berton-Carabin, C. C., van der Linden, E., & Sagis, L. M. (2020). Nonlinear interfacial rheology and atomic force microscopy of air-water interfaces stabilized by whey protein beads and their constituents. Food Hydrocolloids, 101, 105466.

Zhai, J., Miles, A. J., Pattenden, L. K., Lee, T.-H., Augustin, M. A., Wallace, B. A., Aguilar, M.-I., & Wooster, T. J. (2010). Changes in β-Lactoglobulin Conformation at the Oil/Water Interface of Emulsions Studied by Synchrotron Radiation Circular Dichroism Spectroscopy. Biomacromolecules, 11(8), 2136-2142.

Zhang, Z., Dalgleish, D., & Goff, H. (2004). Effect of pH and ionic strength on competitive protein adsorption to air/water interfaces in aqueous foams made with mixed milk proteins. Colloids and Surfaces B: Biointerfaces, 34(2), 113-121.

Summary

Emulsions and foams are two thermodynamically unstable systems. In many food emulsions or foams, multiple components can be involved in stabilizing these systems. A common example are dairy proteins, which are widely used as stabilizers. In specific cases, a mixture of casein and whey proteins is used for stabilization of emulsions or foams, for example, milk protein isolate or skimmed milk powder. In dairy emulsions, some polar lipids can be present in milk fat due to hydrolysis during oil storage, for example, monoglycerides or diglycerides. Stabilizers can also consist of mixtures of stabilizers in different aggregation states (e.g. monomers in coexistence with micelles or aggregates). In a complex multi-component emulsion or foam system, where various surface-active components are present, it is difficult to distinguish the real surface-active species responsible for stabilizing oil-water (O-W) or air-water (A-W) interfaces. The aim of this thesis was therefore to improve our knowledge about the absorption behavior of surface-active ingredients at O-W or A-W interfaces in mixed systems and the resulting interfacial properties. Two types of systems were investigated, namely monomers coexisting with micelles/aggregates and emulsions stabilized with high melting point emulsifiers.

In **Chapter 1**, an overview of the characteristics of dairy proteins and polar lipids and the interfacial rheology methods used in this thesis are presented.

In **Chapter 2**, the adsorption kinetics and rheological properties in the nonlinear viscoelasticity regime of O-W interfaces stabilized with whey protein isolate (WPI) and whey protein aggregate (WPA) were investigated. At a low concentration (0.1 wt%), WPI proved to be more surface-active than WPA, but the rheological properties of interfaces stabilized with the mentioned proteins showed little difference, and both formed a viscoelastic solid-like interfacial layer with a predominantly elastic response at low amplitude. At a higher concentration, the difference in surface activity between WPI and WPA disappeared. Both decreased the surface tension quickly and to a similar extent. WPI displayed strain yielding behavior at a large amplitude (30%), while WPA mainly showed an elastic response, and the layer was more stretchable. At a high concentration and under dynamic conditions (i.e., when subjected to high speed shear), emulsions made with WPA were more stable against creaming, owning to the higher bulk viscosity, but less stable against coalescence. This could be because of the different

structure of the layers formed by these two components at the O-W interface. WPI formed a dense and stiffer interfacial layer, which was brittle but could prevent coalescence by a mechanism similar to the Marangoni effect after the breakage of the layer. The interfacial layer formed by WPA was coarser, thicker and less brittle, but once the layer was broken, the particles could not protect the interface efficiently due to the low mobility of WPA at the interface.

Casein micelle dispersions are composed of several fractions, including micellar caseins, casein monomers, and small aggregates. In **Chapter 3**, we studied the interfacial properties of these dispersions. We fractionated the dispersions into a fraction containing mostly casein micelles and one containing monomers and small aggregates, then investigated their interfacial properties separately. It was shown that micellar caseins can adsorb at neither O-W nor A-W interfaces. When a casein dispersion was used to stabilize interfaces, A-W interfaces were mainly dominated by monomers, while O-W interfaces were mainly occupied by small aggregates.

After studying the behavior of whey protein or casein at O-W and A-W interfaces separately, systems containing both proteins were prepared to study their interfacial behavior in mixtures, which is the topic of **Chapter 4**. Based on rheology results and interfacial visualization, casein was found to be dominant at the O-W interface, even at low casein : whey protein ratio (CA:W = 0.1 wt% : 1.9 wt%) in the mixture. Even though casein preferentially adsorbed at O-W interfaces, it could not form a stiff layer due to its relatively weak in-plane intermolecular interactions at O-W interfaces. At the A-W interface, casein could co-adsorb with whey proteins. With an increasing proportion of casein in the mixture, casein disrupted the solid-like network formed by whey protein, and as a result the layer became less stiff.

In **Chapter 5**, we used glycerol monostearate (MAG-S) as a high melting point emulsifier to study the mechanism by which these crystallizable emulsifiers stabilize O-W interfaces (i.e. bulk versus interfacial stabilization). We confirmed the growth of MAG-S crystals at a planar oil-water interface. The crystallization process of emulsifiers in the emulsion system was observed by optical microscopy. An intriguing phenomenon, repeated deformation-relaxation (RDR), was observed in these experiments. We analyzed the cause of RDR, and it was shown that this was attributable to two factors: the formation of brittle solid interfacial layers by the emulsifiers, and stress build-up in these layers due to shrinkage of the oil bulk phase upon cooling.

Therefore, by interpreting the cause of the RDR phenomenon, we indirectly proved that adsorption of MAG-S happened prior to the crystallization of MAG-S in our tests, and that MAG-S can form a continuous and compact solid layer at the surfaces of emulsion droplets. The mechanism was different from the so-called Pickering mechanism proposed in other work.

In **Chapter 6**, we provided a general discussion to link all the results and findings and put them in a broader context. The effect of molecular properties on the dominating protein species at the O-W or A-W interfaces and mechanical properties of interfaces were discussed in terms of competitive adsorption and displacement among proteins. When small molecular proteins are mixed with larger protein aggregates, small proteins are most likely to adsorb and be dominant at the interfaces, even though sometimes the fraction of these small molecules is not the main component of the used ingredient. Just like the mixtures we studied here, plant protein extracts are often mixtures of various proteins containing several forms, for example, peptides, native proteins, and aggregates. Several suggestions and physiochemical methods were provided for improving the interfacial activity of plant proteins. The methodology we used to identify surface active species of multi-component systems responsible for interfacial properties can also be applicable for plant protein mixtures. Based on the findings in this thesis, we can conclude that the Pickering stabilization mechanism, which is often invoked to explain stability in the complex protein (aggregate) systems and emulsions made with MAG-S, does not hold for these systems. In conclusion, the results presented in this thesis provided new knowledge on the interfacial behavior of complex multi-component systems, which can be useful for designing emulsion formulations or tailoring the functionality of emulsions or foams.

Acknowledgements

Looking back over the past four and a half years of my PhD, I realize how many have people supported me on this journey. My daily supervisor, Leonard, must be the person who invested the most time and effort into me and witnessed my growth. I benefited greatly from your profound knowledge and abundant research experience. You were always patient with me and were never bothered by my repeated questions. Many times, I was deeply touched. I will never forget the moment when I received your feedback on the first draft of my first paper. I was shocked by your explicit remarks and revisions on almost every sentence. I also appreciate the freedom you gave me which allowed me to choose the directions and topics I was interested in. Exactly because of your help, I could finish this difficult and challenging period in my life. Your influences on me originate not only from your knowledge and research skills, but also on the inspiration from your rigorous attitude to science, open mind, friendly and respectful way to treat others, noble sense of morality, and strong sense of responsibility. You made yourself a role model for me and showed me how to treat this world and others. I believe the impression you have left on me will positively and continuously affect my future science career and life. Thank you, Leonard!

My respectful co-supervisor Guido also provided many valuable suggestions on this thesis research. Your professional insights kept me from taking the wrong path on various occasions and your strict guidance on my writing let me realize my shortcomings. Your encouragement and suggestions on my writing will keep echoing around my ears in future and help me to improve.

Besides my supervisors, the help from other FPH staff is also highly appreciated. I am grateful to the technical support and documental assistance from Harry, Floris, David, and Els. I want to especially thank Roy. Besides your help on lab work preparation, I also appreciate our nice discussions on experiments designs, for example, the application of multiphoton excitation microscopy on interface visualization and the coalescence experiment of droplets. Of course, I also want to thank Elke and Erik for encouraging me and sharing your opinions on career perspectives.

If I analogy my PhD training as a voyage, supervisors are like lighthouses, all my other fellows are the sailors, who experienced all challenges and difficulties together with me. Because of your company, my PhD training turned out to be a fantastic and exciting adventure. I first want to acknowledge my most loyal and reliable friend Remco. You helped me with improving my English, being familiar with the Netherlands, and accommodating to my new life when I just arrived in the Netherlands. I enjoyed chatting with you on political topics and sharing your

understanding on this world and people. All of them, together with our laughs on our trip to China, will be the most valuable memories in my life. Naomi, I am glad we were officemates and worked together on the crystal topic. It was a pleasure to make friends with you, as you are one of the most optimistic and enthusiastic people I have met. Next, I would like to thank Jack, Gerard, Melika, and Aref. You guys were never stingy with your knowledge. I benefited from our daily discussions on rheology or other physical topics. Also, dear Annika, your caring greetings could always make my day and sweep away my frustrations. My other FPH fellows, Claudine, Marco, Phillip, Belinda, Ahmad, Huifang, Zhihong, Lei, Bo and Xiaoning, all made FPH a lovely group. I enjoyed the moments I spent with all of you.

Here, I would also like to thank my students, Laurens, Vera, Zhitong and Greg. Due to your hard work, some of the chapters in this thesis could be completed.

在荷兰的求学生涯中，我有幸结识了一圈兄弟们：老蒋，登科，文杰，哲哥，张陈还有桃军。大家一直以来相互的关怀和支持，让我们在异国他乡成为了战友！我很高心我们能在过去的四年中相互见证彼此的成长和年轻时一段奋斗的岁月。除了他们，和我生活在一起的D楼的邻居们：小马，Dan，老马还有文娇也提供了我许多日常生活中的方便与照顾。还有我们中农的伙伴们：小郭，姝辰，贵生，祝缘，砚樵，白莹还有仕杰，缘分让我们在瓦村相聚，感谢你们陪伴我度过了在博士开始的两年里最快乐的时光。

最后我想将最崇高的敬意致以含辛茹苦养育我的父母。没有你们，不会有我的一切。也感谢姐姐以及其他亲人，感谢你们对我从小到大的理解,鼓励与支持。

About the author

Biography

Xilong Zhou was born on Jun 7th, 1993, in Wuxi, Jiangsu province, China. From 2011 to 2015, he studied food quality and safety at Tianjin University of Science and Technology (TUST). After that, he furthered his master education with the major Agricultural Product Processing and Storage Engineering at China Agricultural University (CAU) in Beijing. He was involved in the project to develop UHT recombined dairy cream products. In 2017, after obtaining his master's degree, he started his PhD education sponsored by China Scholarship Council at Wageningen University in the Netherlands. He conducted his research on interfacial properties of dairy ingredients in the group of Physics and Physical Chemistry of Foods. The results of his PhD project are mainly presented in this thesis.

Contact: xlzhou_daily@126.com

Overview of completed training activities

Discipline specific courses

Rheology Course	FPH, the Netherlands	2018
Masterclass Dairy Protein Biochemistry	VLAG, FQD, the Netherlands	2018
Advanced Food Analysis	VLAG, the Netherlands	2019
Big Data Analysis in the Life Sciences	VLAG, the Netherlands	2019

Conferences and symposia

Mini-Symposium Rheology	VLAG, the Netherlands	2019
NRV Rheology Seminar	Wageningen,	2019
International Symposium on Food Rheology[1]	ETH Zürich, Switzerland	2019
18th International Congress on Rheology	Online	2020
EFFOST International Conference[2]	Agroscope, Bühler Group, EPFL, ETH Zürich and Nestlé, Switzerland	2021
18th Food Colloids Conference Structure, Dynamics and Function[2]	Online	2022

General Courses

VLAG PhD week	VLAG, the Netherlands	2017
Career Perspectives	WGS, the Netherlands	2020
Supervising BSc & MSc Thesis Students	WGS, the Netherlands	2020
Scientific Writing	WGS, the Netherlands	2020
Searching and Organizing Literature	WUR library, the Netherlands	2020

[1] Oral presentation, [2] poster presentation

Other activities

Preparation of Research Proposal	FPH	2017
Weekly group meetings	FPH	2017-2022

Teaching and supervision

Food Physics	FPH	2017-2022
Supervision 5 MSc thesis	FPH	2017-2022
Supervision 2 BSc thesis	FPH	2017-2022

Approved by graduated school VLAG

List of publications

This thesis

Zhou, Xilong, Guido Sala, and Leonard MC Sagis. "Bulk and interfacial properties of milk fat emulsions stabilized by whey protein isolate and whey protein aggregates." Food Hydrocolloids 109 (2020): 106100.

Zhou, Xilong, et al. "Are micelles actually at the interface in micellar casein stabilized foam and emulsions?." *Food Hydrocolloids* (2022): 107610.

Zhou, Xilong, Guido Sala, and Leonard MC Sagis. "Composition and rheological properties of oil-water and air-water interfaces stabilized with casein and whey protein mixture." *Food Hydrocolloids*. (**Submitted)**

Xilong Zhou, Naomi Arita Merino, Greg Meesters, Guido Sala, Leonard M.C. Sagis. "Emulsifier crystal formation and its role in periodic deformation-relaxation of emulsion droplets upon cooling." *Food Hydrocolloids*. (**Submitted)**

Other publications

Xia, Wenjie, Linfeng Zhu, Roy JBM Delahaije, Zhe Cheng, Xilong Zhou, and Leonard MC Sagis. "Acid-induced gels from soy and whey protein thermally-induced mixed aggregates: Rheology and microstructure." *Food Hydrocolloids* (2021): 107376.

Han, Jie, Xilong Zhou, Jialu Cao, Yunna Wang, Bokang Sun, Yan Li, and Liebing Zhang. "Microstructural evolution of whipped cream in whipping process observed by confocal laser scanning microscopy." *International journal of food properties* 21, no. 1 (2018): 593-605.

Zhou, Xilong, et al. "Stability and physical properties of recombined dairy cream: Effects of soybean lecithin." International Journal of Food Properties 20.10 (2017): 2223-2233.

Wu, Shaozong, Geng Wang, Zhang Lu, Yan Li, Xilong Zhou, Lintianxiang Chen, Jialu Cao, and Liebing Zhang. "Effects of glycerol monostearate and Tween 80 on the physical properties and stability of recombined low-fat dairy cream." Dairy Science & Technology 96, no. 3 (2016): 377-390.

Colophon

The research described in this thesis was financially supported by the China Scholarship Council (CSC) and the laboratory of Physics and Physical Chemistry of Foods (FPH), Wageningen University.

The financial support from Wageningen University for printing this thesis is gratefully acknowledged.

Layout: Xilong Zhou

Cover design: Xilong Zhou and Timothy Alexander Guth

Printed by ProefschriftMaken